On the Micro-Precision Robotic Drilling of Aerospace Components

John Newberry

B. Eng. Aero. (Hons)

A dissertation submitted in fulfilment of the degree of Doctor of Philosophy

RMIT University

School of Aerospace, Mechanical and Manufacturing Engineering

SET Portfolio

RMIT University, Australia

March 2007

Abstract

This dissertation describes research concerned with the use of advanced measurement techniques for the control of robotic manufacturing processes. The work focused on improving the state of technology in the precision robotic machining of components within the aerospace manufacturing industry within Australia. Specific contributions are the development of schemes for the use of advanced measurement equipment in precision machining operations and to apply flexible manufacturing techniques in automated manufacturing.

The outcome of the research enables placement of a robotic end effector to drill a hole with a positional accuracy of 300 micron, employing an Indoor Global Positioning System for control of the drilling process. This can be accomplished within a working area of 35 square metres where the robot system and/or part positions may be varied dynamically during the process.

Large aerospace structures are capable of flexing during manufacturing operations due to their physical size and low modulus of rigidity. This research work provided a framework for determining the appropriate type of automation and metrology systems needed for dynamic control suited to the precision drilling of holes in large aerospace components.

Disclosure

The material contained within this thesis may be the subject of several patents. This work has not been released into the public arena and is restricted to viewing by thesis examiners.

Statement of Originality

The contents of this thesis report has not previously been submitted for the award of any degree or diploma in any university. To the best of the author's knowledge and belief, this report contains no material previously published or written by any other source, except where due acknowledgement has been make within the text. The content of the thesis is the result of work carried out at RMIT.

John Newberry
August 2007

Acknowledgements

The author would like to offer thanks to those who have given their assistance through the progress of this work, in academic, professional and personal areas.

- Assoc. Prof. Roger LaBrooy as academic supervisor for his timely intervention in accepting a supervisory role and his tireless effort and strained patience throughout this period.

- Other supervisors, both academic and industrial: Mr. Bob Hood (Initial supervisor, RMIT) and Dr. Phil Crothers (HdH) and Dr. M. Mahdavian (RMIT) for their direction and assistance in this research.

- RMIT staff, specifically Mrs. Shoshanna Rudov-Clark, Dr. Alex Kootsookos, Prof. Tom Steiner and Prof. Peter Hofmann for their support over this period.

- Hawker de Havilland, Fisherman's Bend and the CRC-IMST and specifically Messers Geoff Lam, Ashleigh Nesbitt, Alvise Bonghetti, Peter Steele, Jason Braganza, Andrew McConvall and Steven Van Duin.

- The author would also like to thank those who have offered their support throughout this time, Mr Brian Newberry, Mrs. Julie West, Mr. Kevin West, Mr. Robert Newberry and Mr. Matthew Armstrong.

Table of Contents

List of figures

List of tables

Acronyms

CRC-IMST: Cooperative Research Centre for Intelligent Manufacturing Systems and Technologies

IPS: Indoor Global Positioning System, In-factory Global Positioning System

HdH: Hawker de Havilland

QA: Quality assurance

Glossary

Dynamic/static – Dynamic and static refer to characteristics of a measured point – either moving or stationary

Flexibility (manufacturing) – Capability to vary manufacturing process between parts or during operation.

Flexibility (structural) – Tendency for a structure to warp under load.

General/generic – The term “general” and “generic” is used throughout this dissertation to refer to processes that are independent of a specific industry or task, and therefore allowing an inherently flexible process.

Micro-positioning – Ultra small scale movement of an end effector or part, less than 1mm.

Part/Workpiece – Component during manufacturing operation.

Position – Cartesian coordinates of any given point.

Posture – Combination of roll, pitch and yaw for a robot wrist/end effector.

Precision point (data) – Term used for IPS data structures using a large number of samples to create a single, precise measurement.

Precision scale – Scale of work under 1mm. This term is used for measurement and control.

Robot/tool/end effector – Robotic arm with accompanying end effector and tool.

Sensing/measuring/controlling – For the purposes of this dissertation these terms refer to the retrieval of positional data and employment as a means of identifying current location and required move of items including end effector, part and system.

Stability (manufacturing process) – Ability to re-acquire a previously disturbed location and continue manufacturing operation.

System (as in "The System") – IPS (Indoor positioning system), equipment used throughout this research.

Tool – Manufacturing device attached to robot to engage with, or be applied to a part. (eg. a drill.)

Units

The use of units throughout this paper will include both the SI and Imperial units. SI (or metric) units are the norm, however it is necessary to cater to measurements Imperial units required by HdH due to the U.S. influence. Thus millimetres will be the default measurement of length, unless Imperial units are specified.

1 Chapter 1: Introduction

1.1 Preamble

This research is conducted as a part of a project funded by the Cooperative Research Centre for Intelligent Manufacturing Systems and Technologies (CRC-IMST), with Hawker de Havilland (HdH) as the major industrial partner. The research was focused on identifying and developing the basis for a system of micro-precision drilling of aerospace components using a mobile robot. The normal level of positioning accuracy provided by an industrial robot needed to be improved to cope with specific requirements encountered in the aerospace industry. Here usable systems were required to be devised to accommodate the flexibility of large aircraft components even when supported on jigs. A typical product would be a commercial aircraft stabilizer whose span was of the order of 12 metres with similar drilling error requirements common to small products (under 1m length).

Pre-existing robotic systems are incapable of producing the desired level of accuracy over such spans. Hence in order to improve positional accuracy and cater to the inherent flexibility of a structure (even when supported by jigs or fixtures), the candidate needed to use extended sensing to provide inputs for adjusting final end effector location on a precision scale. A potential means of so doing would be to locate a photoelectric diode receiver on the surface of a flexible component so that accurate global location of features could be readily identified by triangulation.

There was then a clear need to establish a means of finer position control beyond what was available for use in the aerospace industry. The candidate researched and investigated the use of an "In-Factory" Global Positioning System (IPS) to attain the final precision positioning and control required in these instances.

1.2 Objective

The overall objective of this research was to investigate whether the use of Indoor Positioning Systems (IPS) equipment was suitable for controlling precision positional information relating to both workpiece and robot when both were required to engage with one another. There needed to be a recognition that both entities were mobile and/or flexible.

It was necessary to eventually design a system to control the precise application-points of a range of tools such as orbital drills or assembly fastener insertion tools, coupled to a robot end effector.

Such a system also needed to cope with multiple robots operating simultaneously on a single component or where the workpiece itself could move. It was envisaged that the proposed system would result in a step change of improving the final manufacturing process accuracy of large aerospace components in a production environment.

2 Chapter 2: Literature review

2.1 Overview of current methods of end effector positioning

Much of the literature on positioning an end effector for manufacturing tasks relies on the robot manufacturer's calculation of the IK (inverse kinematic) solution for determining end-effector position and posture. Inverse kinematics relies on the execution of a robot manufacturer's algorithm to specify individual joint parameters as a function of desired global robot positions. This technique is insufficient because it relies on absolute rigidity of the robot and workpiece and is intolerant of flexibility or other discrepancies in the actual location of critical points on the manufactured surface. As an example, a short summary of the inverse kinematic solution set for a typical robot as described by LaBrooy [1983] and reproduced in McKerrow [1991] are cited in Appendix A.

Paul [1981] provided early methodology to determine joint angles by matrix analysis of the relationship of robot linkages. Additionally, Paul [1981] discussed the derivation of Jacobians based on differential movements to identify the velocity characterisation of an end effector, affecting the dynamics of the manipulator itself.

Young [1973] suggested the need of position measurement feedback for the positioning of a robotic tool, categorising these into either measurement of an absolute nature (where measurement is taken from a global coordinate frame) or incremental measurement (where the measurement is taken from a sequential series of related measurements). This concept is related to an IPS system used throughout this research, which offers an absolute measure. Young [1973] however indicated that at the time, such systems were both large and cost-prohibitive. He suggested that a measurement technique using a steel vane creating magnetic pulses be used to feedback positional information.

Heath [1985] discussed use of the most predominant means of positioning robot used within industry. Here a "teach pendant" was used to manually guide the robot to the correct position and posture. Once this was achieved the operator recorded the robot's position and posture, by recording the joint angles. On replay the robot could rapidly return to "taught" points. The method initially termed joint coordinated motion (JCC) and other related methods are usually referred to as "online" programming. Here the robot must have been pre-driven to taught points and there is no necessity to invoke the inverse kinematic solution set. Heath [1985] suggested that whilst this method allowed the robot to attain end effector locations only, the end-effector path between points was usually indeterminate to form part of robot's in-built trajectory plan.

Hefele and Brenner [2000] discussed the difference between the use of a teach pendant, as described by Heath [1985] and the IK solutions discussed earlier. These authors suggested that robots commonly used for industrial purposes may have a repeatability of 0.1mm. Repeatability is the ability of a robot to reach a known position within a sphere of error. The actual repeatability attained may vary up to several millimetres due to internal robot mechanical factors, such as linkage droop and drive mechanism servo errors. As the teach pendant defines the correct position and posture attained manually, final repeatability is totally dependant on such internal robot factors. The use of the IK solution, in an "offline" programming mode, relies on the mathematical model pre-programmed into the robot. Hefele and Brenner [2000] approached bridging the gap between using the teach pendant and the inverse kinematic solution accuracy by using digital photogrammetric tracking techniques. These two methods were employed, initially placing digital cameras around the robot's end effector and measuring differences between final and expected end effector locations. Secondly, using a camera located at the end effector itself, coded targets placed about the measurement area were measured allowing calibration of the robot system itself and identification of deviations from the expected location.

2.2 Overview of micro positioning research

The first acknowledged attempt at using micro-positioning in addition to the robots IK solution was performed at Arizona State by Davidson [1985]. Since then the general concept of micro positioning has commonly been restricted to robots with operations on a micro scale. This was essentially due to the increasing availability of miniaturised components used in micro-electronics. Large scale deviation measurements were still inaccurate and there was a tendency to use Moire fringe methods for improved accuracy. Adaptation of moire fringes to metrology is commonplace as used in industrial micrometer construction. It's use in *large scale* schemes is restricted and compounded by parallax errors and lens aberrations.

Yi, Na, Chung, Kim and Suh [2002] demonstrated a limited positioning system that was developed specifically for measuring the accuracy of flexure hinges, depicted in Figure 2.1. This system used peizo-electric actuators and possessed overall movement of 0-100μm in two linear dimensions (x and y) with a rotational movement of 0 - 0.1°. The extremely small movement and rotation allowed by such actuators were typical of most micro positioning systems. Whilst being able to position to within a few microns, the scope of the tool itself was extremely limited. Due to the limited nature of these systems, they often required auxiliary micro systems inducing error to operate realistic payloads.

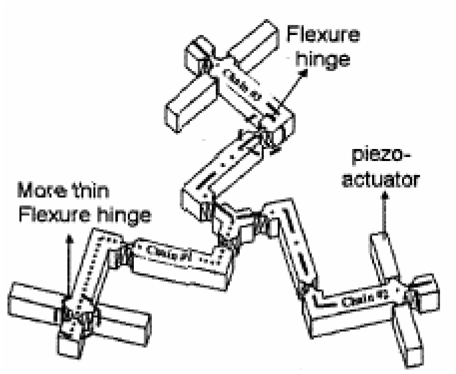

Figure 2.1 - flexure hinge micro positioner

(Yi, Na, Kim and Suh [2002])

Aoyama, Iwata and Sasaki [1995] built micro-robots capable of etching and micro-hammering tasks. These devices comprised a series of miniature robots working in parallel, achieving accuracies at a micron level in a controlled atmosphere. Whilst the use of micro-robots may offer considerable advantages for some manufacturing tasks and are capable of extremely high precision, the use of these schemes with miniscule payloads is only a curiosity in the candidate's brief to manipulate accurately substantial payloads over long distance.

Choi, Han, Kim, Kim, Choi and Na [2003] examined the use of micro positioning grippers for the positioning and pressing of small components. The micro positioning system was based around a rotating module and linear movement axis that was completed by a 3-axis manoeuvring stage prior to pressing of the component. This system employed laser displacement sensors to measure the final position and posture of the parts for determining existing placement error. Again this paper examined a process that focused on small scale items, rather than extending the measurement to larger components where inertia and dynamics played significant and so far unaccounted roles.

Hohn and Robl [1999] considered the use of micro-positioning for existing industrial robotics. Specifically this micro positioning system comprised a precise gripper attached to a standard industrial robot, using a vision system for executive control of the system. This allowed for the prospect of micro-positioning over the range over which the robot operated. It must be noted that adaptation of this system was proposed for the assembly of wristwatch gears and was aimed at the manufacture of micro structures. Many practical watch assembly schemes use extensive micro-jigs and "dead-reckoning" methods used in electronic manufacture. The vision system used for this process was based on a CCD chip, with a maximum measurement area of 30mm x 20mm. Although the accuracy of this system was recorded at 30 μm, it was only achievable over a small area. Positioning accuracy was only possible while the robot arm remained constrained to the work envelope

Huang [2000] examined a micro-positioning system that was based around a tapping cell, using sharp applications of force to effect fine positional adjustments. The scheme appeared beneficial for industrial tasks where static friction needed to be overcome.

Van Duin [2001] performed research examining micro positioning for industrial purposes, allowing measurement and drilling a flat workpiece to within several microns of positional accuracy. This relied on placing static lasers on a part for guiding micro positioning of an end effector. The required payload and movement was well beyond what was demonstrated by prior examples cited. This experimentation however was only able to demonstrate movement with two degrees of freedom and consumed space on the workpiece. Both laser receivers and transmitters were located proximal to each other and 3-D measurements were attempted There was merit in the Van Duin [2001] scheme which was explored by the candidate more fully and described later in this dissertation.

The following section reviews the applicability of several papers in key areas.

2.3 Online vs. offline programming and feedback

Programming of robot operations include two standard methods: Online and offline programming.

Online programming commonly uses a teach pendant. The system must be "online" and the end effector moved to a desired location. The system is rigid in concept and is inappropriate in the context of this research as control must be flexible and may not be pre-programmable.

Offline programming includes the use of robot control programs to be invoked prior to any operation. This relies on a mathematical model of the robot and can result in high errors when used with a flexible workpiece. As there is no scheme for compensating such a robot, offline programming on its own is also unsuitable.

Thus, it is necessary to utilise absolute positional feedback to compensate for the operation of any system, to allow for flexibility and adjustment of pre-calculated position.

2.4 Scale of system

The highest accuracy reported in the examples in section 2.2 was of the order of 100 microns and were attained using of micro-robots, used for micro positioning of small tools. The techniques were inappropriate due to the nature of the micro robots themselves. Firstly their small size heavily restricted both their movement and payload capacity, resulting in operations only being suited to small components and micro structures (demonstrated by Aoyama, Iwata and Sasaki [1995]). While these robots were capable of adapting to differing shapes and situations they remained slow to move and operate. Their applications were very limited. This research focuses on operations on components that are large (several metres in length). The use of micro robots over this space is then not feasible. Additionally, to allow drilling and other operations in aerospace manufacture requires large end effectors and tools, all of which are well above the payload capacity of any micro robot.

2.5 Scale of operation

The examples cited in section 2.2, with the exception of Van Duin [2001] focused generally on micro-components and operations. **The focus of this research is to examine the feasibility of developing a system to operate on aerospace components** (up to12 metres in length). A requirement for appropriate accuracy is needed to be maintained over these distances. Radically different approaches and measurement systems were required over such distances.

Larger scale industrial robots used for aerospace operations must then cater to large payloads and accurate movement over the range of the end effector. While micro-adjustments may be readily available for much smaller scale systems, aerospace robots require dedicated micro-positioning end effectors for accurate tool placement. Additionally, previously reported schemes can introduce mechanical and control instability into the system as the tool positioning trajectory is ill-defined. The parameters to be controlled associated with these robots must be attached to the part surface itself. A micro positioning end effector must be able to operate with great absolute accuracy and repeatability as required by the task and often beyond the specifications of the robot system itself.

2.6 Measurement systems

One of the major issues discussed previously is the scope of the measurement systems to be used to ensure accuracy in micro-positioning. Hohn and Robl [1999] employed standard industrial robots and CCD based vision systems with their micro-positioning system. The processes were again performed on micro-components and accuracy depended on the ability to identify points which could be measured against reference points within a small field of view. This was applicable realistically only to micro-devices, such as the wristwatch gear system cited and not to larger components manufactured for the aerospace industry.

Hefele and Brenner [2000] proposed that increased accuracy may be achieved by employing a photogrammetric system. These systems are frequently used in calibrating manufacturing equipment. This type of system does allow for highly accurate measurement over large areas – however equipment required is often expensive and not robust. Processing using photogrammetry is also problematic as it requires significant computing resources for image resolution and data processing and will not operate effectively in real time applications.

Another prospective method suited to measurement of robot position can be the use of laser trackers. Laser trackers are units that measure the reflection of a laser beam from a scanner head off a reflective tooling ball. The candidate contended that they are unsuitable for comprehensive manufacturing tasks as they are restricted to measuring a single location at a time, are difficult to commission for autonomous measurement and are very sensitive to disruptions in the measurement process.

These methods are further considered in Chapter 3.

2.7 Conclusion

The candidate has reviewed the current literature regarding to the use of measurement systems for automation purposes and deduced that there is a dearth of appropriate methods for control of large-scale, accurate robotic manufacture of aircraft components.

Further detailed review of measurement systems was required to identify prospective systems that may be feasible for this research. Identification of a single suitable method will be detailed later.

3 Chapter 3: Overview of Measurement systems

3.1 Introduction

This chapter will examine and nominate measurement systems available as options for the described manufacturing operations and identify potential candidates for use in this research. Furthermore, a single measurement system to be researched in this dissertation will be identified.

3.2 Measurement systems

A brief discussion was presented in Chapter 2 as an introduction to the state of available and suitable technologies for micro positioning and manufacturing of flexible structures. Central to the concept of micro-positioning for large scale manufacture is the presence of a highly accurate measurement system. This section identifies the most suitable methods for position measurement and feedback for the prospect of automating the scheme to produce positional feedback information for machining large, flexible structures. The following schemes will be described.

3.2.1 IPS

A Global Positioning System (GPS) is commonly employed for geographical location on earth. The systems comprise a number of satellites orbiting the planet, each emitting radio signals. A GPS unit (comprising of a handheld device) can be used with basic triangulation to determine absolute location with an accuracy of approximately 100 square metres normally or 10 square meters using advanced technology. Figure 3.2 demonstrates this concept.

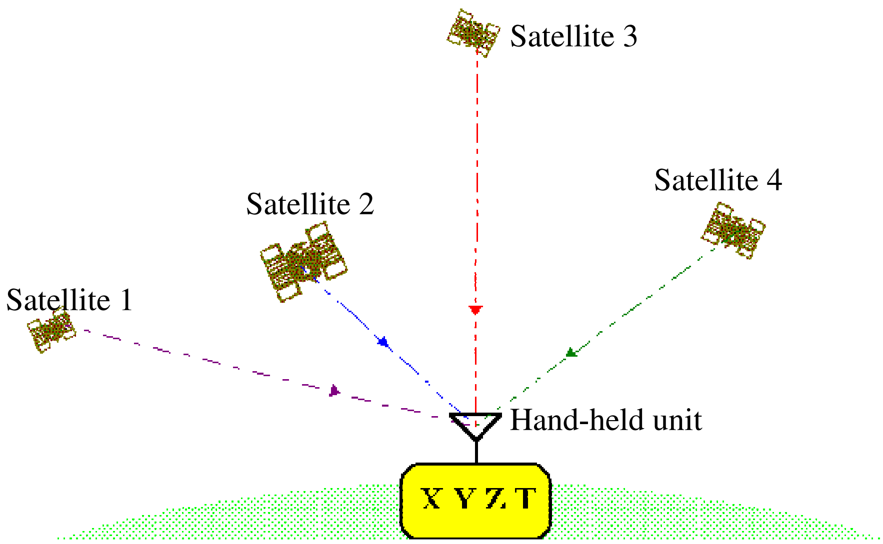

Figure 3.2 - GPS network

Using this principle, manufacturers of IPS equipment developed a system replacing satellites with locally-based, infra-red and laser transmitters and receivers with photoelectric diode receivers. Indoor Positioning System (IPS) is a recent addition available to metrology techniques. Comprising of a series of fixed transmitters producing laser and infra-red pulses at a steady rate, these pulses are recorded by a receiver placed within the measurement area. The resulting pulse timing data can be used to resolve position data into three dimensions.

The intent of this research was to develop a metrology system that could be used to improve automation tasks in manufacturing and be extended to include automotive assembly and autonomously guided vehicles.

The candidate recognised the importance of such equipment and identified the opportunity to extend research into the micro precision control of robotic arms and micro-positioning of end effectors.

Whilst this system is referred to as IPS it is important to note that other terms are frequently employed elsewhere such as Indoor GPS and IGPS. The key advantages of the IPS are:

1. Multiple measurements.

2. Data immediately available at measurement location.

3.2.2 Laser tracker

Laser trackers are new tools used in manufacturing and research for precise measurement. It comprises a laser head and target that is placed manually on or moved across the surface of an object. The system has been used successfully for recent manufacturing of flexible aerospace components, as discussed by Steele [2005] and Bonghetti [2005].

The key advantages of laser trackers are:

3. High measurement accuracy.

4. Readily placed and manipulated targets.

3.2.3 (Digital) Photogrammetry – optical measurement

Photogrammetry is the basis for many traditional optical metrology techniques, Atkinson [1997]. Photogrammetry relies on taking images of an object from a number of locations and comparing the orientation of measured points in each image to determine three dimensional location and data. This method allows multiple measurements to be performed simultaneously. It is however computationally expensive due to the mapping of pixels comprising images particularly if the image moves.

The chief benefits of photogrammetry are as follows:

5. Multiple simultaneous measurements.

6. Large range of equipment options.

3.2.4 CMM – touch probes, scanners

Many CMM's (coordinate measurement machines) are available for manufacturing tasks. These frequently require the object of measurement to be in a fixed location where traverse can be manually controlled. Examples include the touch probes and scanners available through Leica Geosystems (Leica Geosystems [2006]). Manual probe manipulation is common and automated accuracy can suffer. Therefore measurement using CMM equipment can be extremely restrictive.

3.2.5 Theodolites

Theodolites are part of a suite of surveying equipment, consisting of optical tools used to manually determine three dimensional locations. They can be employed in industry, where an example is the MANCAT system employed at Hawker de Havilland used for quality assurance purposes (Bonghetti [2005]). However use of theodolites is time consuming as they are manually operated, making automation difficult.

3.2.6 Laser distancemeters

Laser distancemeters are devices designed to give a uni-directional distance measurement using reflection of a laser unit. They operate on the "time of flight" principle. They are indiscriminate, in that they will not measure to a set target location and can be confused by measuring to the closest object that interrupts the beam. Constant, Mothe, Badia and Saint-Andre [2002] employed a laser distance meter in the measurement of a 1-axis robot arm employed to measure standing tree shapes. They demonstrated that it is possible to use this technology to measure robot position albeit in a limited function.

The method is not feasible where the measurement locations are mobile due to the prospect of beam interruption. A means of identifying a possible end effector position using distancemeters has been discussed by Van Duin [2006], but has so far proven difficult to develop.

3.3 Measurement system characteristics

The following table indicates important characteristics of the measurement system required for this research. These five characteristics must be used to determine the effectiveness of any measurement system to be employed, as described below in Table 3.1.

Table 3.1 - Measurement system characteristics

	Characteristic
1	Accuracy of the system. The accuracy of measurement is the basic definition of the quality of a measurement system. The standard description of accuracy is the distance between the actual and measured values for a position. Accuracy is required below 0.1mm. It is impossible to describe this when the actual location may be unknown, therefore as a standard accuracy usually described as twice the standard deviation of a series of measured values, according to Steele [2005]. .
2	Time to measurement acquisition. The development of precision data is usually achieved by taking a large number of measurements, as a result the time taken to achieve measurement is an important quantity. Measurement must be rapid, of the order of less than 2 seconds to achieve automation tasks.
3	Number of concurrent measurements. Analysis of position and posture of end effectors requires multiple measurements, including the workpiece and other items in the work area. Where only a single measurement is required, this will require movement of the target between measurements, therefore a number of concurrent measurements is an important consideration for automation processes.
4	Portability of operation. Is the system portable, or is a dedicated fixture required?
5	Setup time of system between tasks.

3.4 Laser tracker

The laser tracker is a measurement tool that is often used as an industry standard throughout the world, as discussed by Clarke, Wang, Forbes and Cross [2000]. Its exceptional accuracy and simple operation have made this an appropriate choice for many different manufacturing and research operations.

The laser tracker itself consists of a single unit, with a laser head that measures vertical and azimuth angles of the laser target, coupled with a distance measurement of the beam. The beam itself is reflected by the target, usually consisting of a reflective ball. Depicted in Figure 3.3.

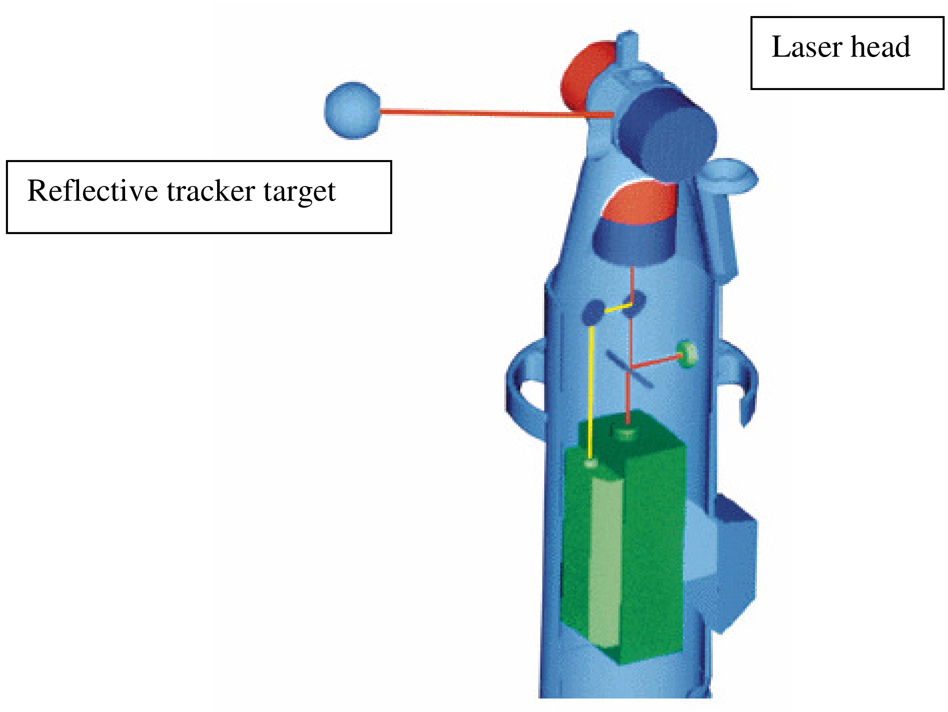

Figure 3.3 - Laser tracker unit and target details

(Kyle, Loser and Warren [1997])

3.4.1 Accuracy

Kyle, Loser and Warren [1997] describe the achievable accuracy of a laser tracker to be as low as 30-50 microns (μm). However the new Leica laser tracker operates with an accuracy of 15 microns (μm) according to Leica Geosystems [2006]. This was confirmed by Steele [2006] and Bonghetti [2006] who demonstrated additionally that the error of the Leica system increased by at least 10 microns for each metre distant from the laser tracker head.

3.4.2 Operation

As the laser tracker itself relies on the reflection of a laser beam by a target, it is sensitive to interruption of the beam. Should the beams be interrupted it is necessary to re-calibrate measurement of the part. This can be problematic due to the environment, particularly where multiple objects operate in the same space and where a key element (head or ball) is mobile.

Additionally, as the laser tracker relies on measurement of the laser head posture, it is not capable of measuring more than a single point at any given time. Where several points are required each must be measured individually by the operator, and the part must remain stationary throughout the measurement period. This causes difficulty as measurement of multiple targets by necessity requires intervention of an operator to change and re-calibrate targets, increasing system down time and increasing the risk of measurement error due to movement between measurements. During testing performed in association with this research the candidate found that taking measurements of points may take up to ten minutes to achieve effectively.

Table 3.2 - Laser tracker characteristics

	Characteristic	Rating
1	Accuracy to within 15 microns with a skilled operator.	Excellent
2	Time taken for individual measurements is negligible, however to achieve high accuracy batches of 100 measurements are taken, usually achieved in under 1 second.	Excellent
3	Single point measurement.	Poor
4	The system requires a dedicated computer and operator, data is commonly taken physically from this system via disk for further use. This increases time for any measurement, however may be improved with system or fixture design.	Poor
5	The system is readily moved and requires little setup time as the measurement component consists of a single unit.	Excellent

3.5 Photogrammetry

Photogrammetry uses two or more cameras placed on, or surrounding an object, with measurements taken from each image to determine three dimensional data.

Traditional photogrammetry, according to Atkinson [1996], involves the use of film-based cameras. This has been largely replaced by digital media allowing images to be available immediately for the purposes of measurement. For the purposes of this dissertation, only digital photogrammetry will be considered.

Photogrammetry relies usually on taking measurement of either flat-colour or retro-reflective targets. As data is derived from images, multiple measurements are available from previously recorded images. Measurements taken at the camera location cannot be assembled and interpreted readily, requiring large computing resources for point mapping between images. As described by Atkinson [1997] photogrammetry is not a feasible option where real-time measurements are required. Although there has been some development into “videogrammetry”, Burner and Liu [2001] suggest this equates to analysis of video footage after the recording, and therefore is quite incapable of real-time measurement.

Automated systems have become available for photogrammetric techniques, such as the V-STARS system employed by VMS (Vision Metrology Systems). This system utilises precision metrology equipment that is capable of acquiring measurement data in seconds. This equipment is however extremely expensive, with each unit in excess of US$100,000. (Geodetic Services Inc. [2006])

3.5.1 Accuracy

Geodetic Services Inc. (Geodetic Services Inc. [2006]) describes that the maximum accuracy for the V-STARS system is however 1:60,000 – which corresponds to an accuracy of 0.33 microns over a 20 metre (maximum dimension) large object. This accuracy is dependant heavily on the skill of the operator and environmental factors.

3.5.2 Operation

Although there are a great number of different photogrammetric systems available, they rely on similar techniques. Whilst high quality photogrammetric systems use calibration to ensure that the image taken is as accurate as possible, “low end” systems adjust identified points on a measured surface to cope with irregularities in the optics and measurement surfaces of camera equipment. (An example of this is the calibration scheme employed by PhotoModeler Pro software, as described by Eos systems Inc [2000].)

Table 3.3 - Photogrammetry characteristics

	Characteristic	Rating
1	With high-quality equipment, setup accuracy may be below 1 micron.	Excellent
2	Using advanced systems measurements may be acquired rapidly (Under 1 second) however these systems are cost prohibitive. Most methods will require large periods of time for data to be available.	Poor
3	No restriction on concurrent measurements.	Excellent
4	Data is acquired at steady points, and image acquisition data is computationally expensive. Systems need to be kept separate from the working and processing areas.	Poor
5	Capable of surveys using highly mobile equipment, following calibration performed setup time is reduced to very little.	Excellent

3.6 IPS

IPS (Indoor Positioning System) is a system that relies on a series of base stations (transmitters) located about a working area. These transmitters emit laser and infra-red pulses at regular intervals, which are recorded by receivers within the working area and are then used to calculate receiver positions. This arrangement is demonstrated below in Figure 3.4.

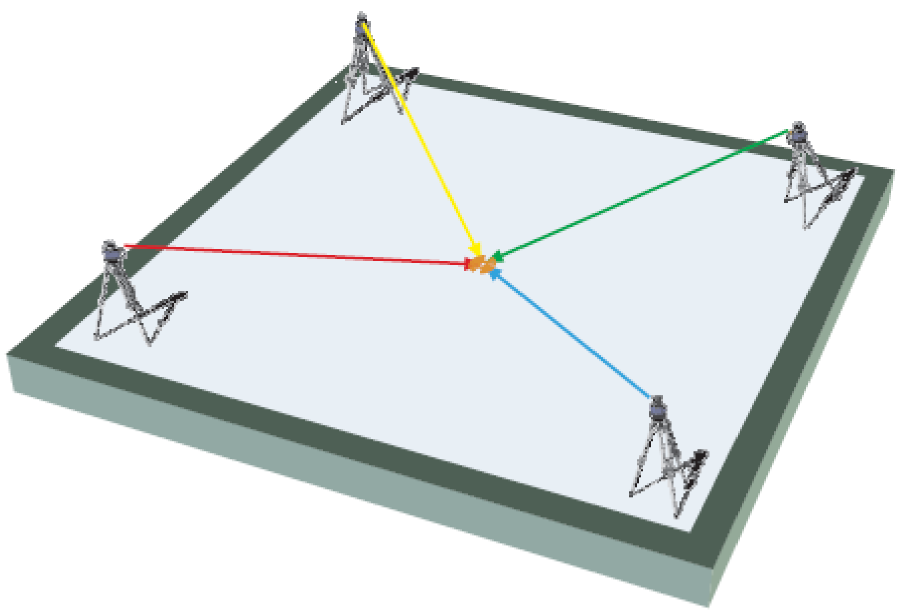

Figure 3.4 - IPS operation

(ArcSecond Inc [2003])

3.6.1 Accuracy

The accuracy quoted for the Indoor GPS equipment is 0.37mm, described as 3 times the uncertainty – or the error registered in 99% of all measurements, according to ArcSecond Inc. [2002]. Further study by the candidate has demonstrated that a measurement accuracy of 0.1mm is achievable over the working area of the IPS, a total of 35 meters square. This is discussed further in Appendix B.

3.6.2 Operation

The operation of the IPS is based on rapid analysis of laser and infra-red pulse timing data from several transmitter base stations. As the signals recorded from each base station consists of timed pulses of laser and infra-red light from the transmitters there may be as many concurrent measurements as receivers available. Blocking transmission does reduce system accuracy but it does not prevent measurement. Successive measurements can be used to restore measurement quality immediately, hence the system is resistant to interruptions in the working area. The IPS is a difficult system to prepare initially however once set up, measurement can be taken continuously and data is available readily. As a result, aside from initial setup and calibration there is virtually no need for operator intervention during operation. Finally, the data can be made available readily to measurement software and applications making use of simple languages such as Visual Basic for programming purposes.

Table 3.4 - IPS characteristics

	Characteristic	Rating
1	Accuracy to below 0.1mm with skilled setup and calibration	Good
2	Time taken for individual measurements is approximately 0.1 second; however to achieve high accuracy large numbers of measurements are needed. This will commonly take up to 10 seconds, however it is readily varied by the operator.	Good
3	Number of measurements only limited by available receivers.	Excellent
4	The system is operated independently by any terminal with access to USB ports and receivers, and may therefore be readily accessed by any terminal including those dedicated to the tasks. As a result this may be integrated into most processes.	Excellent
5	The system consists of several independent components which may be readily moved and installed, however movement of the system required fresh setup and calibration procedures.	Good

3.7 Choice of measurement system

3.7.1 Key indicators for assessment of measurement systems

Table 3.5 - Measurement technique comparison

Characteristic	Laser tracker	Photogrammetry	IPS
1	Laser tracker accuracy may be as high as 15 microns when employed by a skilled operator.	Accuracy varies with the size of measurement taken; however may reach micron level accuracy. Advanced systems may produce measurements superior to 1 micron accuracy.	Described as "sub millimetre accuracy" however through testing achievable accuracy of below 0.1mm may be achieved.
2	Measurement speed of approximately 100Hz, with precision measurement at approximately 1Hz	Time dependant on system employed, may be as low as 1Hz for advanced systems.	Measurement speed of approximately 10Hz, precision measurements may be set from 2Hz and higher.
3	Only one measurement at any given time.	Number of measurements not restricted.	Number of concurrent measurements only restricted by available hardware.
4	Tracker requires dedicated terminal, and interface software for all equipment.	Analysis is computationally expensive, frequently requiring dedicated terminals for advanced systems.	Measurement may be performed in parallel with operations, thus dedicated terminal is not required.
5	Rapid setup of single unit.	Requires movement and setup of multiple sets of photographic equipment.	Requires setup and calibration of transmitters and access to receivers.

From the above table it can be demonstrated that the most problematic areas are the rapidity of measurement coupled with cost of the system in the case of photogrammetry, and the restriction to measurement of a single point in the case of a laser tracker.

On the basis of the investigation, the candidate has chosen to nominate the IPS system to investigate the issue of providing feedback to position an end effector accurately at the end of a robot.

3.8 Conclusion

An overview was conducted of suitable measurement systems and focus was placed on the IPS scheme. This method of measurement can readily be established within a work area offering robust measurements and readily available data.

Laser trackers, IPS and photogrammetry were also reviewed, and although both laser trackers and photogrammetry are able to achieve superior accuracy to the IPS, they are limited by the number of concurrent measurements that can be made. Computational effort is also high. Future development will be based on the IPS to provide numerical feedback where required to a robot system.

4 Chapter 4: Industry participation

4.1 Introduction

This chapter outlines the participation through the industrial partner, Hawker de Havilland (HdH) throughout the process of this research. A series of research questions are presented as a means of developing a set of Key attributes for the assessment of a micro-positioning system employed using IPS.

4.2 Project background

The candidate undertook to perform research on behalf on the CRC-IMST where HdH was a contributor. The firm HdH identified a need to pursue a means of controlling a machine tool to drill large flexible structures to a high degree of accuracy. The candidate researched suitable means of achieving these objectives which led to the investigations reported in this thesis.

The candidate was offered access to production facilities within HdH as well as assistance with familiarisation of the system and programming. As a consequence of association with the CRC, this led to knowledge of the current means of robotic control, procedures within the industry and further knowledge of techniques under research. The candidate was funded to visit Boeing facilities in Seattle as part of this project. At the time of writing HdH relied largely on using basic teach pendant and physical markers on the workpiece for end effector location. Laser tracker measurements have also been used by the candidate to compare some drilling and trimming trials. Such tracker measurements were found to be time consuming and required the presence of a skilled tracker operator throughout the process. Additionally the tracker did not allow the opportunity for measurement of multiple locations simultaneously and therefore was unable to offer real-time identification of the end effector position and posture with respect to the workpiece. The advent of IPS allows this measurement to be made, allowing for more rapid identification, correction and micro-positioning. Nevertheless laser tracker measurements were used as a datum against which to compare IPS data where nominated.

4.3 Research objectives and Outcomes

4.3.1 Research questions

The following questions were the basis of work performed throughout this research.

i. How may a TCP (Tool Centre Point) be located in an absolute frame of reference?

ii. How may key points on a workpiece be adequately located absolutely and transmitted to a central processor?

iii. How may a system be instituted to modify robot controls to cater to flexibility in both robot and workpiece?

iv. How may a point be located absolutely and have a scheme in place to drive the end effector to reach the desired location of a workpiece?

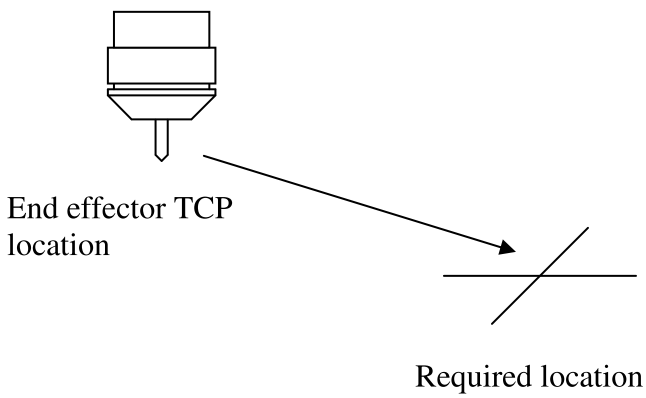

Figure 4.5 - Desired movement of an End Effector TCP

v. How may a point be located absolutely and a robot reach the location of a *large* workpiece supported in a jig using the same method?

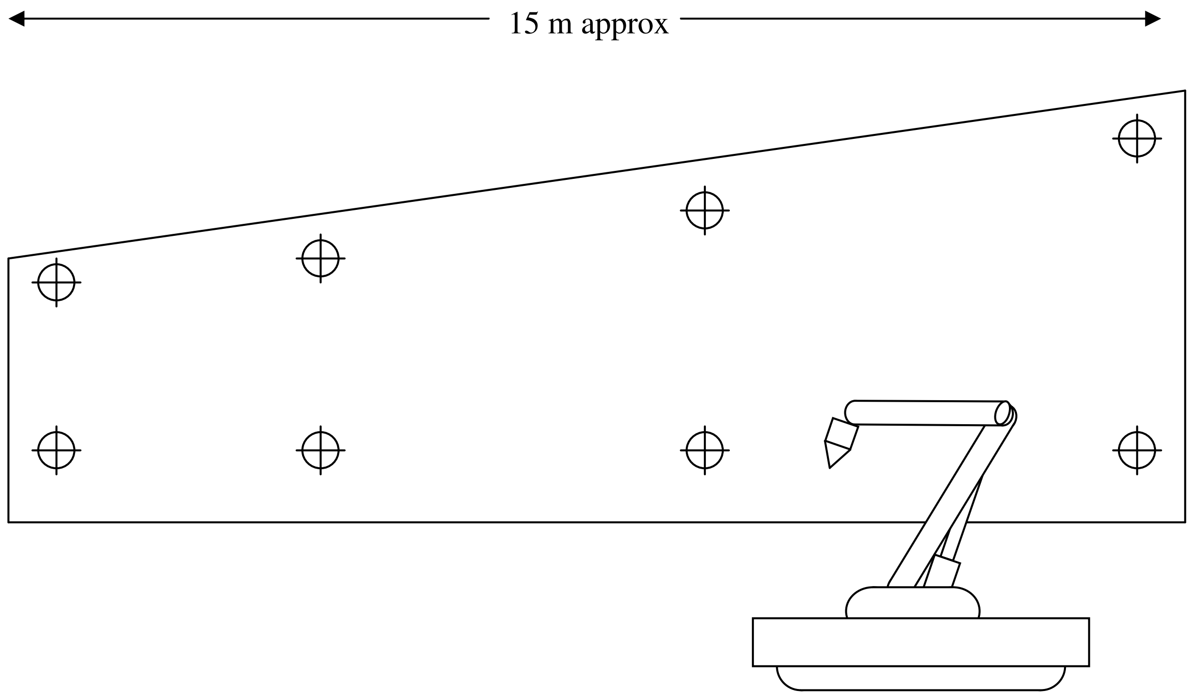

Figure 4.6 - Example of mobile robot working on a large component (wing section)

vi. How can the above system be made dynamic to cope with moving workpieces in an assembly line situation?

4.3.2 Key attributes

The questions above dictate a path toward improving manufacturing techniques with the aid of sophisticated measurement and data acquisition systems. These questions additionally set the requirements for a series of attributes that a system developed as part of this research must achieve. The key attributes of this system are described in Table 4.6.

Table 4.6 - Key attributes

Key	Attribute
1	System must be able to identify objects rapidly, including, but not restricted to, robotic tools, and workpieces.
2	Measurement and control of systems must be capable using a minimum of workstations.
3	Must be capable of micro-measurement, and micro-positioning of both end effectors and *large* workpieces to an accuracy of less than 0.1mm.
4	Must be capable of taking measurement in under 2 seconds.
5	System must be capable of measuring and deploying multiple robots simultaneously, along with workpieces and additional requirements.
6	System must be capable of adjusting tool centre point locations to allow for workpiece movement during the operation.
7	Equipment must be readily portable and robust.
8	The system should be applicable to a number of different industries with minimal variation to the initial components.

4.3.3 Project outcomes - deliverables

4.3.3.1 Robotic drilling data

The primary outcome of this research is to produce data that demonstrates the applicability of advanced control techniques for manufacturing operations. This will take the form of drilling procedures, such as have been completed previously through research with the CRC-IMST and Hawker de Havilland. (Van Duin [2001])

This data should include details on the effects of a flexible environment, ensuring that a system developed in a such a way is not only capable of rapid alteration of process, it is also capable of identifying and dealing with unexpected movement of either the workpiece and/or the end effector.

4.3.3.2 Data feedback methodology

A further deliverable is a methodology for employing the data provided by the above section, and ensuring that it may be employed by the process to ensure the quality of the process. This methodology is in a very basic form demonstrated by the feedback loop below in Figure 4.7.

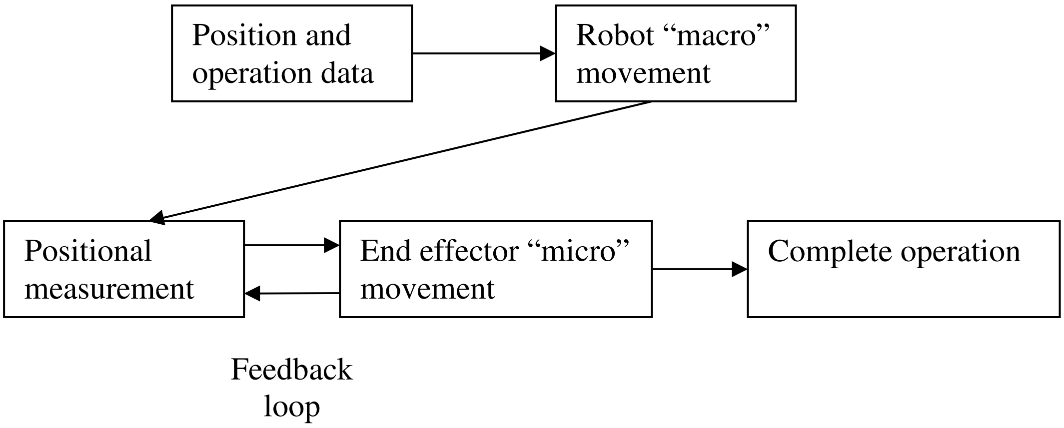

Figure 4.7- Data feedback philosophy

4.3.3.3 Software for employing feedback

The developed system for coping with data and feedback on position should then be used to produce software to easily identify part and tool locations, with data reflecting required movement of all components.

4.3.4 Conceptual design of robotic tools

The deliverables above are to be developed with the intention of comparing these to current technology for systems that fit broadly into two categories.

4.3.4.1 Mobile platform

The feedback system must be capable of identifying the process as applied to a mobile robot, specifically ensuring that the robotic platform is able to be placed randomly and the system will identify movement of the robotic arm and end effector to complete operations. The mobile robotic platform used for testing during this research was the mobile robotic platform developed by HdH (Hawker de Havilland) and UoW (University of Wollongong), as demonstrated in Figure 4.8.

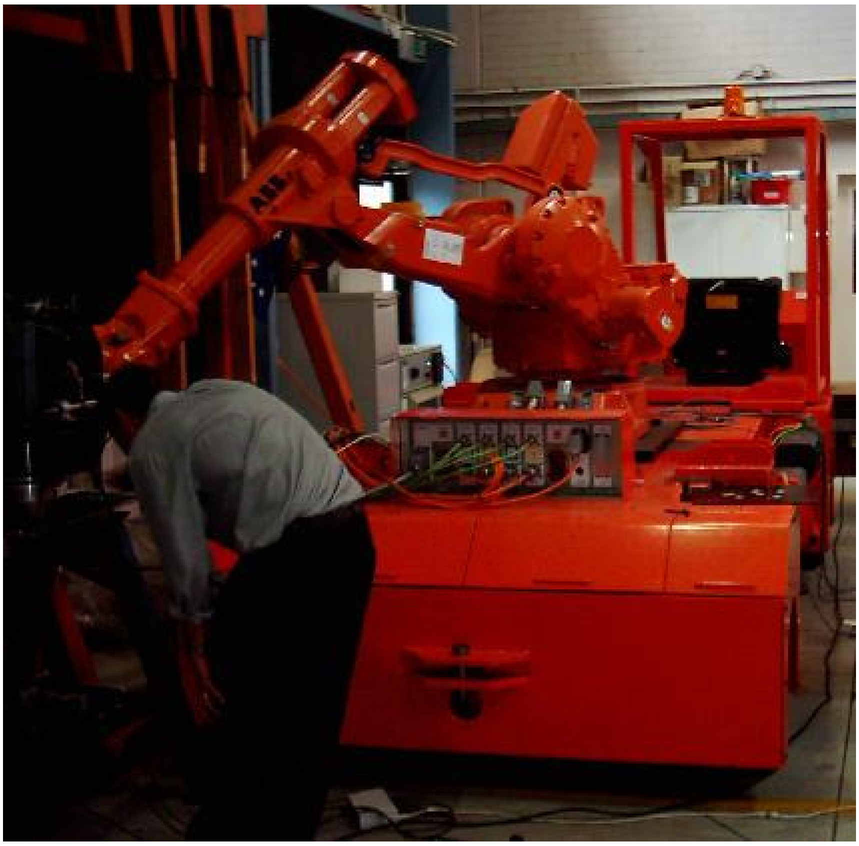

Figure 4.8 - Mobile robotic platform

This platform consists of an IRB 6400 robotic arm, and a custom designed mobile platform and end effector, discussed later in this dissertation.

4.3.4.2 Mobile assembly line process

Although demonstrating this concept physically is beyond the capabilities of the research, the work offers indications of how such automated systems can be used on moving assembly line.

4.4 Conclusion

The chapter has outlined the interaction of the candidate with industry and identified key research questions associated with the research. A Table of Characteristics was presented listing Key attributes of the selected measurement system. These Key attributes were used as a means of assessing the outcomes of this research.

5 Chapter 5: Outline of testing procedures used in this research

This chapter provides a brief but concise outline of the various tests proposed and conducted by the candidate to effect the project outcomes.

The first phase (Phase 1) of testing was aimed at identifying the characteristics of an IPS system. This included identifying absolute levels of accuracy afforded, the time to sample a location and the quality of that sample. This work is described in Chapter 6.

The second phase (Phase 2) of testing involved comparing the accuracy afforded by an IPS in relationship to a laser tracker. Whilst the laser tracker was used as a basis for demonstrating accuracy of IPS positional measurement is was noted that the laser tracker was grossly inhibited by it's inability to be used in the context of this research because of it's inflexibility. This work is described in Chapter 7.

The third phase (Phase 3) of testing was performed to demonstrate how the IPS data could be used to effect micro-positioning control of a robot end effector during a drilling operation. In these tests both workpiece and robot move relative to each other in a dynamic environment. These tests exposed issues of practical importance needed to devise a system for operating in a real manufacturing environment. This work is described in Chapter 8.

6 Chapter 6: Testing Phase 1 – Initial testing and commissioning of IPS

6.1 Introduction

This chapter presents and discusses the initial phase of testing. Chapters 3 and 4 have identified why the IPS scheme was the most suited to the tasks of precision drilling of flexible components. A pre-release version of an IPS system was purchased for evaluation and testing. There was a dearth of information on its use, operation and effectiveness. Phase 1 testing was aimed at commissioning the system and identifying characteristics of performance of the IPS, it's operational accuracies including time to sample and the quality of sampling in accordance with the criteria established in Chapter 3.

6.2 Details

6.2.1 Setup and operation of system

Details for the setup and operation of the system remain consistent throughout this research. To reduce repetition within this dissertation, the IPS process and suitable configurations for transmitter locations are presented in Appendix B. Improvements to the technique have been developed during this research and will be identified where appropriate. Specific setup procedures individual to each section will be discussed.

6.2.2 Outline of Phase 1 testing

Phase one testing consisted of many separate tests, where the key tests are listed as follows:

- Test One – System operation
- Test Two – Area measurement
- Test Three – Precision point accuracy
- Test Four – Movement
- Test Five – Drift measurement

6.3 Test one – System operation

At the outset of this research equipment supplied was inoperable, with paltry levels of information dealing with the setup and use of the system. The aim of Test 1 was to ensure that the IPS equipment was (a) operating and (b) capable of measurement. The accuracy of the system was not yet under investigation.

6.3.1 Setup

Appendix B is a thorough description of the procedure used by the candidate in the described tests. The arrangement of the system was not critical for this test, therefore testing was performed on a table within the cell's working area. The setup as is demonstrated in Figure 6.9 was established by the candidate for the purpose of commissioning the IPS.

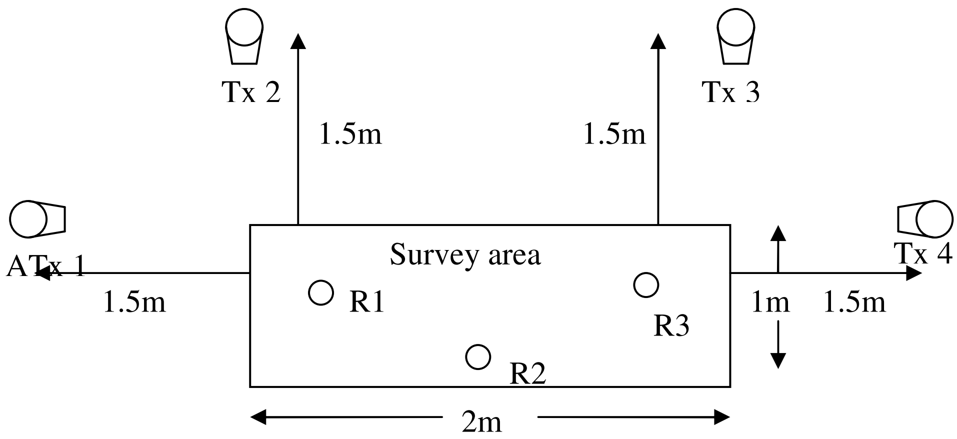

Figure 6.9 - Test 1 arrangement

ATx1 to Tx4 are transmitters, R1-3 are reciever locations. These were not specified locations as they were to move during measurement.

6.3.2 Method

Test One was specifically aimed at demonstrating whether the equipment was capable of making measurements. Therefore the methodology was limited to the following:

1. Set up transmitters as shown in Figure 6.9.

2. Set up 1 receiver, as described in Appendix B.

3. Effect calibration procedure, as described in Appendix B.

4. Identify operation, record data and M-values. (Defined in Appendix B.)

6.3.3 Results

Results for Test 1 are as described in Table 6.7.

Table 6.7 - part 1 results

Day	Pass or fail?	Detail
1 – 2 Nov 2004	Fail	Non-convergence*
2 – 3 Nov 2004	Fail	Non-convergence*
3 – 18 Nov 2004	Fail	Non-convergence*
4 – 24 Nov 2004	Fail	Non-convergence*
5 – 3 Dec 2004	Pass	Erratic measurement**
*Non-convergence. System failed to initialize, specific cause impossible to determine, most likely being insufficient ray convergence in bundle adjustment procedure. See Appendix B for details. **Erratic measurement. System initialized and calibration was successful, however visual inspection of measurement identified that this was highly erroneous.		

The final testing performed on day 5 resulted in the data presented in Table 6.8.

Table 6.8 - Data for successful measurement

Configuration	Square
Maximum dimension	2m
M-value	25mm
Estimated error of final target point	20mm

The value used for assessment was the "M-value" (metric value). This is described as the maximum distance between the measured location and an intersection "ray". This concept is described more fully in Appendix B.

6.3.4 Conclusions

The error of this measurement, at 20mm representing 1% of the maximum dimension, was judged to be **far too high** for the requirements set in Chapter 4.

The small area for measurement additionally led to high error due to proximity with the transmitters, therefore the measurement demonstrated was highly unstable, with large variations of measured position and little correlation with movement of the receivers.

6.3.5 Recommendations

- Accuracy must be improved – setup areas need to allow sufficient distance from transmitters. (Minimum of 2 metres was suggested by the manufacturer.)

- Use of metric value appears too simplistic to quantify the complexities of error now envisaged, and a further identifier must be developed.

- Measurement must be shown for the measurement of moving receivers.

- Need to show movement of measured location over time. (Drift).

6.4 Test Two – Area measurement

As IPS relies heavily on triangulation it is evident that measurement accuracy will be heavily dependant on the geometry of the measured location and stations from where measurement is taken. Suitable configurations of transmitters are described in Appendix B.

Test 2 is aimed at measurement taken over a working area where the working area was set to the size of a robotic cell, with approximately 10 metre square working space. Due to the presence of obstructions as shown in Figure 6.10 a regular pattern of measurement was not possible.

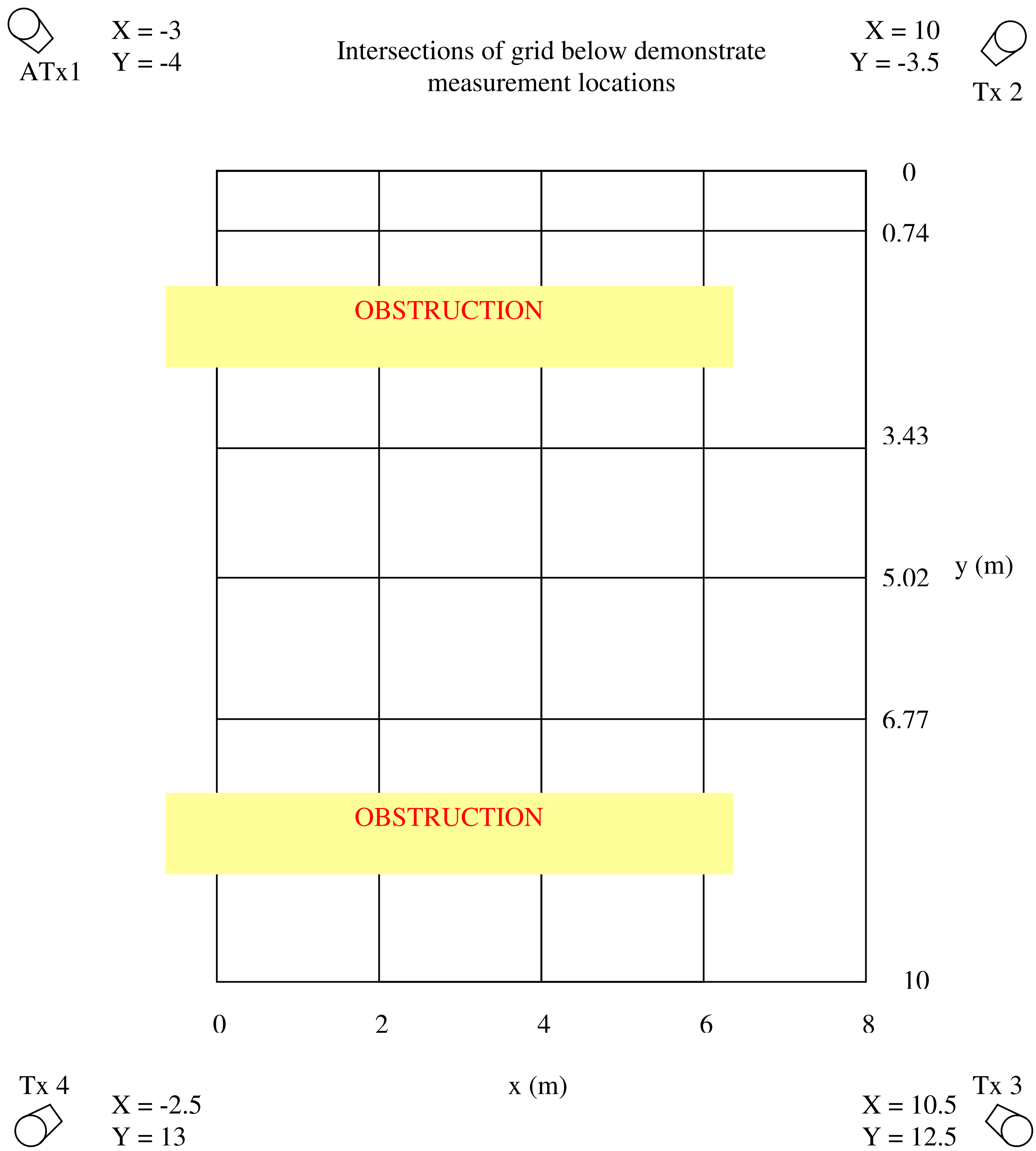

Figure 6.10 - Area testing layout and configuration

6.4.1 Error calculation

Test 1 described in Section 6.3 demonstrated a need for a more suitable measure of error. To deal with this, the use of a standard measure of 90th percentile error is employed. (Error being twice the standard deviation of a large number of measurements, as shown in Equation 6.1). Thus, a large number of data points was required to give an indication of error and hence a larger measurement time, or a previous estimation of error in the measurement volume must be made.

$$Error = 2\sigma \qquad \text{Equation 6.1}$$

6.4.2 Precision point data

An improvement available at the time of Test 2 was to use the "Precision Point" function described in Appendix B. This function takes a number of data points set by the operator, using analysis of the data to provide a single precise measurement. This has been employed in the following sections, and details of this are provided where appropriate.

6.4.3 Setup

The setup procedure is detailed in Appendix B. The arrangement for this measurement is an exaggerated square configuration, as depicted in Figure 6.10. This arrangement was required due to obstructions in the testing area.

6.4.4 Method

The methodology for test two was as follows:

1. Set up transmitters as shown in Appendix. B.

2. Set up 1 receiver, as described in Appendix B.

3. Calibrate system as described in Appendix B, ensure accurate measurement by analysis of a specific data point.

4. Place receiver in first location, represented by intersection in Figure 6.10.

5. Record data for later analysis.

6. Repeat for each location in Figure 6.10.

7. Determine position and error for each location from recorded data and separate measurements by different levels of precision point data.

This process was completed in an established location where several days were available to ensure the optimum operation of the IPS.

6.4.5 Expected results

As this testing was based on the use of triangulation principles, due to this it was expected that locations with the highest intersection angles between rays from transmitters to receivers will have the lowest error. (This concept was described in Appendix B.) This suggested that the measurements taken in the centre of the working area result in the lowest error.

The use of precision point data is also expected to reduce error.

6.4.6 Results

Error was calculated based on precision point method described in Section 6.4.2. Subsequently the following error maps were generated. The following Figure 6.11 through Figure 6.15 demonstrate the error of measurements taken over the working area described in Figure 6.10 and specified in Section 6.4.4 where the receiver was placed in 30 separate locations within the range x = 0m to x = 8m and y = 0m to y = 10m. Numerical data is included in Appendix C.

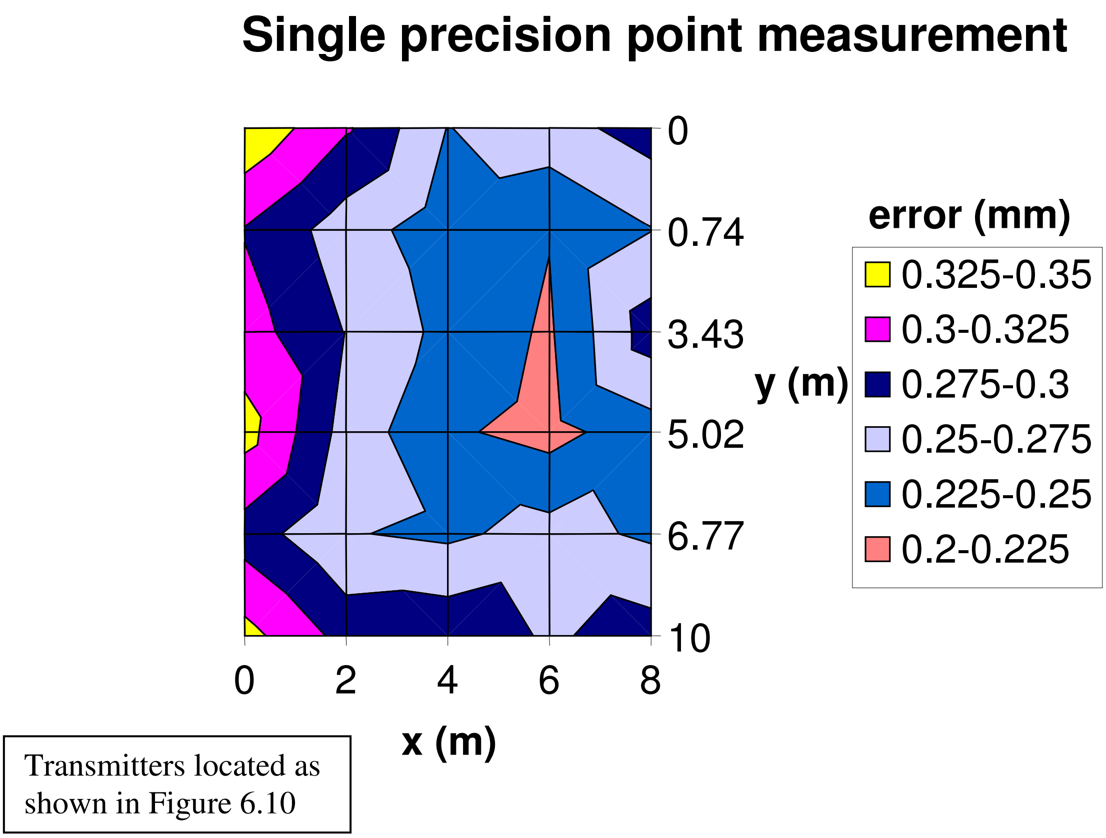

Figure 6.11 - 1 sample measurement

The candidate noted that large errors occurred when in close proximity to transmitters (Txi). The geometry caused poor error resolution due to steep ray angles close to transmitters. This was accounted for in setup of further experimentation. The lowest error is between 0.2 and 0.225mm within an area at approximately x = 6m, and 0.7m< y < 5m. This high variation should be characteristic of low precision point sample sizes.

This test also demonstrates that locations with higher intersection angles towards the centre of the measurement area will produce the lowest error.

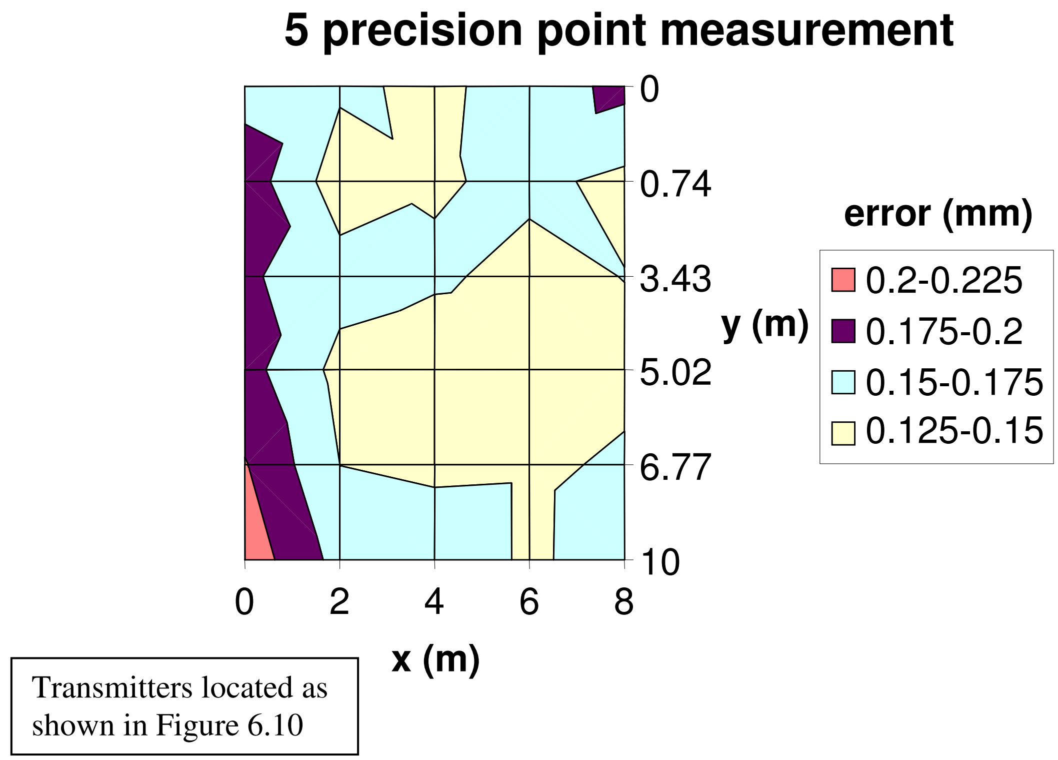

Figure 6.12 - 5 sample measurement

The candidate next investigated 5 precision point data measurement to reduce the recordable error. Figure 6.12 now demonstrates the lowest error occurred in a similar band, with an improvement of 47% over the region 4m<x<6m, and y = 5m. This demonstrates a significantly lower error than the previous measurements, due to the increase in Precision point data. The lowest error recorded is in the range 0.125-0.15mm.

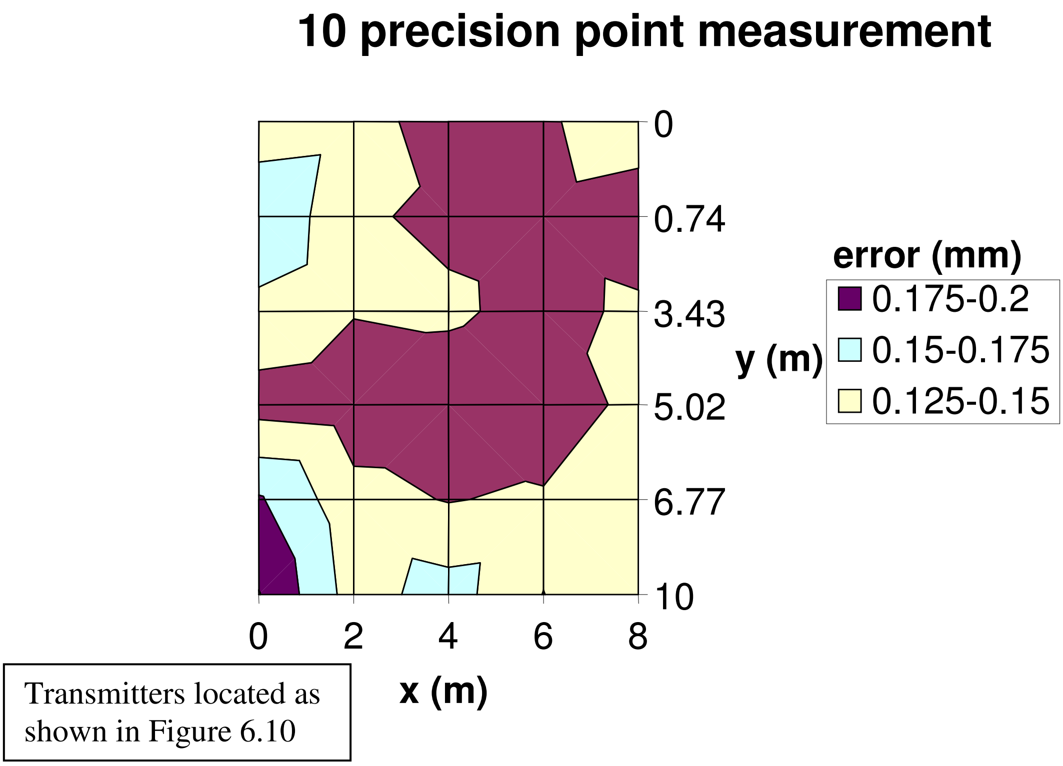

Figure 6.13 - 10 sample measurement

The test was repeated for 10 Precision point data. Figure 6.13 shows again this improvement at y = 5m, and improvement in overall measurement error. The lowest error recorded is within 0.1-0.125mm, a 50% improvement on single precision point measurement. The region of lowest error is again central to the measurement area, with lower error along edges away from the transmitter locations. This is expected as these locations also provide excellent geometry.

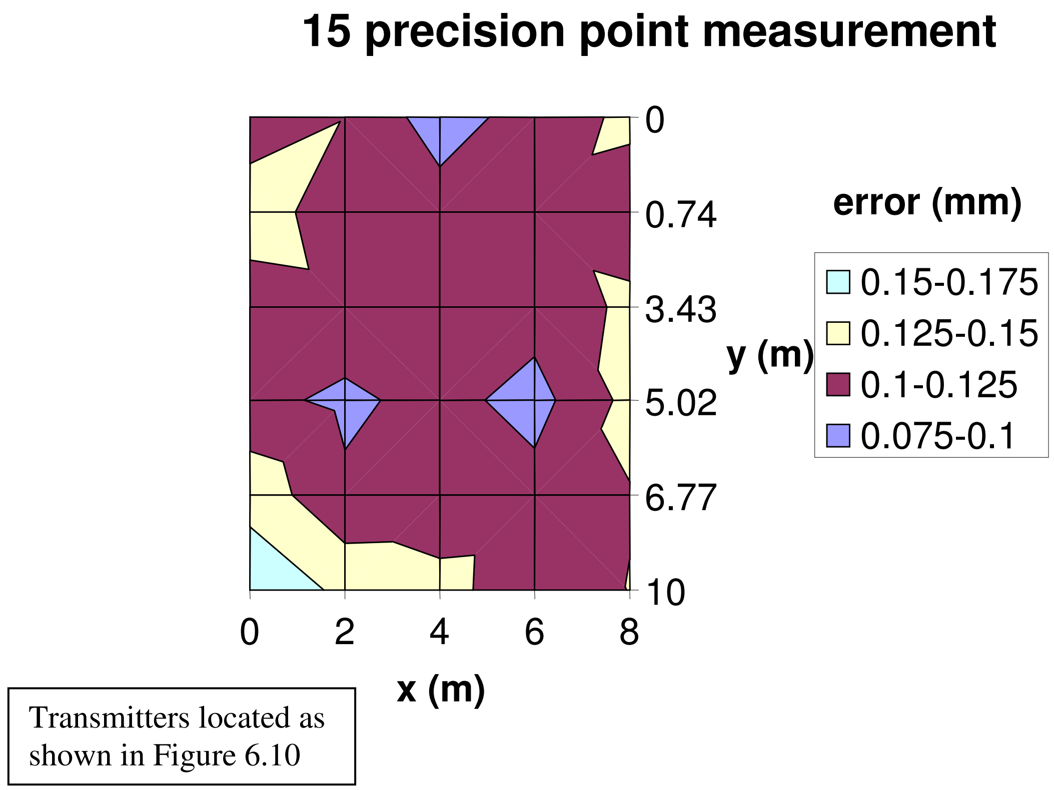

Figure 6.14 - 15 sample measurement

The test was repeated for 15 precision point data. Figure 6.14 shows again this improvement at y = 5m. At this point there is a distinct band of high accuracy, with points at x = 2 and 6m. The lowest error recorded is within 0.075-0.1mm, an improvement of 73% on single precision point data.

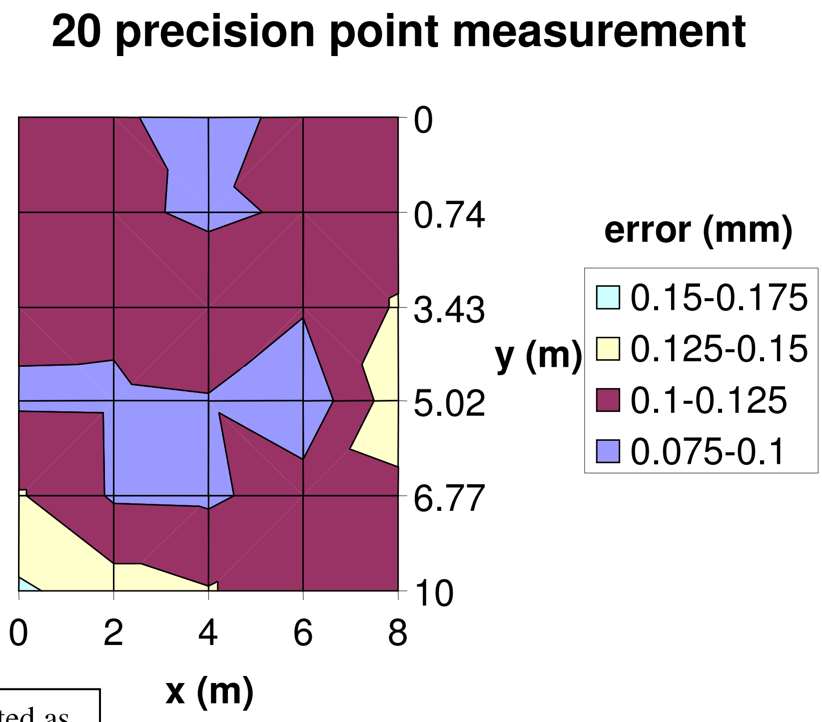

Transmitters located as shown in Figure 6.10

Figure 6.15 - 20 sample measurement

Figure 6.15 again demonstrates the characteristic band of high accuracy at y = 5m, with a minimum error in the region 0.075-0.1mm, with only a marginal improvement over 15 precision point data.

The above figures demonstrate a distinct tendency towards lower error in a band at approximately y = 5m, and x = 6m. The lowest error recorded is within 0.075-0.1mm. These correspond to an area in the centre of the measurement area, with higher intersection angles. The increase in Precision Point data reduces the error, and the time to sample.

Table 6.9 – Variation of recorded error with increasing precision point

Precision point	Improvement	Error band	Time per sample
1	NA	0.2-0.225mm	0.05 seconds
5	47%	0.125-0.15mm	0.25 seconds
10	50%	0.1-0.125mm	0.5 seconds
15	73%	0.075-0.1mm	0.75 seconds
20	73%	0.075-0.1 mm	1 second

6.4.7 Conclusions

- In the square configuration this experimentation has demonstrated that the system is capable of recording an error of between 0.075mm and 0.1mm, this is within the specifications set in Chapter 4.

- The above diagrams demonstrate that a distinct improvement will be gained towards the centre of the measurement area. This agrees with the theoretical concepts of triangulation, and manufacturer suggestions of arrangement of the IPS. The higher error demonstrated towards the transmitters themselves also demonstrates the interference due to proximity with the transmitters and poor geometry of the location.

- The improvement of measurement at the centre of the area is in agreement with the concept that intersection angles that intersect at as close to 90 degrees as possible will afford the lowest error.

- As suggested, using the "Precision Point" data to make calculations with larger sample sizes dramatically improved the results. Further experimentation is required to demonstrate this improvement and determine a suggested number of points for measurement. The minimum error recorded varied from 0.225mm down to 0.075mm.

6.4.8 Recommendations

- Further experimentation should investigate the improvements to be gained from increasing the precision point data.

- Locations requiring highest measurement accuracy should be placed central to measurement areas, with intersection angles as close to 90 degrees as possible.

6.5 Test 3 – Precision Point data

Section 6.4 identified the need for further evaluation of the use of Precision Point data, which is the focus of Test 3. This testing aims to vary the number of data points employed for Precision Point data from 1 to 100 points, and allow an assessment of the accuracy improvement compared to time taken for each individual measurement. The aim of this is to identify the highest accuracy return on measurement time.

6.5.1 Setup

The setup for Test 3 is identical to that for Test 2, as described in 6.4.3.

6.5.2 Method

The methodology for test three was as follows:

1. Set up transmitters as shown in Figure 6.10.
2. Set up 1 receiver, as described in Appendix B.
3. Calibrate system as described in Appendix B, ensure accurate measurement by analysis of a specific data point.
4. Place receiver in a central location.
5. Record data for later analysis.
6. Determine position and error for each different level of precision point data.

6.5.3 Results

Table 6.10 demonstrates the effect of Precision Point as a percentage improvement on measurements.

Table 6.10 – Reduction in error with multiple precision point data

Samples taken	Sampling rate (Hz)	X	Y	Z	Relative accuracy to single point measurement	Error (mm)
1	10	100.00%	100.00%	100.00%	100.00%	0.385928
5	2	56.35%	55.49%	46.35%	55.64%	0.21466
10	1	44.91%	44.25%	35.64%	44.35%	0.17463
15	0.666667	40.01%	39.52%	31.37%	39.67%	0.15574
20	0.5	34.94%	35.55%	28.15%	35.17%	0.136772
30	0.333333	36.08%	35.09%	27.66%	35.61%	0.138689
40	0.25	27.83%	26.28%	22.26%	**27.21%**	0.104249
50	0.2	24.25%	23.34%	20.91%	23.91%	0.091135
60	0.166667	22.03%	21.47%	19.31%	22.01%	0.0828
80	0.125	19.86%	17.90%	17.76%	19.16%	0.075076
100	0.1	17.54%	16.36%	17.79%	17.11%	0.065715

The data demonstrates the nature of increasing number of measurements taken. This specifically notes that at approximately 40 samples the improvement to accuracy becomes marginal.

Table 6.10 demonstrates that for 40 samples error of only 27% compared to single point data, however by increasing the data to 100 samples this will reduce to 17.11%. The average error varied between 0.38 and 0.065 mm.

For manufacturing tasks employing this technology, time to measure is an important factor. According to Table 6.10 using a sample of 40 points will require approximately 4 seconds (0.25 Hz), while 100 points requires 10 seconds (0.1 Hz). However, comparing this to the initial requirements that data be taken within two seconds it is evident that 10 to 20 points should be taken, allowing for a maximum of 45% error for a single point measurement.

6.5.4 Conclusion

As expected, this testing has demonstrated the improvement of employing Precision Point data.

- Improvement in relative accuracy of 55% was attained where measurements were taken for a minimum of 2 seconds.

- A best absolute error of 0.066mm was attained when using 100 sample precision point data.

6.6 Test 4 – Movement

Measurement of a number of stationary receivers is normal for the operation of IPS as described. However as the system provides continuous measurement it is capable of measuring a moving point. The previous experiments have shown that increased time allows for more precise measurements, this however assumes that the receiver remains stationary throughout the measurement time. Test 4 is aimed at quantifying the error induced due to movement of the receivers, and identifying a "safe measurement speed" for IPS operation.

6.6.1 Setup

6.6.1.1 IPS

The setup for Test 4 is identical to that for Test 2, as described in 6.4.3.

6.6.1.2 Receiver mount

To allow movement of a receiver a "ball bar" is used. This is a calibration tool for laser tracker units employed to offer a moving mount for Test 4. This consists of a rotating bar that can be set to move at a constant angular velocity. This bar was modified to rotate about a vertical axis (horizontal plane) with an IPS receiver fixed in place of the laser tracker target. Measurements were then taken on the rotating arm, and the measured data was compared to the known length of the rotating bar to determine accuracy.

This arrangement is depicted in Figure 6.16.

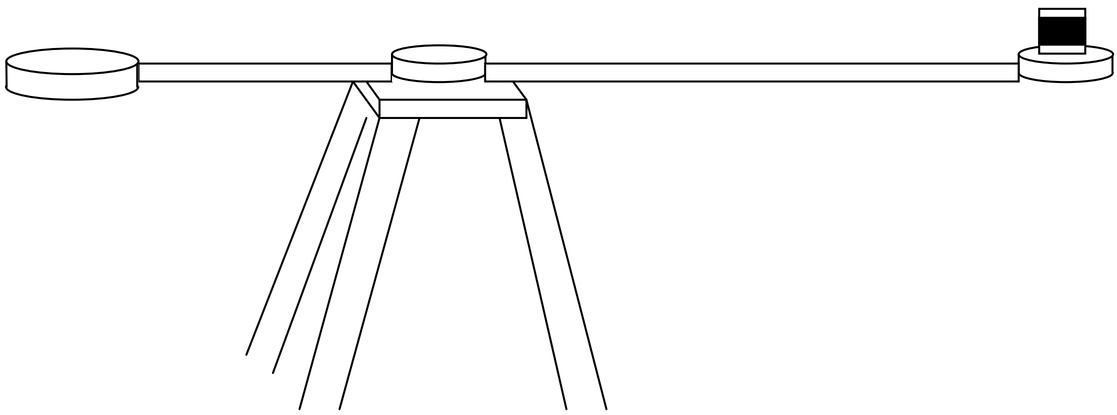

Figure 6.16 – Rotating "ball" bar

6.6.2 Method

The methodology for test four was as follows:

1. Set up transmitters as shown in Figure 6.10.

2. Set up 1 receiver, as described in Appendix 0.

3. Calibrate system as described in Appendix 0, ensure accurate measurement by analysis of a specific data point.

4. Place ball bar in a central location.   Attach receiver to the ball bar mount.

5. Start ball bar.

6. Record data for later analysis, repeat for varying speeds.

7. Compare recorded data at different speeds and Precision Points.

6.6.3 Results

The receiver was moved in a circular path of radius 549mm as described previously. The rotating bar was halted to take measurements at fixed locations on the perimeter of the circle. Tests were subsequently made as the receiver was rotated at a constant speed. These results were compared to those taken when the receiver was stationary.

The minimum measurement speed employed in this testing was 2.5rpm (approximately 0.144m/s tip speed), with results as shown in Table 6.11. More extensive results are contained in Appendix C.3.

5 separate ball bar locations were used as depicted in Figure 6.17.

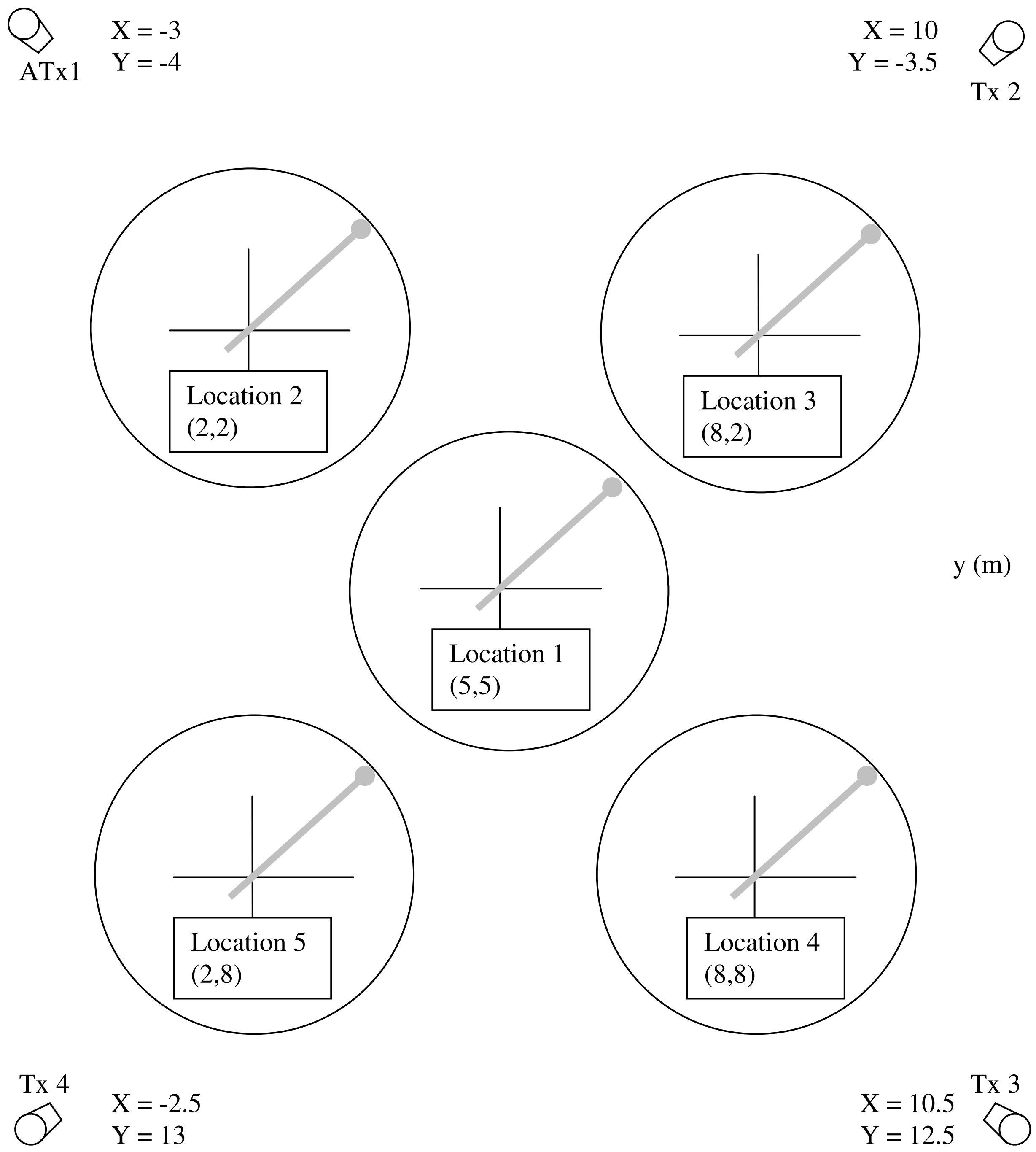

Figure 6.17 - Arrangement of ball bar locations

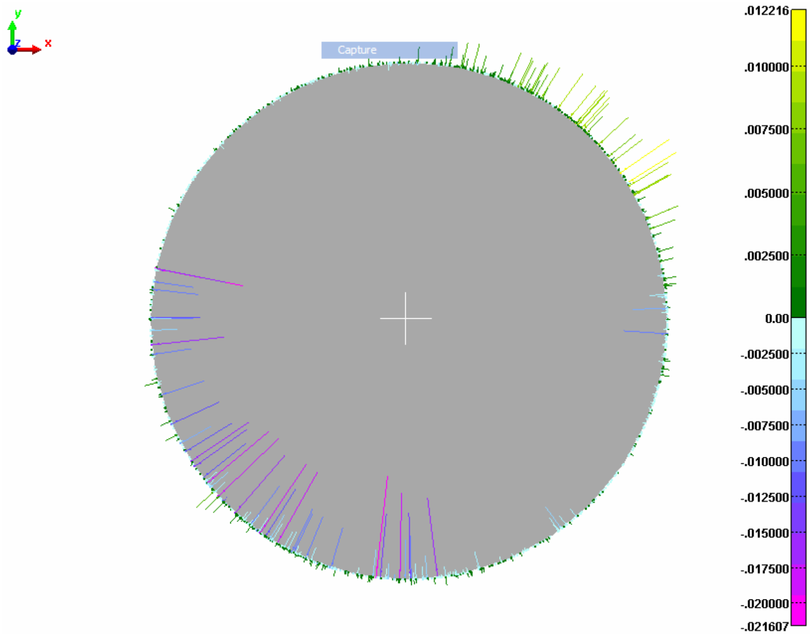

Figure 6.18 - Example of circular element

The element depicted in Figure 6.18 is an example of a circular element developed by analysis of the IPS data. The whiskers in the plot depict the error of individual measurements when compared to the actual path of the receiver with a radius of 549mm.

Table 6.11 - Dynamic point standard deviation at 2.5 RPM

	Precision points							
	1		10			20		
	Radius (mm)	2σ (mm)	Radius (mm)	2σ (mm)	% increase	Radius (mm)	2σ (mm)	% increase
Location 1	549.04	1.978	548.849	9.36	373.21%	550.863	11.878	218.27%
Location 2	548.495	2.072	548.256	14.214	586.00%	546.242	34.92	495.90%
Location 3	548.792	2.706	548.516	11.924	340.65%	547.827	15.294	348.96%
Location 4	548.946	2.142	548.296	14.99	599.81%	552.363	32.168	436.30%
Location 5	548.67	3.146	549.469	14.042	346.34%	548.069	31.366	805.63%
Mean	548.7886	2.43	548.6772	12.862	429.30%	549.0728	26.536	518.12%

σ = standard deviation.

Further data is presented in Appendix C.3. As can be seen in Table 6.11 moving receivers present significantly higher standard deviation, and error, than that identified in previous sections – with the best accuracy at 1.978mm. This clearly demonstrates that measurement of a moving object will result in data with a larger error. Additionally, it can be seen that the use of precision point data will further increase error because of changes in position between measurements. Using 20 samples deviation increases up to 32.168mm (805% increase on single sample data). This was expected by the candidate as analysis for a set of data comprising moving point.

Table 6.12 – Dynamic error for a variety of reciever speeds (mm)

	Precision points					
Speed	1		10		20	
Rpm	Radius	2σ	Radius	2σ	Radius	2σ
2.5	548.973	1.994	549.145	9.054	549.54	11.738
3	548.973	7.14	549.145	9.178	549.54	12.666
5	548.973	2.23	549.145	15.94	549.54	34.52
7.5	548.973	3.052	549.145	18.538	549.54	100.668
10	548.973	4.56	549.145	25.622	549.54	63.118
average	548.973	4.29	549.145	16.736	549.54	54.058

Table 6.12 demonstrates the results from location 1. It shows an increase in error recorded with receiver speed.

6.6.4 Conclusions

- Precision Point data should not be recorded during any movement of the receiver.

- Movement during measurement should be avoided for precision measurements, there is no "safe operating speed" for such measurement.

6.7 Test 5 – Drift measurement

The concept of drift is a steady degradation of measurement continuity and quality. This takes the form of a perceived movement of a measured point over time, usually due to thermal effects on analogue componentry. In the case of IPS this was expected to result in the need to recalibrate the equipment. A secondary effect of drift was observed by the candidate as a result of tidal movement within HdH's location on the Melbourne foreshore. Hence, the candidate believed that if drift existed it ought to be quantified.

6.7.1 Method

The methodology for test five was as follows:

1. Set up transmitters as shown in Figure 6.10.

2. Set up 1 receiver, as described in Appendix B.

3. Calibrate system as described in Appendix B, ensure accurate measurement by analysis of a specific data point.

4. Place receiver in a central location.

5. Record data over a long period of time.

6. Analyze data to identify movement of the measured location.

6.7.2 Primary drift measurement – three day

The following data describes the results examining drift over the measurement area described in 6.4.3 and were taken *over a period of three days*.

Due to software employed at the time of measurement, Precision Point data could not be employed where multiple receivers are operating over extended periods of time, as a result all data provided in the following section is based on single sample measurement taken at intervals throughout the test time. The locations within the working area of the system are recorded in Table 6.13.

Table 6.13 – Location of drift measurements

Location	X	Y	Z
1	1225.202	4212.177	-889.67
2	8636.803	4556.198	-750.07
3	3790.793	7282.607	-637.44

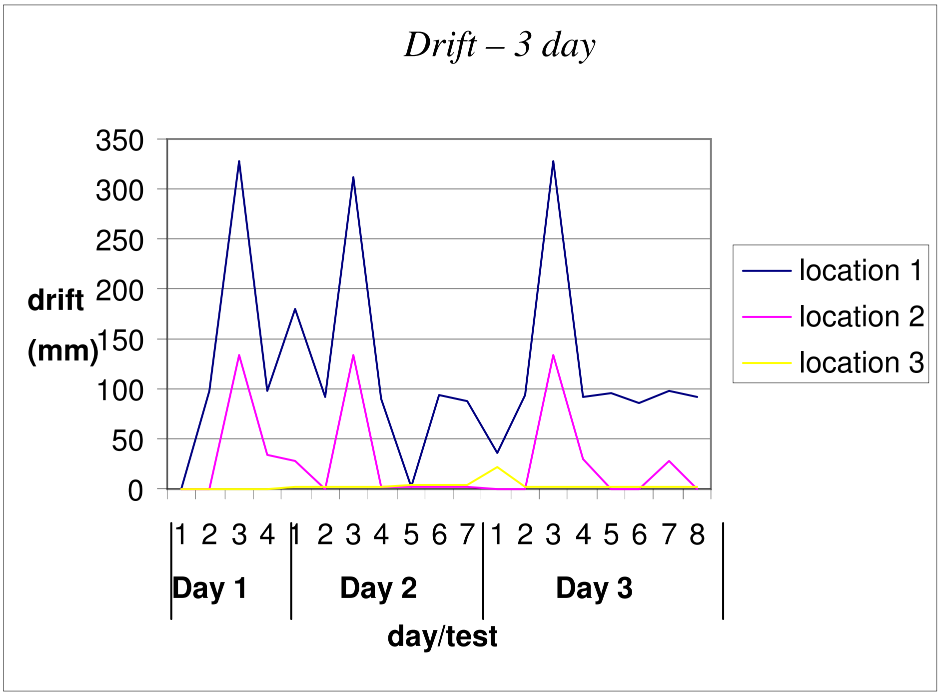

Figure 6.19 - Primary drift (3 day period)

Figure 6.19 demonstrates movement of the measured points over this period. As can be seen this may reach over 300mm, which is clearly excessive. This highlighted two causes of variation in measurement:

1. Initialization of IPS system. High variation is demonstrated in the first measurement taken for each day. (This is more evident in data presented in Appendix C.4.) This suggests that the IPS may take 30-50 minutes to warm up and operate effectively following initialization of the system. As can be seen above (most clearly in location 1 data in Figure 6.19) following a period for starting the system, it will settle at a given location – in this case it produced a variation of approximately 100mm from the initial measured location.

2. Transmitter loss. Several measurements (Figure 6.19) demonstrate extreme variations. Analysis of raw data, and diagrams presented in Appendix C.4, suggest that this high variation is due to blockage of a transmitter. Further analysis suggests that this variation is strongly effected by the quality of the measurement and most recent calibration. Where the calibration quality is poor this will lead to a high sensitivity to loss of a transmitter. This has been the case with these measurements, and should these be repeated with recent calibration data this high error should not

occur. A scheme for automatic calibration should be investigated

Additionally, testing highlighted the problems with this software. Most importantly the confusion of separate IPS receivers, which resulted in the swapping of point data with a sudden shift in location. This was a greater problem when using precision point data, as these points impact on the calculations, and increase error to well above that expected from single data measurement. This problem was rectified with updates to software provided.

A further source of error was the unstable ground for mounting of equipment, this effect is due to tidal forces and cannot be reduced. Due to the poor results of this test, further secondary drift measurements were performed during a single day to reduce movement of the system, as discussed in Section 6.7.3.

6.7.3 Secondary drift measurement – single day

Figure 6.20 demonstrates drift measurements taken over a single day. This clearly demonstrates that a high variation is seen from the initial measurement. However, variation is lower in later measurements suggesting that the system may require time to initialize correctly.

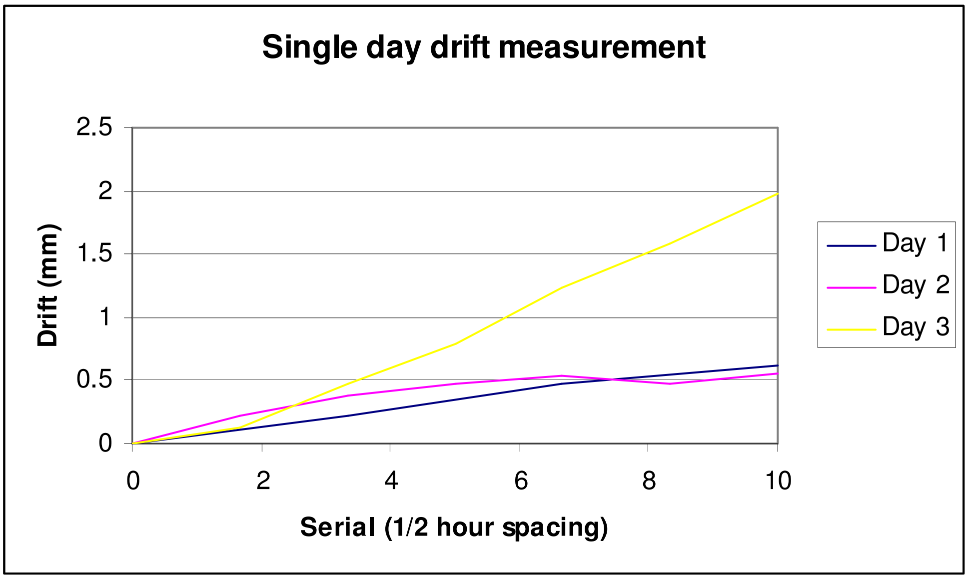

Figure 6.20 – Secondary drift (single day)

6.7.4 Discussion

As may be seen from Figure 6.20, the greatest variation is from the initial measurement. Movement following this variation remains at approximately 0.5mm or less for each 30 minute interval. This suggests that the largest factor effecting drift will be initialization of the system prior to use. Additionally, this movement is below the standard deviation presented in previous sections, suggesting that this may be due to the quality of measurement taken rather than movement of the actual location. The largest variation (aside from the initial setup) was between measurements 2 and 6, which suggests that to keep drift below 0.15mm, calibration may be repeated within two hours.

As may be readily seen from section 6.7.1 and 6.7.3, the initial 3 day tests show a variation of 100 – 300mm for initial tests, reducing to below 0.35mm for the tests over a single day. The factor effecting this most is the software confusion between separate receivers. This issue has been dealt with in an updated software package, and is unlikely to cause any problems at a later date. The variation demonstrated in Figure 6.20 suggests that calibration may be repeated every two hours to maintain variation of 0.15mm or below.

6.8 Conclusion

The IPS was commissioned and it's characteristics including operational accuracy and measurement quality was examined. In particular:

- Improvement in relative accuracy of 55% was attained where measurements were taken for a minimum of 2 seconds.

- A best absolute error of 0.066mm was attained when using 100 sample precision point data. This will occur towards the centre of a square configuration.

- Precision Point data should not be recorded during any movement of the receiver.

The candidate now believed it important to compare the accuracy of IPS to the laser tracker to compare the proposed system to one of a more established means.

7 Chapter 7: Testing Phase 2 – IPS measurement on Aerospace Manufacturing Equipment

7.1 Introduction

In Chapter 6 the first phase of testing demonstrated the characteristics of operation of IPS and allowance was made for an estimation of measurement accuracy. This was demonstrated early during the research and therefore continual improvements in measurement process were expected to lead to greater accuracy in the following testing phases.

Phase 2 testing described in this chapter developed the IPS in a static condition as a means of identifying the locations of real objects within a measurement area. Additionally this phase of testing was able to develop the IPS as a means of QA (Quality Assurance) for aerospace manufacturing jigs. Throughout this testing the IPS was applied to measurement of specified target locations on assembly jigs used in Hawker de Havilland's (HdH) manufacturing operations.

7.2 Details

7.2.1 Setup of IPS for Aerospace assembly jigs

Setup of the system varied for measurement of differing jigs, as prospective transmitter locations were restricted by the manufacturing environment. Each section of the chapter details setup arrangements individually.

7.2.2 Parallax error in IPS measurement

Testing Phase 1 in Chapter 5 demonstrated the accuracy of the IPS to be approximately 0.2mm, however the setup arrangement was maintained square. The jigs discussed in *this* chapter all employ a spatial "C" configuration for transmitter location and receivers on the jigs and were restricted in operation as explained later. It was postulated that this would lead to errors due to parallax, and initial testing was designed to identify this.

Figure 7.21 depicts how error can be generated depending on the relative location and orientation of transmitters to the receiver. The receivers use between 8 and 32 photovoltaic cells of diameter 8mm to absorb a signal. However the physical shape of the receiver can partly block the transmitter signal. For example Figure 7.21 shows that receiver *A* receives the signal from the transmitter over its length *A1*. Receiver *B* can receive the same signal but only over length *B1*. The transmitter will then have more difficulty accurately pinpointing the location of *B* due to the parallax error over this length.

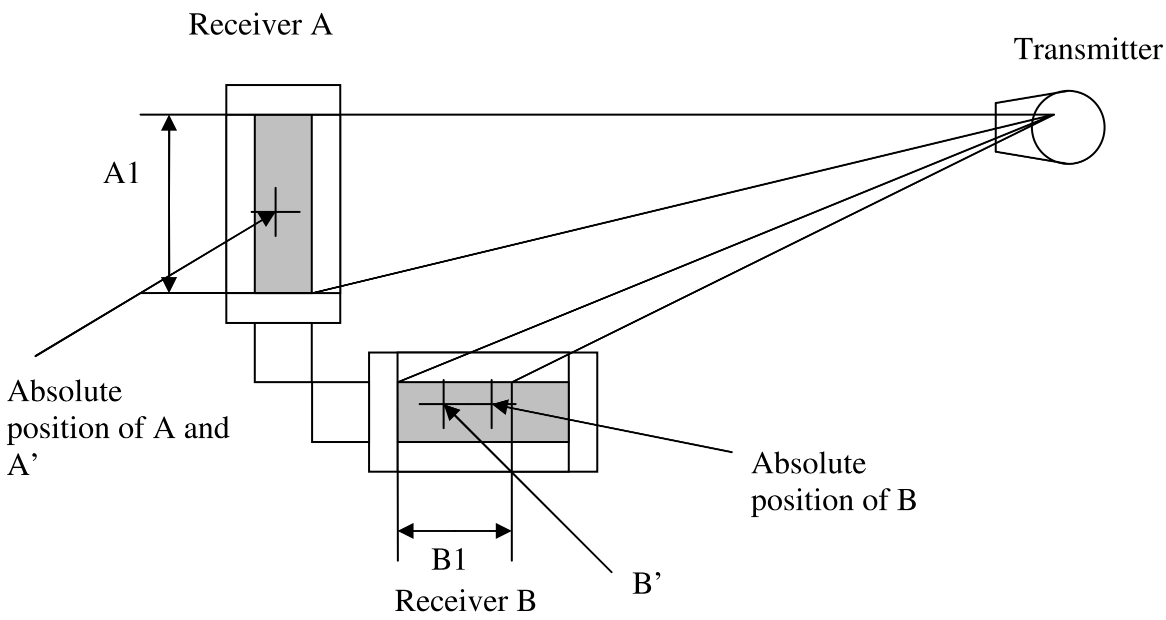

A' and B' are the centroidal locations of the visible footprint from the transmitter.

Figure 7.21- Receiver parallax

For the IPS, transmitter data comprises laser and infra red signals and the system had difficulty discriminating well enough to identify the absolute locations of receiver *B* when compared to laser trackers.

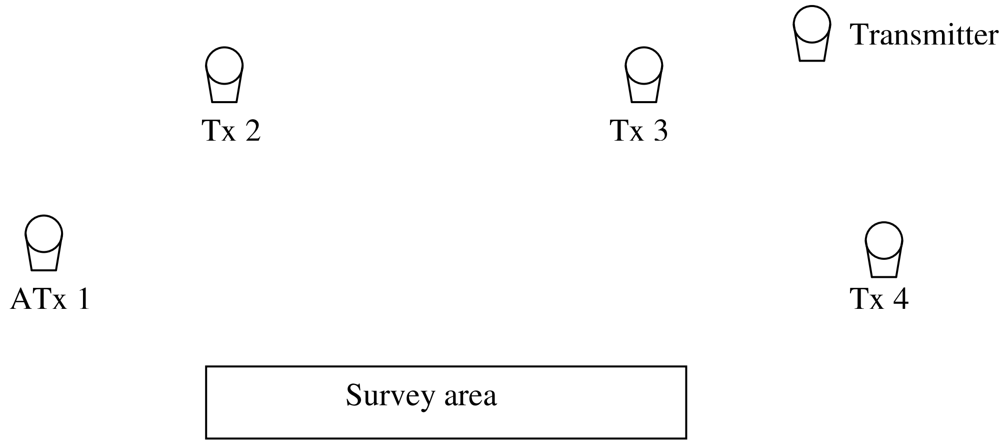

Figure 7.22 - "C" configuration

Figure 7.22 depicts a typical “C” configuration of the IPS. For this arrangement the parallax problem is compounded for receivers that are horizontal mounted with transmitters in the horizontal plane. The visibility of lengths *A1*, *B1*, etc are obscured by the physical features of the receivers, as shown below in Figure 7.23. This will therefore result in a measurement forward of the actual location of the receiver. As the calculation for position includes each transmitter data this can lead to a large zone of uncertainty due to an enlarged footprint caused by the obliqueness of incident rays. The effects of parallax error may be reduced by keeping all transmitters distant to the jig, however this may lead to increased error due to the low intersection angles. This has been discussed in Chapter 6 and Appendix B.

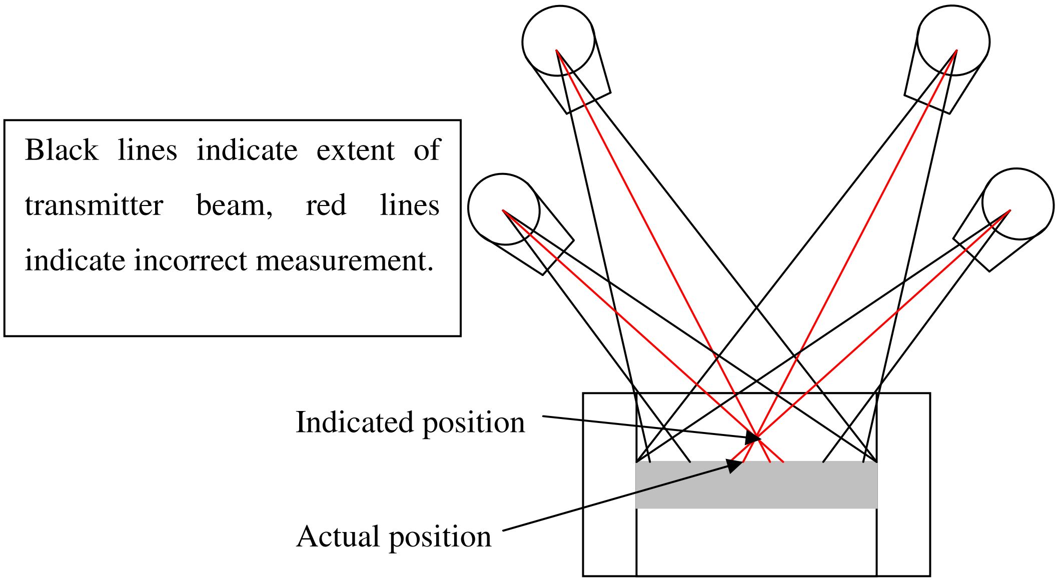

Figure 7.23 - Parallax of a single receiver in "C" configuration

7.2.3 Assembly jigs for IPS measurement

The following assembly jigs were used in measurements.

- Krueger flap assembly jig:

The Krueger flap jig was used to produce the flap for a number of aircraft including several Boeing 700 series aircraft and Airbus A380.

- Boeing 757 vertical stabiliser jig:

The Boeing 757 vertical stabiliser jig was employed to produce the structural spars and final assembly of the vertical stabiliser for the Boeing 757 aircraft. This equipment was readily made available for testing.

- 777 vertical stabiliser jig:

The Boeing 777 aircraft is the most popular Boeing airliner in production. The related equipment used by the candidate was used as a means of assembling the vertical stabiliser and was employed throughout the experimental period. Tests needed to be conducted on the equipment even though the latter was in use for production purposes.

7.3 Krueger flap assembly jig QA measurement

Initial testing involved measurement of a Krueger flap assembly jig, of overall length 1.5m, as shown below in Figure 7.24. This testing was performed to assess the ability of the IPS to survey a relatively small assembly jig and demonstrate the effect of parallax error discussed previously in Section 7.2.2. Additionally, this testing was used to compare the IPS to a laser tracker where it was expected that parallax would lead to high errors.

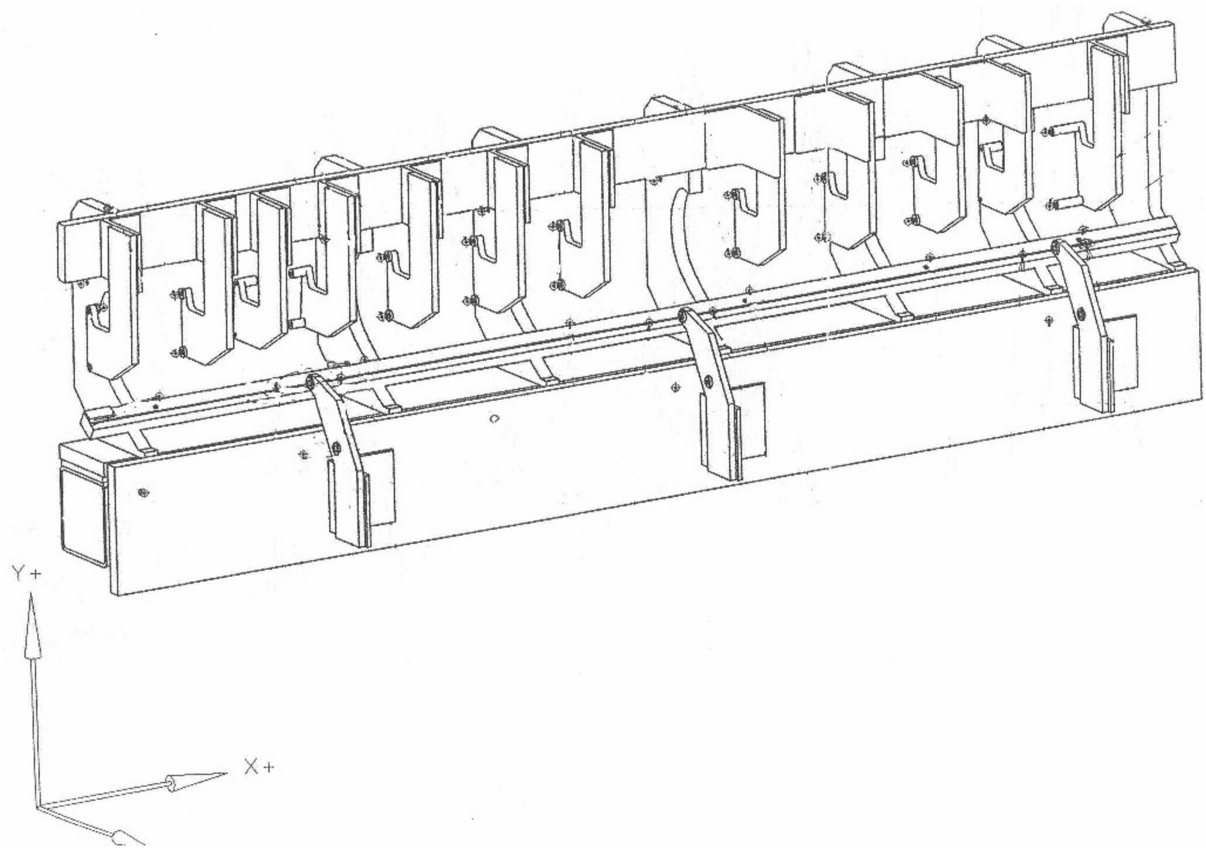

Figure 7.24 - Krueger flap assembly jig

7.3.1 Setup of IPS for measurement of Krueger flap assembly jig

Setup of the IPS was achieved in the "C" configuration layout, as depicted in Figure 7.25. Transmitters were constrained to locations as depicted, to operate within the Krueger jig area. The measurement area and test component are far smaller than other experimentation described in Chapter 5. It was expected that the impact of survey size would not adversely affect accuracy of measurement as previous measurements in Phase 1 testing suggested. However the candidate suggested that parallax was likely to result in high error.

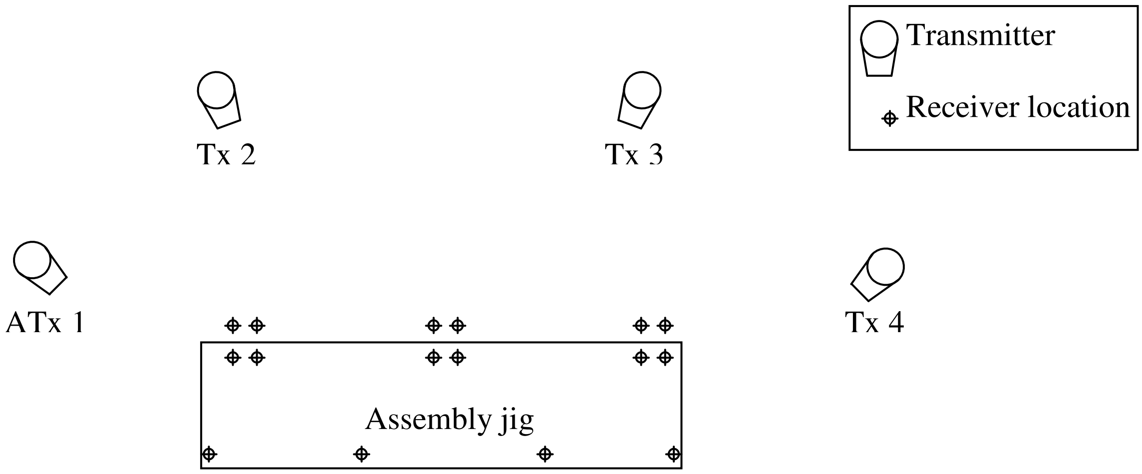

Figure 7.25 - Krueger test setup

7.3.2 Measurement locations

The target locations for measurement were co-located with the locations employed for conventional laser tracker used in QA measurement. Hence a comparison between the two methods could be made and discussed later in this dissertation. Measurement of jig targets was required at an offset distance from attachment to the jig depicted in Figure 7.26.

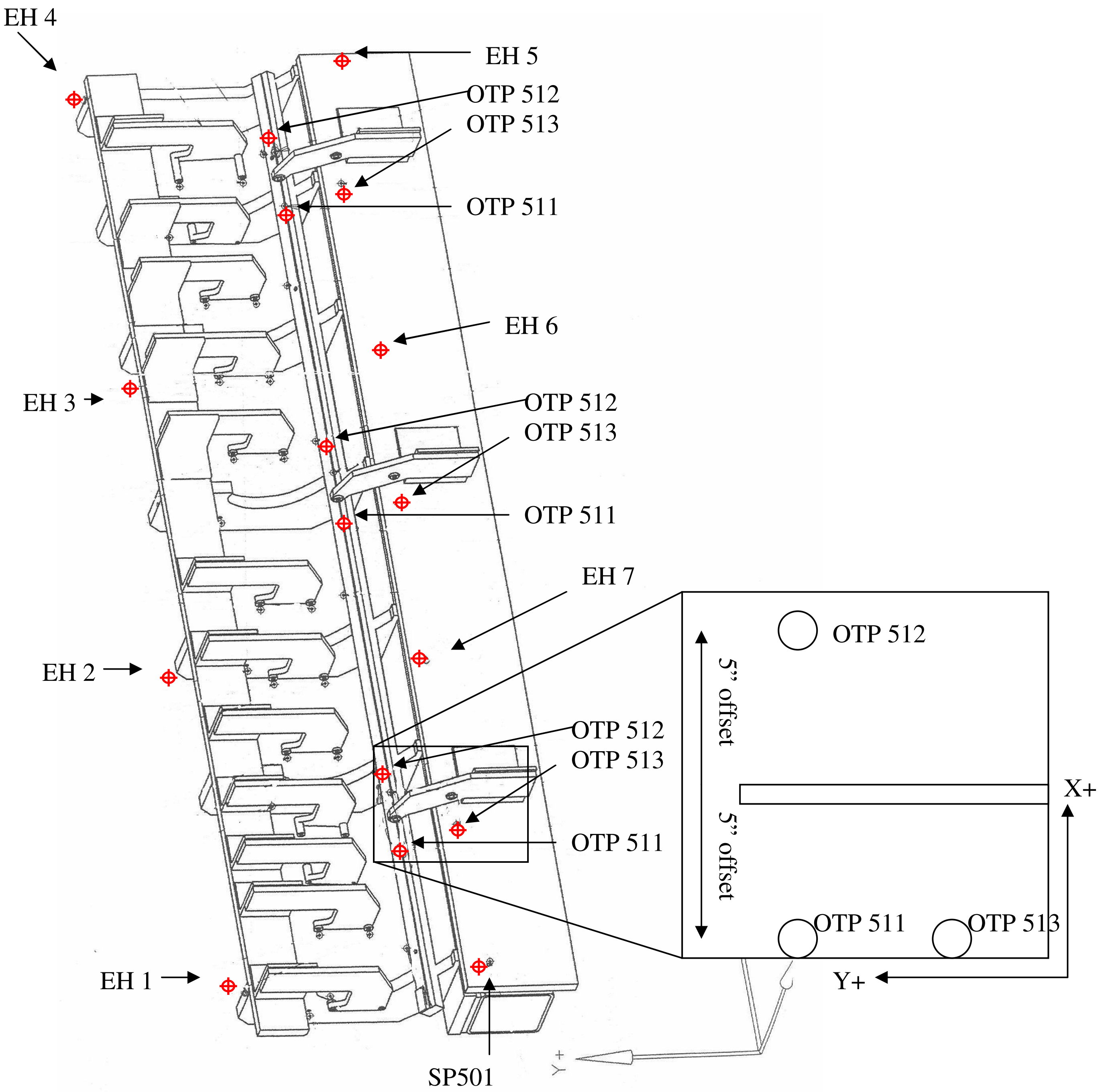

Figure 7.26 - Krueger measurement locations

7.3.3 Orientation of receivers for Krueger measurement

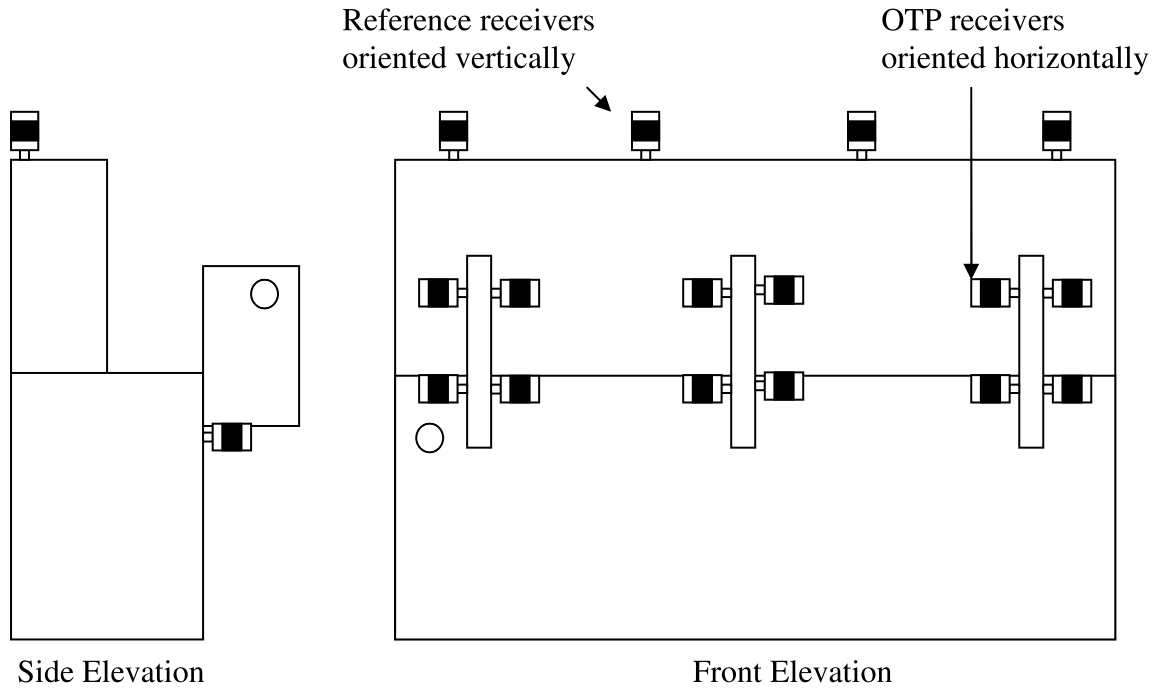

Figure 7.27 - Orientation of Krueger receivers with transmitters located in one horizontal plane.

Figure 7.27 shows that *receivers* located at OTP targets along the front of the jig are oriented akin to receivers depicted previously in Figure 7.23. The reference points are located generally in a vertical plane. This scheme has resulted in errors as described is Section 7.2.2 therefore analysis of data from receivers has been split into two sets: one for OTP targets and the other for reference targets.

7.3.4 Adapters

To allow for measurements to correctly locate OTP receivers OTP offset adapters are required, the design of which is shown in Figure 7.28.

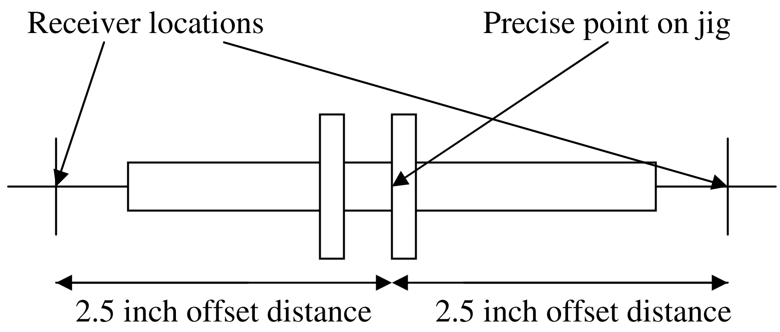

Figure 7.28 - Krueger test OTP adapters

7.3.5 Results

Full results are included in Appendix D.1. Figure 7.29 depicts the error between laser tracker (or expected) established data points and IPS data points.

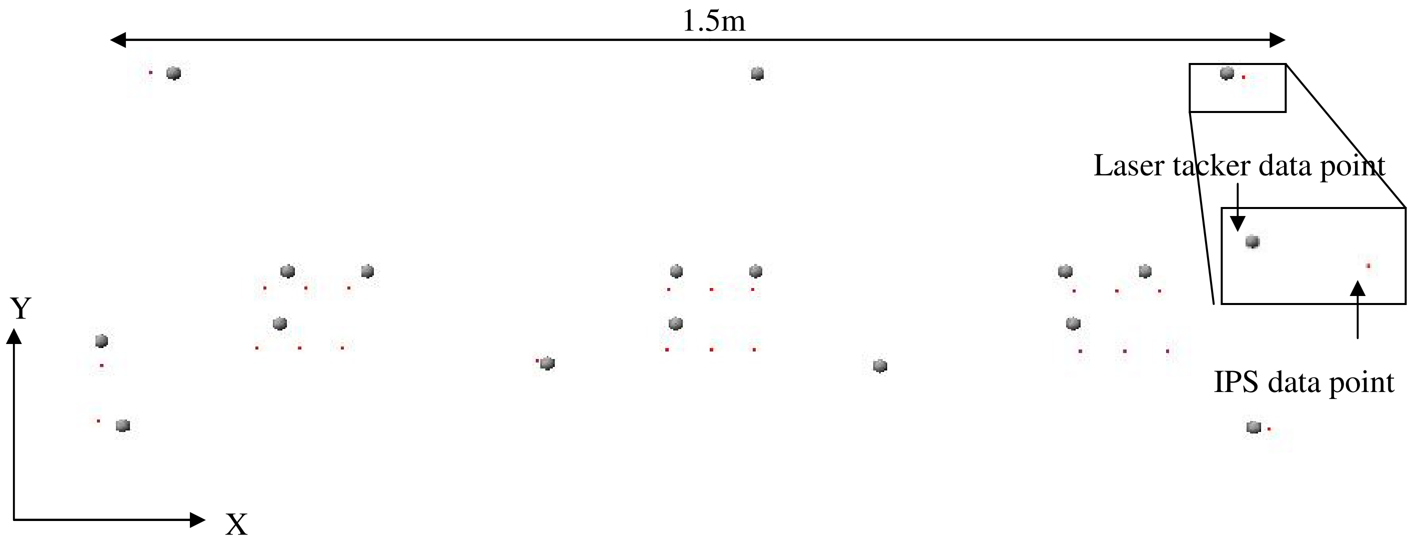

Figure 7.29 - Error between IPS target measurements and Laser tracker data

The above image shows that error between the laser tracker and IPS from the targets was not acceptable. It should be noted that Figure 7.29 is not to scale, and therefore only intended to be representative with the real x-scale error of Figure 7.29 being approximately 7mm.

The following data demonstrates there is a large variation between the OTP target and reference target sets as defined in Section 7.3.3. To investigate this variation data has been aligned in two different manners as follows:

1. Aligned by reference target sets.
2. Aligned by OTP target sets

Extensive data is included in Appendix D.1, however the reduced results is included in Table 7.14.

Table 7.14 - Kruger jig measurement variation (mm) with laser tracker data applied to jig of maximum dimension 1.5m

Oriented by	OTP		Reference (EH)	
Data set	OTP	Reference (EH)	OTP	Reference (EH)
Maximum	1.46	15.95	12.36	4.87
Minimum	0.23	5.90	9.94	1.37
Average	0.97	11.23	11.35	2.85

In the context of this research, Laser tracker data is presumed to be absolute and accurate in comparison to the IPS-generated data. Where these two data sets exist (Laser tracker and IPS) points can map from one data set to another.

It has been shown that the IPS data corresponding to receivers located on the horizontal plane (located on the front of the jig) are more prone to parallax error. Correspondingly receivers located in the vertical plane (located on top of the jig) are less prone to error.

Acquired data can be considered as thus:

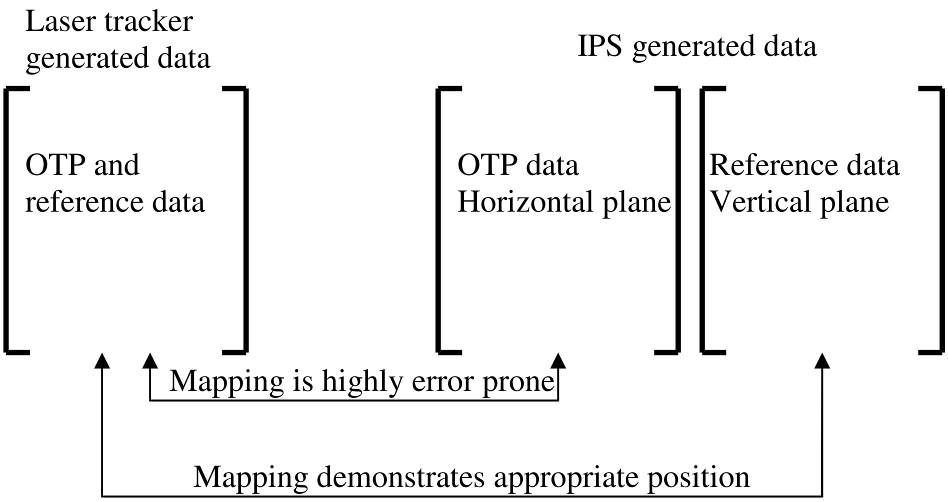

Figure 7.30 - Data mapping error matrix

In order to present this data the following representations will be used:

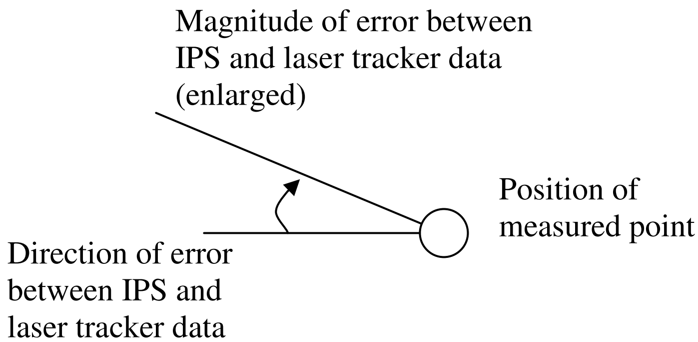

Figure 7.31 - Representation of data

When laser tracker and IPS generated data sets are compared the diagrams following in Sections 7.3.5.1 and 7.3.5.2 result.

7.3.5.1 Krueger data aligned by reference points

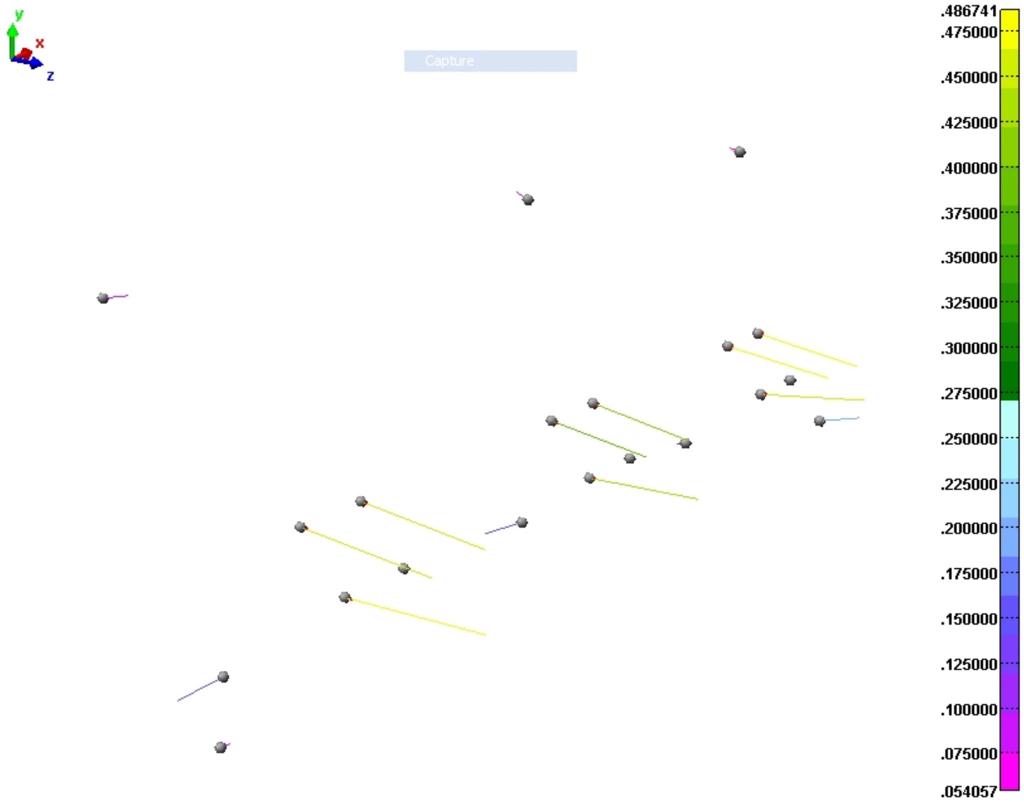

Figure 7.32 - Krueger data oriented by reference targets (Offset in inches)

Alignment by reference target sets along the main body of the jig demonstrates that the measurements of OTP targets are not adequately measured with respect to their expected locations. This is depicted in Figure 7.32. The long "whiskers" above clearly demonstrate that large error has been generated where OTP positions are systematically situated in front of the accurate laser tracker locations. This is the expected result as discussed in Section 7.2.2. Table 7.14 demonstrates that the error of OTP measurement points is on average 11.3mm, while the error of reference target points is 2.86mm.

7.3.5.2 Krueger data aligned by OTP targets

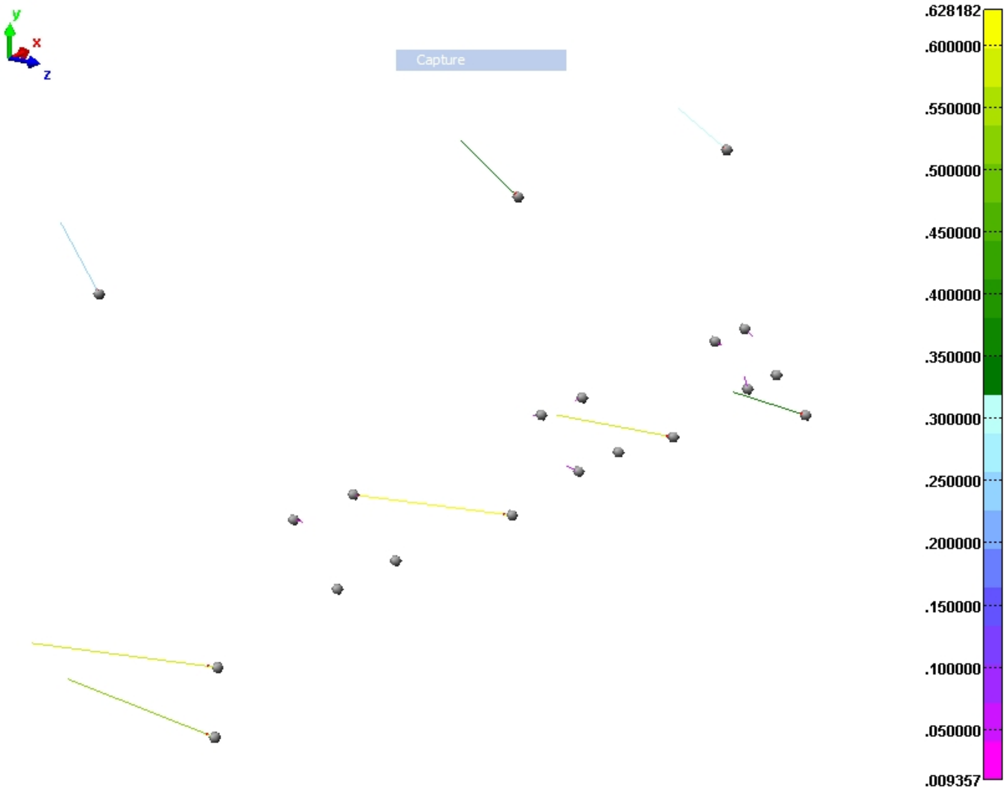

Figure 7.33 - Krueger data oriented by OTP targets (Offset in inches)

Aligning by the OTP target sets demonstrates that the measurements of the attachment targets are not appropriately placed with respect to their expected locations, as shown above in Figure 7.33. The long "whiskers" on the above data clearly demonstrate that large error has been generated where reference targets have been located behind the accurate laser tracker locations. This agrees with the details discussed in Section 7.3.5. Table 7.14 demonstrates that the error of OTP points is on average 0.976mm, while the error of reference points is 11.23mm.

It now becomes clear that in all cases the IPS data is located in front of the laser tracker data for every measured OTP point. This systematic error observation occurs because of parallax error.

7.3.5.3 Krueger data basic measurement error

Experimentation in the previous chapter demonstrates that the system is operating sufficiently accurately as defined in Chapter 3. Error of individual points from IPS data is presented in Table 7.15. This suggests that the accuracy of the data points was improved well below sub millimeter accuracy, demonstrating that the error determined in the previous sections was due to parallax error rather than by poor measurement accuracy.

Table 7.15 - Krueger data accuracy

Number of data samples	1	10	20	50
eh1	0.297967	0.100279	0.085039	0.065938
eh2	0.285852	0.085954	0.067894	0.047676
eh3	0.237363	0.085039	0.072923	0.054178
eh4	0.247752	0.089611	0.072415	0.051029
eh5	207.4751	0.344373	0.240055	0.198018
eh6	725.6869	249.3486	2.885567	2.943835
eh7	4.004132	0.105689	0.080848	0.060046
SP501	0.683946	0.086741	0.06477	0.048717
OTP 511	0.167589	0.06604	0.051283	0.031572
OTP 512	105.4371	0.116002	0.094336	0.070739
OTP 514	0.20381	0.065049	0.049327	0.027762
OTP 515	0.266421	0.082093	0.070612	0.043078
OTP 517	0.371678	0.09398	0.074041	0.060096
OTP 518	0.218364	0.066167	0.045212	0.030861
OTP 513	0.233274	0.08382	0.05776	0.039751
OTP 516	0.530454	0.129515	0.115138	0.08067
OTP 519	0.240386	0.071044	0.053035	0.030836

It is clear that the measurement accuracy of the IPS is very high, especially for Precision point data employing large numbers of samples. The error reported in Table 7.15 is the error compared to the length of the error whiskers in Figure 7.31.

It is also clear that eh6 and OTP 512 error is far larger than expected, this is due to interference of the measurement by external factors.

7.3.6 Krueger flap assembly jig conclusions and recommendations

Following the Krueger experimentation, the following recommendations are made:

- Small setup areas should be avoided, whilst several small jigs may be included in one survey area, the transmitters should be arranged in a larger setup.

- Where possible allowing parallax error due to relative position and orientation of the transmitter and receiver should be avoided, thus orientation of receivers should be vertical to reduce parallax error. Following return of this data to the manufacturer an effective angle of 120º was suggested, relating to 60º from the horizontal to the receiver. Data from this experimentation has assisted with documentation for the official release of IPS equipment.

- Where receivers must be located horizontally, transmitters must be located distant to the receivers to reduce parallax error.

- IPS error was 11mm over 1.5m which corresponds to 0.7%.

7.4 757 Vertical Stabiliser Assembly Jigs

A 757 vertical stabiliser jig was employed for the second stage of aerospace assembly jig measurements; t6his experimentation included the measurement of the main assembly jig and rudder spar assembly jigs.

7.4.1 Setup of IPS for measurement of 757 vertical stabiliser assembly jig

The candidate has demonstrated in Section 7.3 that consistent placement of the receivers in a vertical orientation would reduce the parallax error and allow transmitters to be placed around the jig. This would lead to an improvement by:

- Reducing the IPS error.

- Reducing error between "accurate" location and IPS data.

Measurement of the 757 vertical stabiliser assembly jig consists of two separate tests, involving measurements taken off rudder spar assembly jigs, and main assembly jig. The spar jigs consist of two linear jigs within a workspace, and allows for a square configuration. The main assembly jig is a vertical planar jig, requiring a "C" configuration. These are depicted in Figure 7.34.

The testing in Section 7.3 demonstrated the effects of parallax on measurement accuracy, therefore all measurement of the 757 jigs receivers were constrained to remain vertical to avoid the increased error discussed in Section 7.2.2.

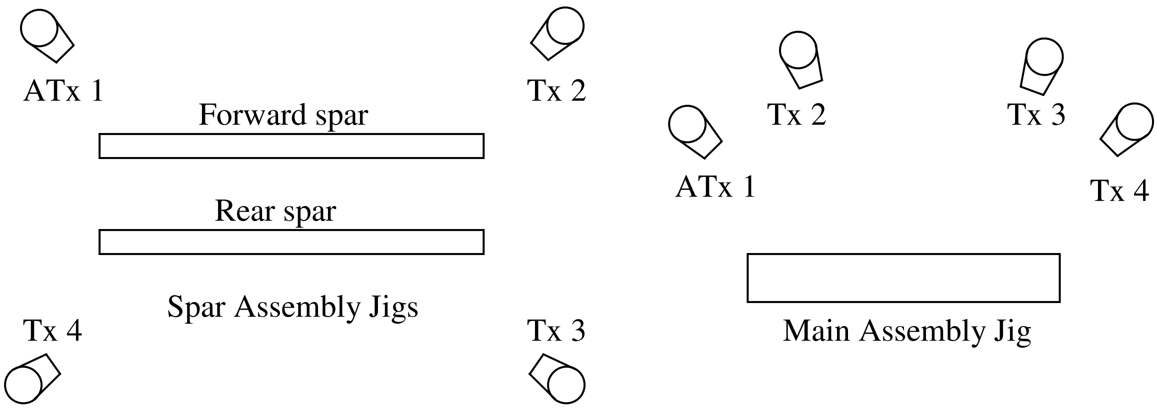

Figure 7.34 - 757 assembly jig setup

7.4.2 757 vertical stabiliser assembly jig measurement Locations

The measurement locations presented in the following sections, depicted in Figure 7.34 and Figure 7.35.

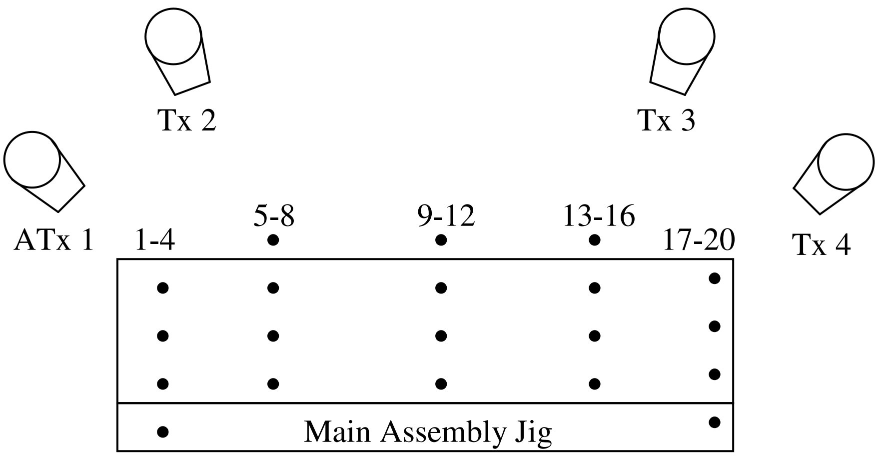

Figure 7.35 - 757 Main assembly jig target measurements

7.4.3 Results – 757 spar assembly jigs

Measurement data for the 757 spar jigs is demonstrated in Table 7.16. This demonstrates that a sub-millimetre accuracy was readily achievable, with the expected improvement in accuracy using increased data samples that has been demonstrated in Chapter 6.

Table 7.16 - 757 spar measurement results

Summarized from Appendix D.2 and D.3

Samples	Test 1		Test 2		Test 3		Average	
	Front	Back	Front	Back	front	Back	Front	back
1	0.71509	1.76775	0.80362	0.857281	0.703214	0.96887	0.740643	1.197968
10	0.29361	1.37851	0.40348	0.414632	0.322631	0.528714	0.33991	0.773954
20	0.23340	1.40284	0.29743	0.285388	0.268568	0.505749	0.266471	0.731327
50	0.16028	1.13339	0.21560	0.343471	0.217339	0.423822	0.197742	0.633563

Table 7.16 also demonstrates that the measurements taken for the rearward spar in test 1 have produced an error of 1.13mm, which is significantly high. This result was due to interference with the system at the time of measurement by staff working in the measurement area.

7.4.4 Results – 757 stabiliser assembly jig

Due to the state of the 757 assembly jig it was not possible to take measurements from specific targets fixed to the structure, therefore measurements were taken off physical scaffolding and other locations on the jig itself. The results of these measurements are recorded below in Table 7.17.

Table 7.17 - 757 main jig measurement results

Location	data points			
	1	10	20	50
1	0.42503	0.185989	0.150232	0.122843
2	NA	NA	NA	NA
3	NA	NA	NA	NA
4	0.556853	0.192479	0.123675	0.073268
5	0.542744	0.208694	0.140526	0.073006
6	0.535217	0.211576	0.146088	0.064967
7	0.558743	0.22307	0.151689	0.045682
8	0.52059	0.200086	0.119662	0.067896
9	0.43258	0.167623	0.140448	0.07726
10	0.71583	0.338948	0.287024	0.180393
11	0.648198	0.249739	0.209989	0.137142
12	0.516132	0.269384	0.237148	0.148451
13	0.573317	0.265688	0.224399	0.140382
14	0.593567	0.227461	0.168712	0.080204
15	0.522523	0.224955	0.177544	0.08946
16	0.604026	0.301736	0.247722	0.182118
17	0.462492	0.158678	0.122478	0.069674
18	0.500716	0.217161	0.166347	0.11332
19	0.489563	0.195216	0.126016	0.089146
20	0.554072	0.218276	0.146903	0.075528
Max	0.71583	0.338948	0.287024	0.182118
Average	0.541788	0.225376	0.171478	0.101708
Min	0.42503	0.158678	0.119662	0.045682

Data from the 757 measurements for the main jig demonstrate achievable accuracy of under 0.2mm using samples of 50 data points.

7.4.5 Laser tracker application to 757 measurement

Laser tracker measurement was not possible on the 757 measurement jig as interference with the scaffolding and technical failures of the equipment rendered this section of the experimentation unfeasible.

7.4.6 757 experimentation recommendations

- Further experimentation should be completed employing laser tracker data to verify the accuracy of the IPS on large components.

- Such measurement must employ the laser tracker with all scaffolding removed and specific adapters fixed into locations on the jig body.

- Measurement using IPS is appropriate for larger components such as assembly jigs.

7.5 Testing of 777 jigs

Previous testing of 757 assembly jigs in Section 7.4 suggested that measurements taken should be compared to laser tracker measurements of attached targets on the structure, which was unavailable. To achieve this, measurements have been performed on the 777 rudder jig which at the time of experimentation was used for production. The 757 measurement demonstrated the improved measurement capable by ensuring the receivers were kept vertical and allowing the "C" configuration with good spacing to ensure higher intersection angles.

This testing included two phases:

- Initial measurement and accuracy identification.

- Laser tracker comparison measurements.

7.5.1 Setup of IPS for measurement of 777 vertical stabiliser assembly jig

Setup in "C" configuration, as depicted in Figure 7.36.

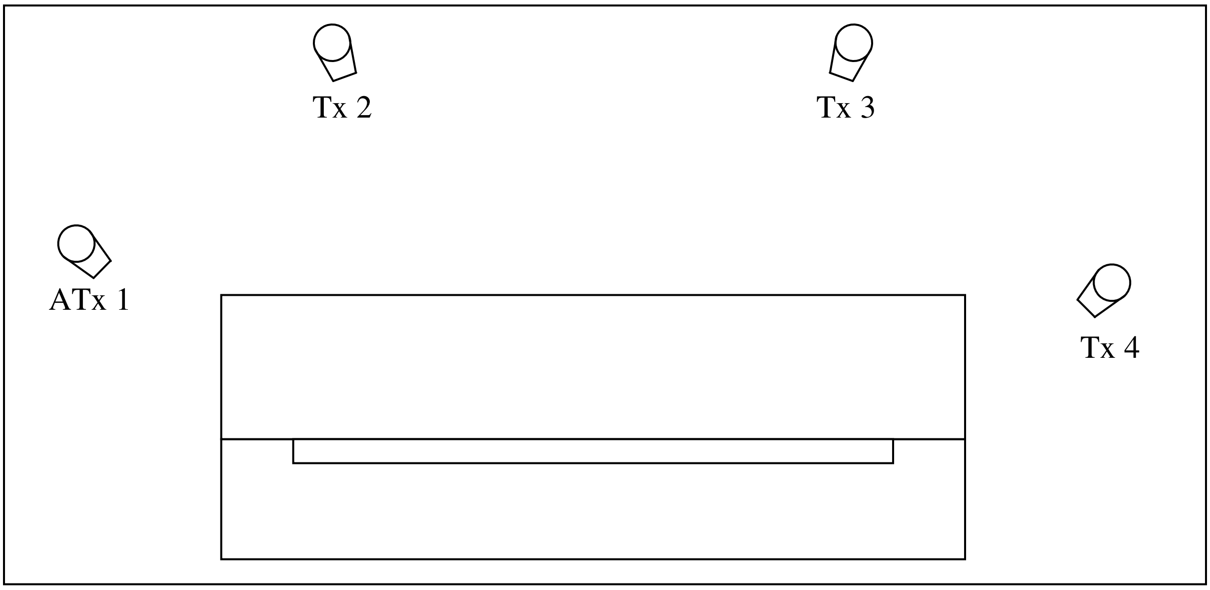

Figure 7.36 - 777 measurement setup

7.5.2 Setup – adapters for 777 vertical stabilizer assembly jig

The candidate demonstrated in Section 7.3 that special adapters were required to ensure that measurement could be taken in appropriate locations. Therefore adapters were designed to take measurements from the 777 jig, and allow receiver placement in appropriate target measurement locations. Following this the receiver was to be replaced with a 1.5 inch diameter laser tracker measurement ball. These adapters additionally ensure that the receivers remain vertical to ensure adequate visibility of the transmitters, and avoid the parallax error as discussed in Section 7.2.2.

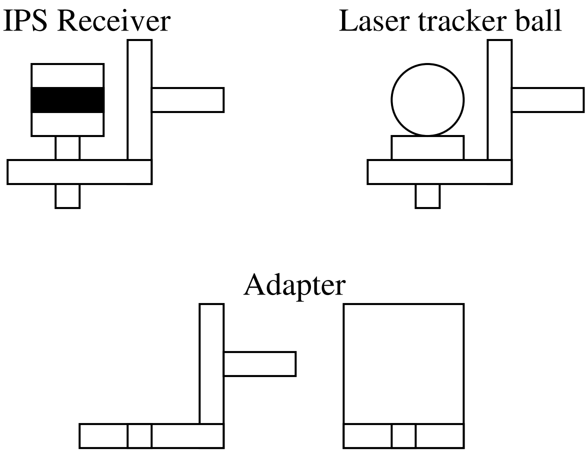

Figure 7.37 - 777 adapters

7.5.3 Setup – 777 assembly jig arrangement and measurement location

Setup of the 777 vertical stabilizer jig is depicted in Figure 7.38. Target locations have been noted in the diagram. A further location has been included on the scaffolding for use as a "control target". The control target was employed to provide a stationary point. The distance between the measured target and the control target was then compared in subsequent readings to offer an indication of the stability of the system. Additionally, the control point demonstrates that the IPS is capable of measuring multiple locations at any given time.

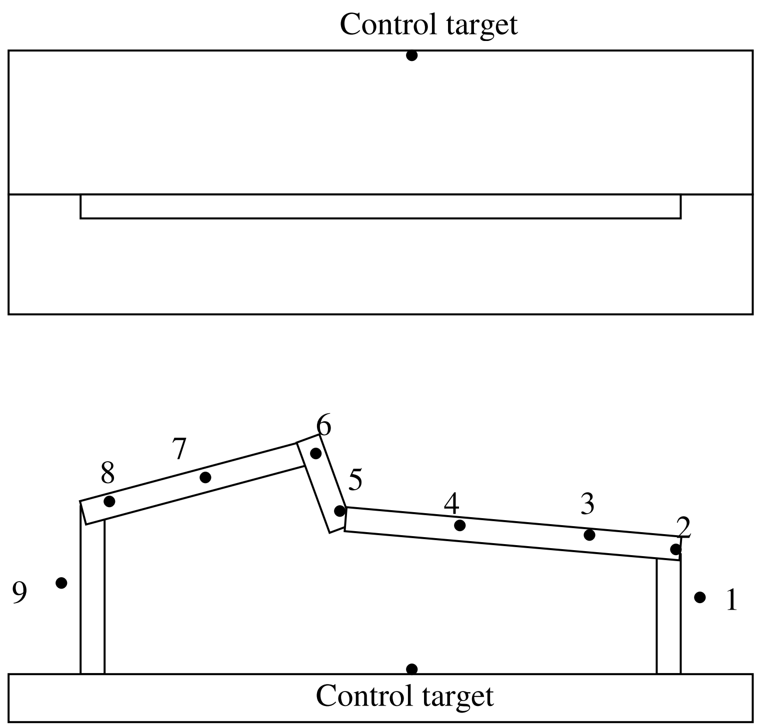

Figure 7.38 - 777 measurement locations

7.5.4 Results – measurement

Measurement results taken over the 777 vertical stabilizer jig are demonstrated in Table 7.18, additionally these have been compared to the control target in the workspace. The "shift" value expressed below is the average variation of the distance from the measured target to the control target. The extremely low shift value suggests that while the error of the measured target point may be as high as 0.25mm, the point was stable and physical error is likely to be less than the indicated error.

Table 7.18 - 777 measurement results (measurement average in mm)

Day	1		2		3		4	
	Error	Shift	Error	Shift	Error	Shift	Error	Shift
1	0.245287	0.087424	0.196598	0.006874	0.236556	-0.02399	0.252292	0.021196
2			0.197894	-0.00174	0.253218	-0.06956	0.261959	0.041761
3			0.205771	0.001795	0.229658	-0.01701		
4					0.370886	-0.05475		
5					0.446502	-0.16618		
6					0.263593	-0.06053		
7					0.207596	0.025185		

7.5.5 Results – Laser tracker comparison of 777 assembly jig measurement

The variation of laser tracker and IPS data is recorded in Table 7.19, with extended results recorded in Appendix D.4.

Table 7.19 - 777 laser tracker variations

IPS data			Laser tracker data				variation
X	Y	Z	X	Y	Z		
0	0	0	-1.24921	0.473852	0.600302		1.464725
336.8096	-159.543	3.289431	337.4875	-159.297	2.92065		0.809963
865.3327	-899.275	951.3632					NA
1103.442	-1018.81	514.5708	1103.413	-1018.85	514.7568		0.191848
1869.183	-1388.49	843.6558	1869.891	-1388.89	843.0904		0.989834
3311.854	-2101.91	212.2807	3311.904	-2102.71	212.2342		0.803521
3697.879	-2265.73	849.8959					NA
6819.897	-3759.59	1017.501	6821.829	-3760.96	1018.161		2.459139
7909.411	-4290.91	792.8863	7910.793	-4291.14	792.7844		1.403889
9038.37	-4840.85	550.919	9039.013	-4840.56	550.6899		0.739855
9988.721	-5303	349.5877	9989.253	-5303.45	349.7844		0.721334
11064.47	-5812.49	115.6685	11065.68	-5813.48	115.8382		1.573794

Measurement with the laser tracker was used as a means of verifying the accuracy of employing IPS, however it was found that this equipment was effected by the following:

- Repeated failure of laser tracker due to technical difficulties and interference with surrounding items.

- Adapter errors as discussed in Section 7.3.

- Obstructions to the laser tracker beam.

This experimentation concluded that while the current use of the laser tracker is an effective option for some measurement tasks, it can be expected that it will not perform well in environments with a large number of obstructions. Standard laser tracker measurement of the 777 assembly jig must be performed while the base platform is removed, and all manufacturing operations must cease while this is occurring.

The use of IPS was possible while rudders were being produced and caused no impact on the duties of personnel in the area. For further development IPS should be permanently affixed in place, and tool verification would be achieved far more effectively than using the standard laser tracker equipment.

7.5.6 777 experimental recommendations

- Measurement can be achieved on jigs used for manufacturing tasks by the IPS without affecting productivity. This additionally suggests that the IPS may be employed during production as a means of QA of the produced part.

- Where tolerance is 0.2mm or higher IPS is readily capable of use in QA tasks.

- Use of a control point measured simultaneously allows a further estimation of accuracy, however multiple targets may be used to speed up measurement process.

- IPS is more flexible in a manufacturing environment, and less sensitive to adapter errors.

7.6 Review of Key objectives

The key objectives as listed in Chapter 3 are as follows. Phase 2 testing has investigated the use of IPS for measurement of large assembly jigs and quality assurance tasks, and therefore attributes referring to its use for automation cannot be demonstrated. Table 7.20 lists the achievements of the system compared to the original key attributes.

Table 7.20 - Key attributes as of Phase 2

Key	Attribute
1	*System must be able to identify objects rapidly, including, but not restricted to, robotic tools, and workpieces.* • The system is able to identify measurements, however at this stage ability to rapidly identify items and report on posture is not demonstrated.
2	*Measurement and control of systems must be capable using a minimum of workstations.* • All measurement and control performed using a single portable computer.
3	*Must be capable of micro-measurement, and micro-positioning of both end effectors and workpieces.* • Capable of fine measurement with accuracy below 0.2mm, positioning not yet demonstrated.
4	*Must be capable of taking measurement in under 2 seconds.* • Measurement requires approximately 5 seconds to complete accurately.
5	*System must be capable of measuring and deploying multiple robots simultaneously, along with workpieces and additional requirements.* • Not yet demonstrated.
6	*System must be capable of adjusting tool centre point locations to allow for workpiece movement during the operation.* • Not yet demonstrated
7	*Equipment must be readily portable and robust.* • All equipment readily moved by hand/vehicle with installation within an hour.
8	*The system should be applicable to a number of different industries with minimal variation to the initial components.* • All tasks are not industry specific.

7.7 Conclusions

The IPS was successfully employed for the measurement of large aerospace manufacturing jigs, and it's accuracy compared to that of the laser tracker to verify the quality of measurement. It was noted that:

- The IPS is a suitable choice for quality assurance tasks, however it's error may be in excess of the tolerances required. Additionally it may be capable of QA of parts throughout the manufacturing process. Testing has suggested that the accuracy may be superior to that quoted of 0.2mm, however this has been impossible to demonstrate.

- The IPS is capable of measuring multiple targets simultaneously. Further analysis is required to employ this system for manufacturing tasks.

- The IPS is a poor choice for highly restricted locations where transmitters must be placed close to the targets, however multiple smaller jigs may be included in a larger survey area.

- The use or "C" configurations results in a high parallax error unless receivers are kept vertical and not constrained to a given orientation, or the transmitters are kept distant from the receivers.

- Laser tracker data is insufficient to prove accurate measurement where there is no ability to ensure accurate machining of adapters.

8 Chapter 8: Testing Phase 3 – Robotic drilling trials

8.1 Introduction

The objective of this research is to develop a methodology for the application of advanced measurement equipment (IPS) for control of automated aircraft manufacturing operations. Testing Phase 3 is aimed at demonstrating this through a dynamic robotic drilling trial on a carbon composite panel to simulate a drilling operation on an aerospace component.

This chapter additionally examines the capability of the system to cope with an unpredictable environment, where not only the article being manufactured may move, but also the robot platform may move.

8.2 Required tasks for the system

8.2.1 Manufacturing issues

The use of IPS is envisaged as a means of control for robotic manufacturing tasks that will improve the robotic manufacturing of aerospace components. The following issues were identified as important in this research:

- Control via IPS.

IPS is considered as a means of control for a manufacturing process.

- Control of a mobile robotic platform.

With the development of mobile robotics there is a need for precise control of the manufacturing process. Precise control of a robotic system usually requires a clear knowledge of the position and orientation of all components in the system. For a mobile robotic system the location of the platform itself varies frequently. To account for this, the IPS is used to measure the end effector location and attitude only. Movement of the end effector is introduced relative to the initial end effector location, bypassing the need for robot positional knowledge. The following situation is common:

- Coping with an unexpected movement of workpiece.

A common manufacturing problem is flexure and movement of the part during the manufacturing process. For a pre-programmed process this can result in damage to the part and likely damage to both part and tool.

As drilling is performed on a completed assembly (eg. Wing, flap, rudder etc) damage can result in tens of thousands of dollars. A methodology for the measurement of the part throughout the process must be developed, allowing corrections within the manufacturing process to be automatically achieved.

8.2.2 Tasks for Testing Phase 3

Tasks described in this chapter were based on the use of IPS data as feedback of positional information for both a robot end effector with a drill and the workpiece. To test this several tasks were completed as follows:

- Identification of positional data for TCP (tool centre point), robot and part;

- Determining positional correction of the TCP as applied to part locations;

- Development of a feedback loop for the utilisation of IPS data.

8.2.3 System testing

To achieve the tasks the following tests were completed:

- Test 1 – Measurement of pre-programmed drilling operation.

Preset positional movements were programmed into an ABB IRB6400 robot, using a teach pendant dedicated to the robot. This task formed the basis of the first set of drilling trials involving only movement of the end effector without any control from the IPS. The positional accuracy of this measurement produced an estimation of end effector repeatability and drill pattern quality.

- Test 2 – Control of a drilling operation utilising the IPS.

The IPS guided trial involved control of the end effector solely by use of IPS data. Ideally data should be automatically fed into the robot and applied however due to the lack of an online control for the robot and safety concerns with unproven equipment the choice was made to input data manually.

- Test 3 (Bump 1) – Control of a drilling operation employing IPS and involving simultaneous movement of the drilling platform.

The “Bump 1” testing was as per Test 2, however during the drilling trial the robot platform was moved to simulate unintentional movement of the end effector and/or movement of the platform between operations. This is referred to as “Bump 1” testing as the tests simulated the capacity of the system to correct itself when one or more components were accidentally moved.

- Test 4 (Bump 2) – Control of drilling operation employing IPS with movement of the part.

Bump 2 testing was as per Test 2, however during the drilling trial the workpiece was moved to simulate unintentional movement of the drilling plate to observe how the system compensated for the disturbance. This is referred to as “Bump 2” testing as it assesses the capability of the system to self correct when one or more components were accidentally moved.

8.2.4 Feedback loop

Throughout the testing a feedback loop for controlling these operations was gradually developed. This is presented in the following sections in the manner it was developed to deal with the experimentation.

8.3 Experimental arrangement

The experimental arrangement is depicted in Figure 8.39. This comprises of the IPS system, two test drilling plates and the mobile robotic platform, with a micro-positioning drilling end effector attached. The working area covered by the IPS is approximately 30 square meters.

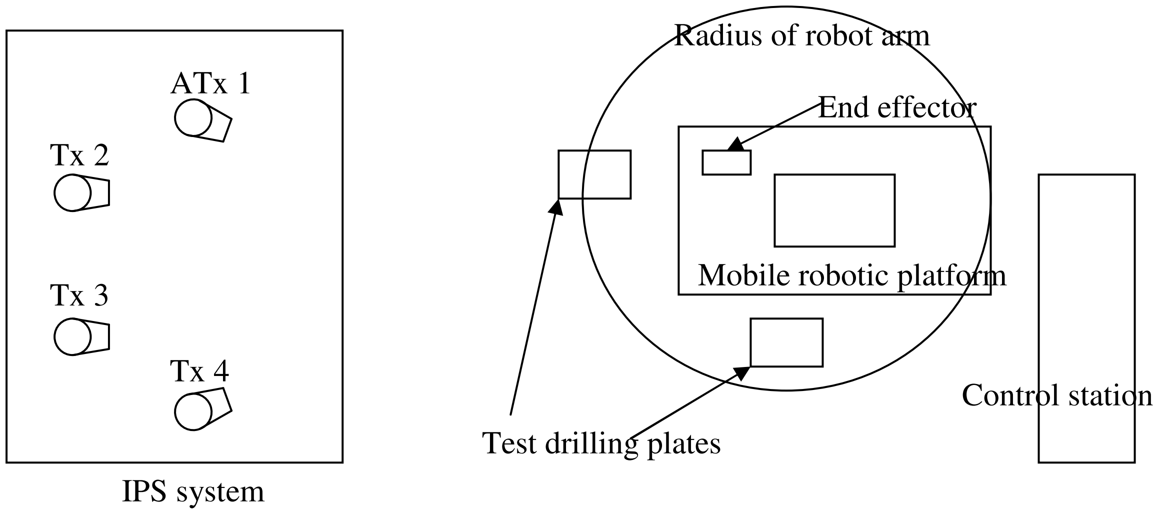

Figure 8.39 - Experimental drilling arrangement

8.3.1 IPS setup

The IPS setup is arranged in the C-configuration utilized previously where extensive setup time can be minimized and measurement achieved from a single side of the measurement area. The receivers were mounted horizontally on the end effector. Chapter 7 identified that this may cause high error, and the "visible" angle must be adequate for appropriate measurement. This is shown below in Figure 8.40.

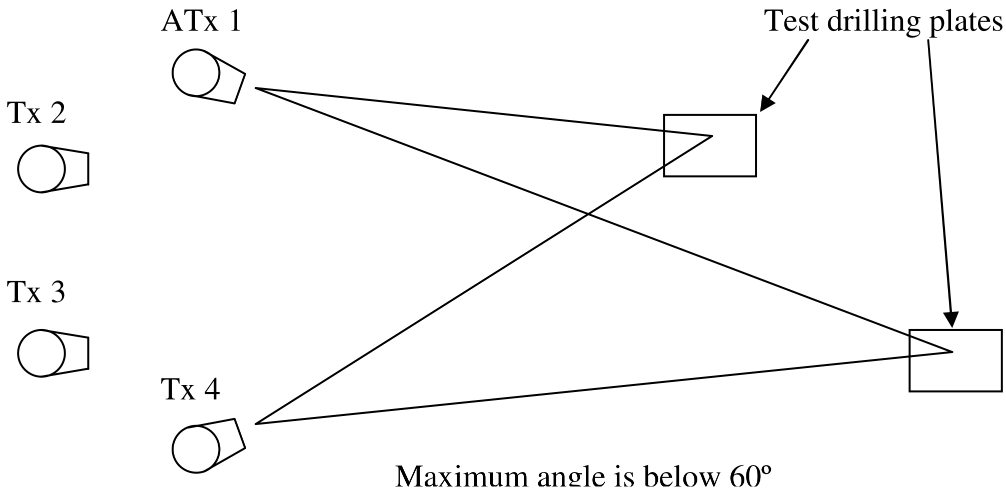

Figure 8.40 – Visible zone in IPS system

As depicted, the maximum angle for interference with the measurement is less than 60º, which is suggested to be effective in Appendix B. This results in an insignificant shadowed area, which is expected not to effect the measured accuracy.

8.3.2 Mobile platform and drilling plate setup

Figure 8.41 demonstrates the setup of the mobile robot and drilling plates. The diagram depicts two separate drilling plates so that the robot can move its end effector throughout its entire range between drilling trials.

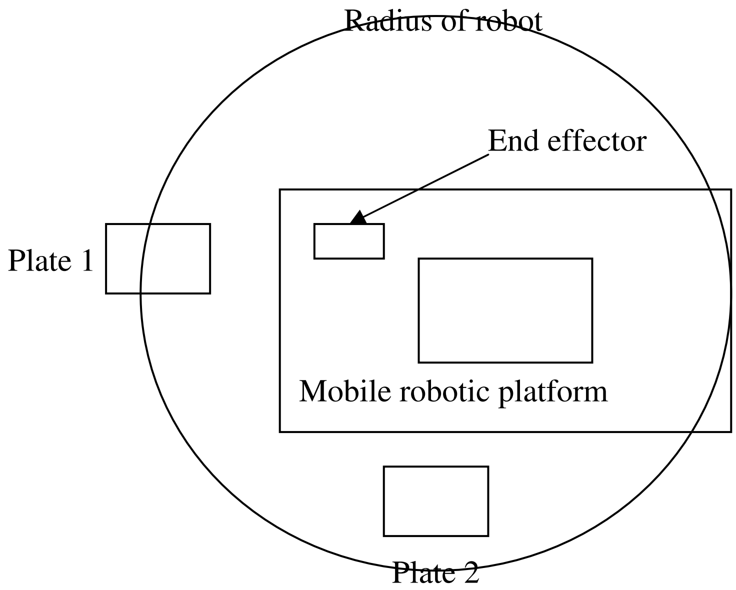

Figure 8.41 - Mobile platform and drilling setup

8.3.2.1 Mobile robotic platform

The “Mobile robot” platform employed has been developed as part of a project within HdH. It was also envisaged that the IPS could be used to guide the platform itself in addition to positioning the end effector. As fine measurement is achieved on the tool, guiding and positioning of the platform may be ignored at this stage because this task is less complex than manipulating the end effector.

The platform itself is a custom built platform of size 1.5[m] x 3[m] developed for HdH. At the time of experimentation an IRB6400 robot was mounted on this platform. The platform is shown in Figure 8.42.

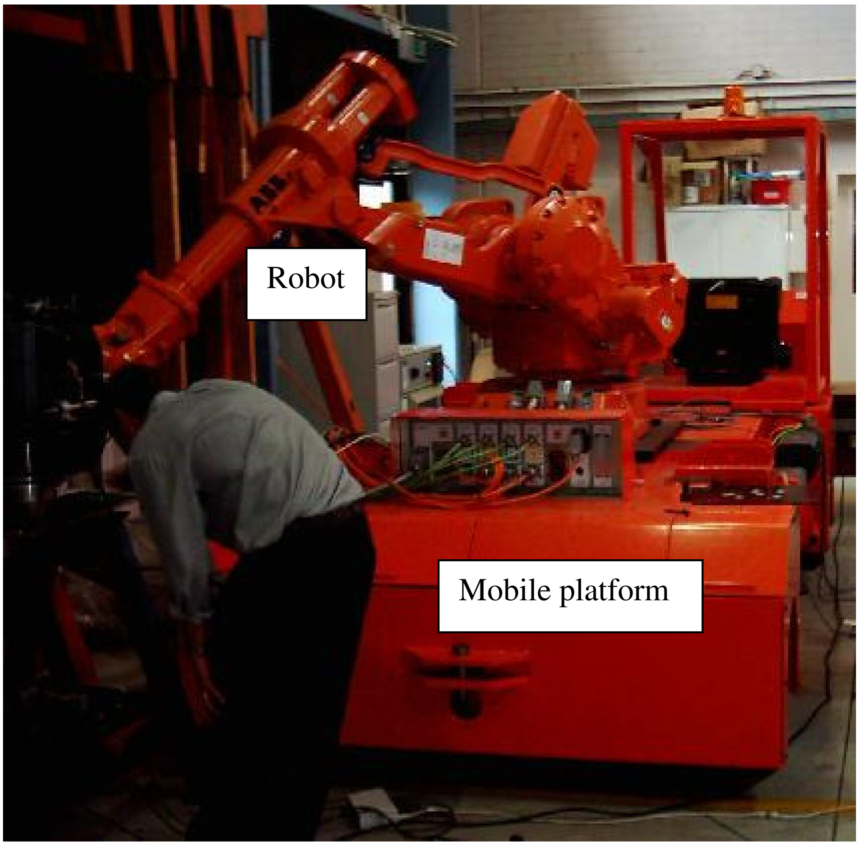

Figure 8.42 - Mobile robotic platform

Figure 8.43 illustrates an example of the drilling plate setup used in the trial. Plates are mounted on steel frames of 50kg mass used previously on drilling trials. The setup ensures that there is no unintentional movement of the part throughout the trial and the frames are light enough to be shifted manually when required. The plates themselves are made of aluminum alloy with mounting provided for composite panels. The plates incorporate a window for drilling as shown in Figure 8.43.

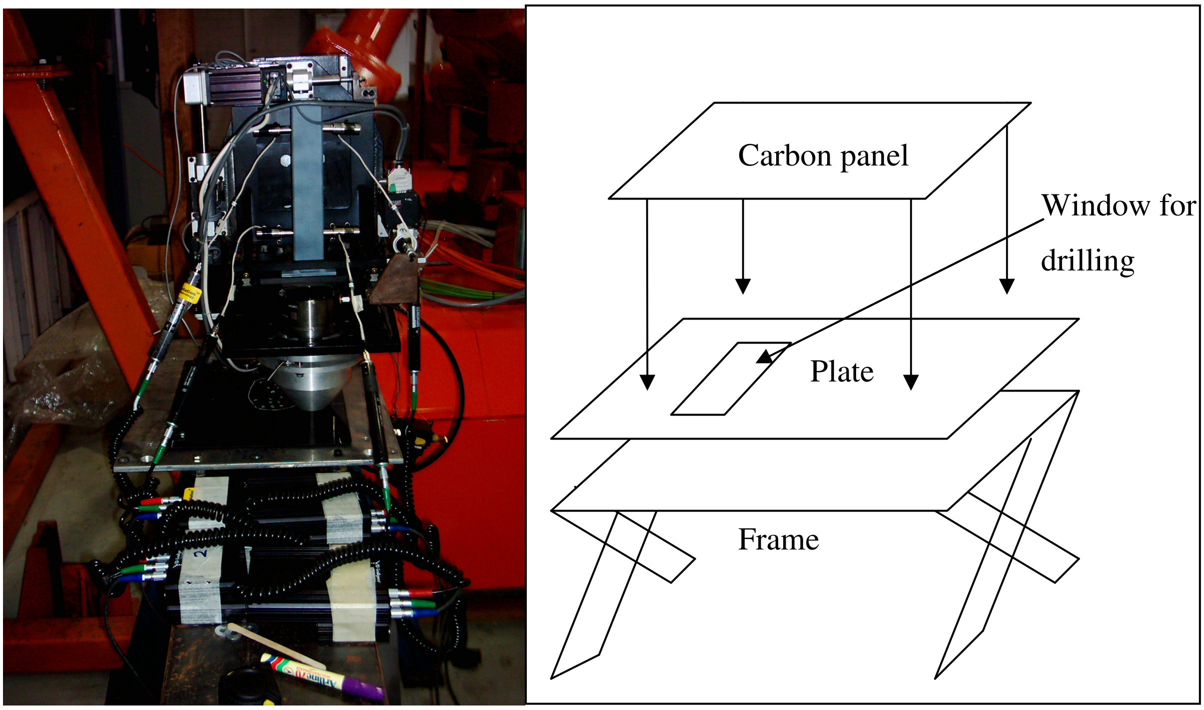

Figure 8.43 - Drilling plate setup

8.3.3 End Effector setup

The drilling end effector employed for this research is a micro-positioning end effector previously used for drilling trials. The end effector is depicted in Figure 8.44.

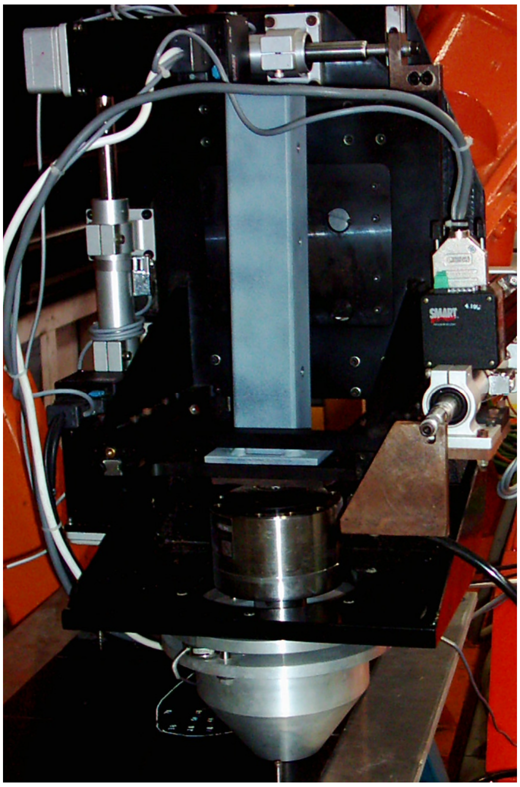

Figure 8.44 - Micro-positioning drilling end effector

The following details of the end effector are relevant to this research:

- Maximum traverse: 100mm.

- 3-axis movement; translation only in all 3 axes.

Placement of the end effector was achieved by movement of the robot arm, with fine positioning achieved by end effector micro-positioning. This fine positioning was achieved using only two axis of the end effector, with the third axis used to raise and lower the tool.

Therefore the end effector had only two <u>effective</u> degrees of freedom.

Receivers were placed on a metal bar fixed rigidly to the end effector as shown in Figure 8.44. This resulted in the receivers being placed close together and horizontally. The distance to the TCP from the receivers will however make this arrangement sensitive to errors in measurement.

8.3.4 Drilling panel

The testing was performed on a 5mm thick carbon composite panel. Following the drilling process, the panel was measured accurately using CMM equipment, results are included in Appendix E.

8.3.5 Drilling pattern

The drilling pattern employed was a pattern of four 4mm diameter holes comprising a central hole with three surrounding holes equally spaced at 120º intervals on a 50mm radius circle, as shown in Figure 8.45.

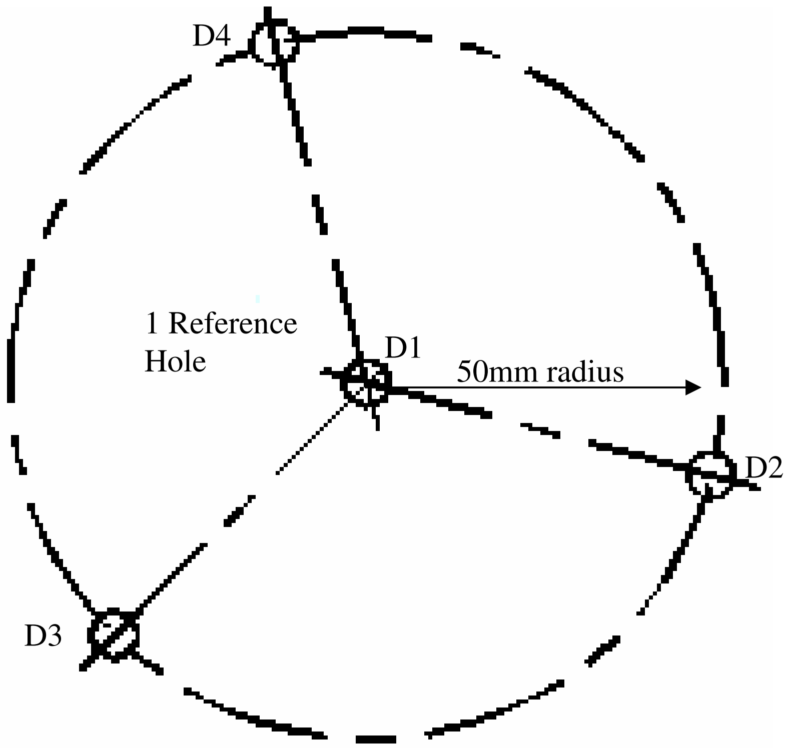

Figure 8.45 - Drilling pattern

8.4 Coordinate frame – Measurement and identification

This testing included precise identification of components within a working area using a series of coordinate frames to identify key components. These coordinate frames are depicted in Figure 8.46.

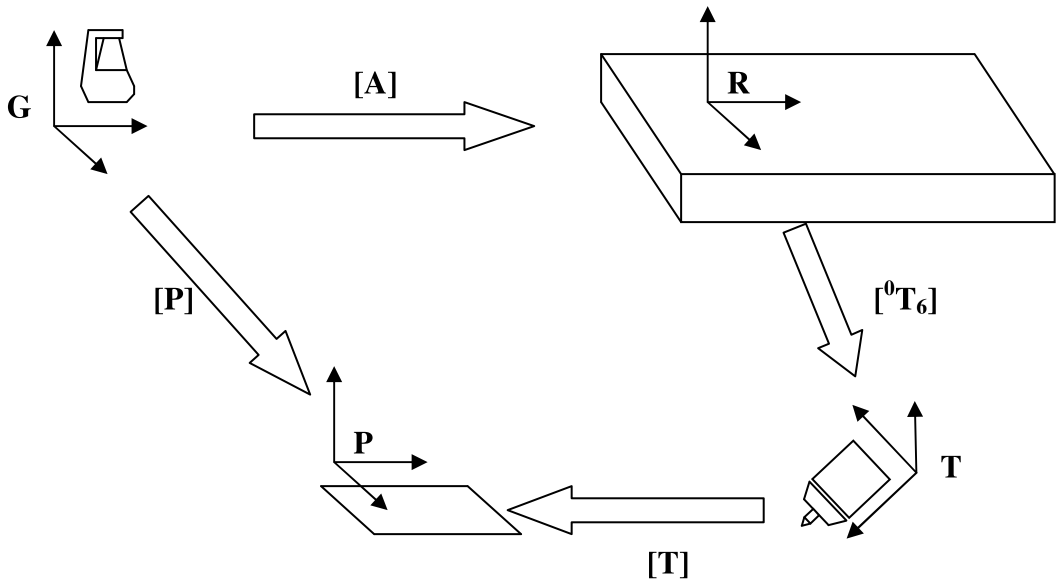

Figure 8.46 - Coordinate frames

The environment consists of the following coordinate frames and transformations:

- Global coordinate frame - G
    - The Global coordinate frame was a stationary inertial coordinate frame characterized by the IPS system. All coordinates were measured in this frame in order to compare tool to part vectors.
- Robot location frame - R
    - The robot coordinate frame is the coordinate frame that describes the positioning of the robot with reference to the global system. This coordinate frame can be passed by taking measurements directly from the tool frame, and referring results to the Global frame using coordinate transforms.
- Inertial Robot Transformation - $[{}^{0}T_{6}]$
    - $[{}^{0}T_{6}]$ is a set of internal robot frames denoting the wrist centre (at the origin of the last internal robot frame) from the robot's base frame.

- Tool coordinate frame - T

    - The tool coordinate frame is used to describe the location of the TCP from frame 6 of the robot. This point is most frequently located at the origin of the tool frame. All measurements can then be taken with reference to the TCP, allowing displacement to be readily input by the operator.

- Part coordinate frame - P_i

    - The part coordinate frame was the frame where coordinates specify measurement points on the part with respect to the origin of the part frame. The most commonly referred points describe the location of required holes to be drilled.

Figure 8.47 shows the relationship between the frames as a transform map.

8.4.1 Transformations

The mathematics controlling transformations is based on methods described by Paul, R. [1981]. The basic methodology is described as follows:

$$Rot(X,\theta)=\begin{bmatrix}1 & 0 & 0 & 0\\ 0 & \cos\theta & -\sin\theta & 0\\ 0 & \sin\theta & \cos\theta & 0\\ 0 & 0 & 0 & 1\end{bmatrix}$$

$$Rot(Y,\theta)=\begin{bmatrix}\cos\theta & 0 & \sin\theta & 0\\ 0 & 1 & 0 & 0\\ -\sin\theta & 0 & \cos\theta & 0\\ 0 & 0 & 0 & 1\end{bmatrix}$$

$$Rot(Z,\theta)=\begin{bmatrix}\cos\theta & -\sin\theta & 0 & 0\\ \sin\theta & 0 & \cos\theta & 0\\ 0 & 0 & 1 & 0\\ 0 & 0 & 0 & 1\end{bmatrix}$$

$$Trans(a,b,c)=\begin{bmatrix}1 & 0 & 0 & a\\ 0 & 1 & 0 & b\\ 0 & 0 & 1 & c\\ 0 & 0 & 0 & 1\end{bmatrix}$$

To allow transformations between matrices the transformation matrices, and their inverses need to be known. The methodology used to determine the inverse matrices was described by Paul [1981] and LaBrooy [1991], given the orthogonal nature of the transforms:

If : $$[A_n]=\begin{bmatrix}n_x & o_x & a_x & p_x\\ n_y & o_y & a_y & p_y\\ n_z & o_z & a_z & p_z\\ 0 & 0 & 0 & 1\end{bmatrix}$$

Then: $$[A_n]^{-1}=\begin{bmatrix}n_x & n_y & n_z & -\vec{p}\bullet\vec{n}\\ o_x & o_y & o_z & -\vec{p}\bullet\vec{o}\\ a_x & a_y & a_z & -\vec{p}\bullet\vec{a}\\ 0 & 0 & 0 & 1\end{bmatrix}$$

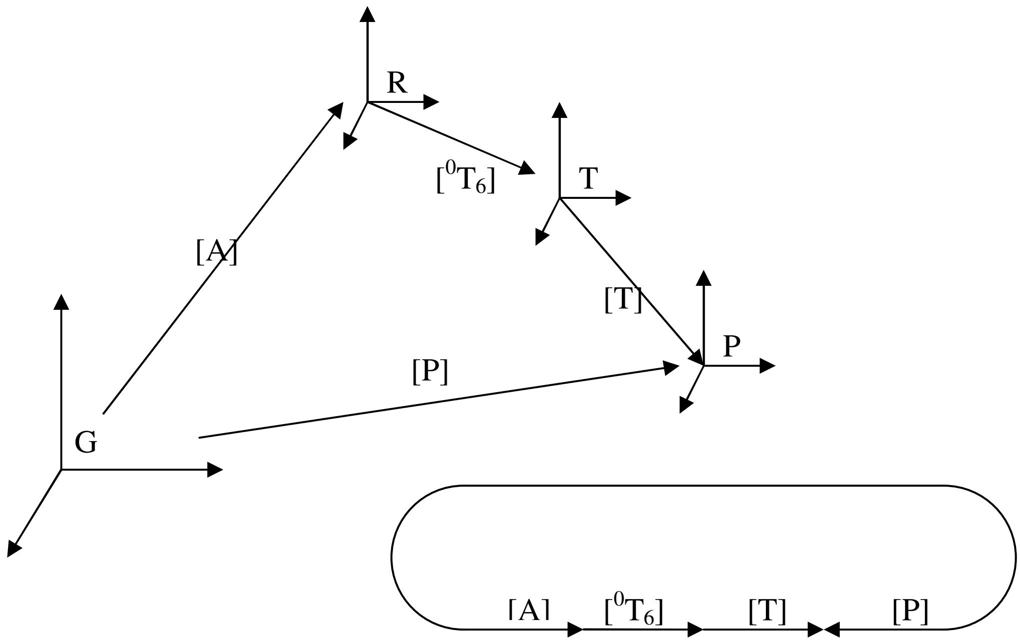

Figure 8.47 - Transform map

$$[A]\cdot[{}^{0}T_{6}]\cdot[T]=[P]$$
$$[A^{-1}]\cdot[P]=[{}^{0}T_{6}]\cdot[T]$$

8.4.2 Calculation of Rotations and Translations

Calculation of rotations and translations were completed using Microsoft Excel Solver functions. An example of the spreadsheets and function description is also included in Appendix E.

This methodology included setting boundary values known to be above and below the actual values for each rotation and translation entity followed by iteration of these values. As each measurement included four separate receivers the accuracy of solution was determined using the minimum difference between the calculated and measured results, again described in Appendix E.

8.4.3 Data analysis – TCP correction

To complete measurements and identify movements required, all measurements were required to be adapted into coordinate frames represented in Figure 8.48:

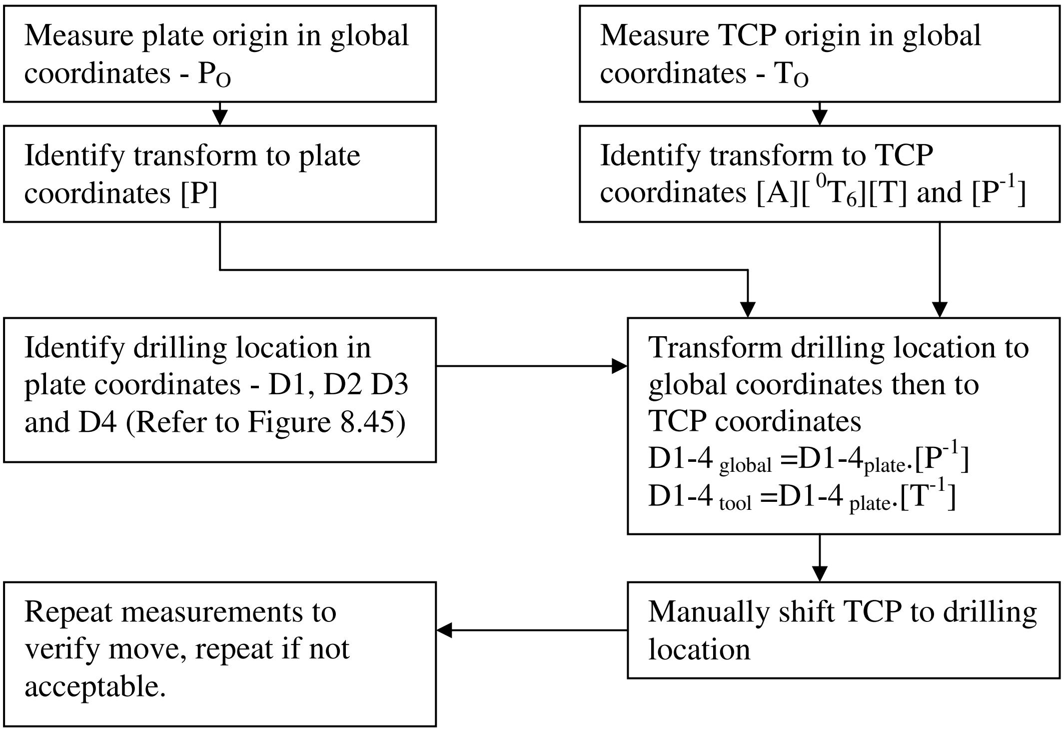

Figure 8.48 - Coordinate frame conversions

8.5 Test 1 – Measurement of pre-programmed drilling operations

In Test 1 a robot's tool was firstly positioned arbitrarily at a location D1 (Drilling location 1, as depicted in Figure 8.45) on a carbon fibre panel. The robot was moved under program control to 3 other locations (D2, D3, D4) on the carbon fibre panel relative to D1. Any accuracy errors resulting from reaching subsequent holes will be generated by the robot's inability to precisely reach D2, D3 and D4 due to computational error in the ideal mathematical model programmed into the robot. The physical location of the resulting holes was then measured by CMM measurement.

8.5.1 Feedback loop – Stage 1

The data employed for test 1 comprised of recording the drilling locations and identifying the accuracy of positioning the tool of the robot via robot transforms. Error related to the inability of the robot tool to reach a desired position. Hence only recording of positions was performed. The loop for this data analysis is depicted in Figure 8.49.

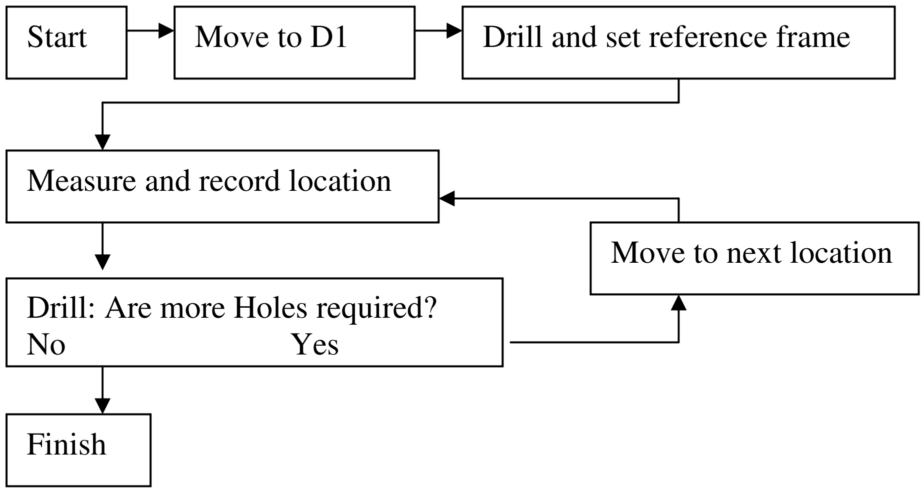

Figure 8.49 - Feedback loop Stage 1

8.5.2 Measurement results

Table 8.21 demonstrates the average error of drilling these holes in 4 trials. This measurement (the expected locations compared to the CMM measurement) used the central hole as a reference point. Expanded results are included in Appendix E.

Table 8.21 – Physical error of drilled holes: Test 1

Test 1	
Trial	Mean Error (mm)
1	0.565329
2	0.204471
3	0.181868
4	0.424021
Average between trials	0.343922

The results in Table 8.21 demonstrate that the accuracy of actual drilled locations was within 0.34mm over the robot span of 2800mm. The error presented here is the variation between the actual measured location of the drilled hole, and the expected location of the hole, as shown below in Figure 8.50.

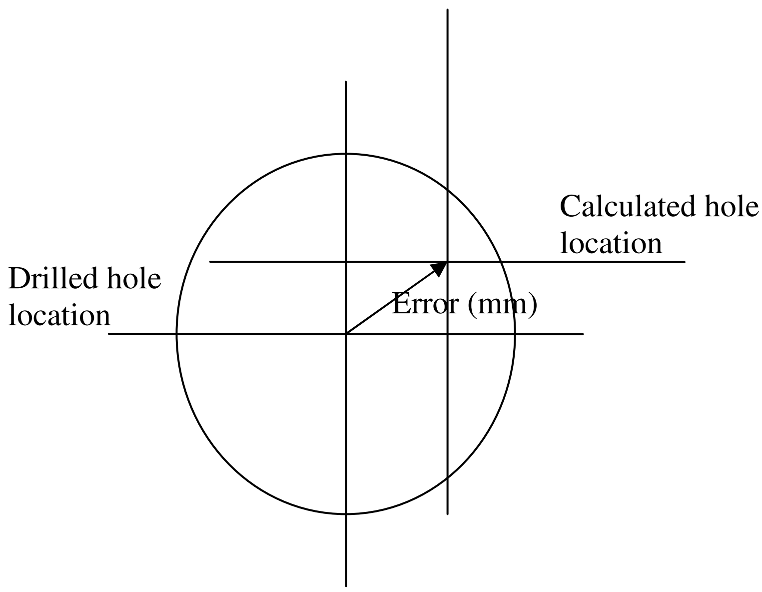

Figure 8.50 - Drilled hole error

8.5.3 Recommendations

- Measurement demonstrated at approximately 0.34mm accuracy was well above the micron level stated in Van Duin (2000). It can be assumed that the system was inherently incapable of achieving these levels of accuracy without additional precise control. This will impact on the accuracy of the IPS controlled drilling trials.

- Further drilling trials are required employing the IPS as a means of control to identify if this will affect the accuracy of drilling trials.

8.6 Test 2 – IPS guided drilling operations

Test 2 consisted of drilling operations guided by the IPS system. Due to the process employed IPS data was entered manually to move the end effector.

Receivers were located on the tool and part as shown in Figure 8.51. Receivers 1-4 were fixed rigidly to the end effector relative to the TCP, and receivers 5-8 were located on the part. The tool was located by analysis of measured locations of receivers 1-4. The location of the TCP was calculated with respect to these. Hence the location of D1, D2, D3 and D4 were calculated using data from all eight receivers. The end effector was manually moved and the process repeated with points D3 and D4.

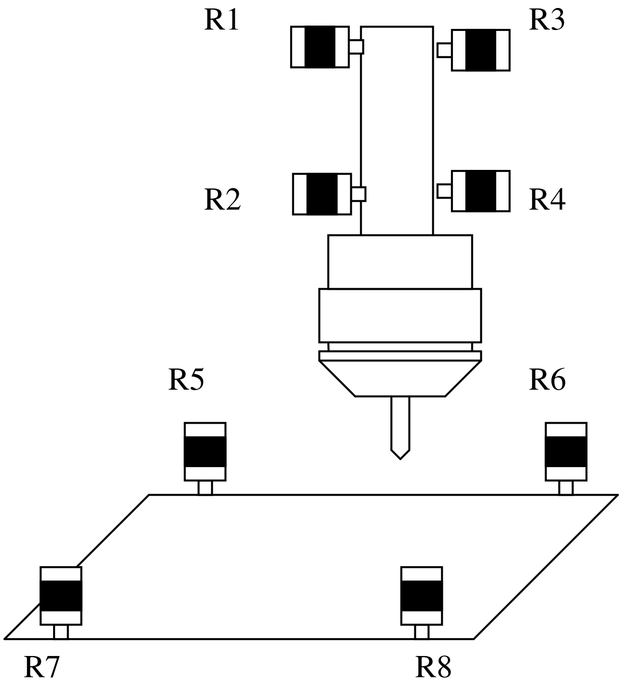

Figure 8.51 - IPS receiver locations on End Effector

8.6.1 Feedback loop – Stage 2

The feedback loop described in section 8.5.1 was adjusted to include data returned to the system. The feedback loop for this operation is depicted below in Figure 8.52.

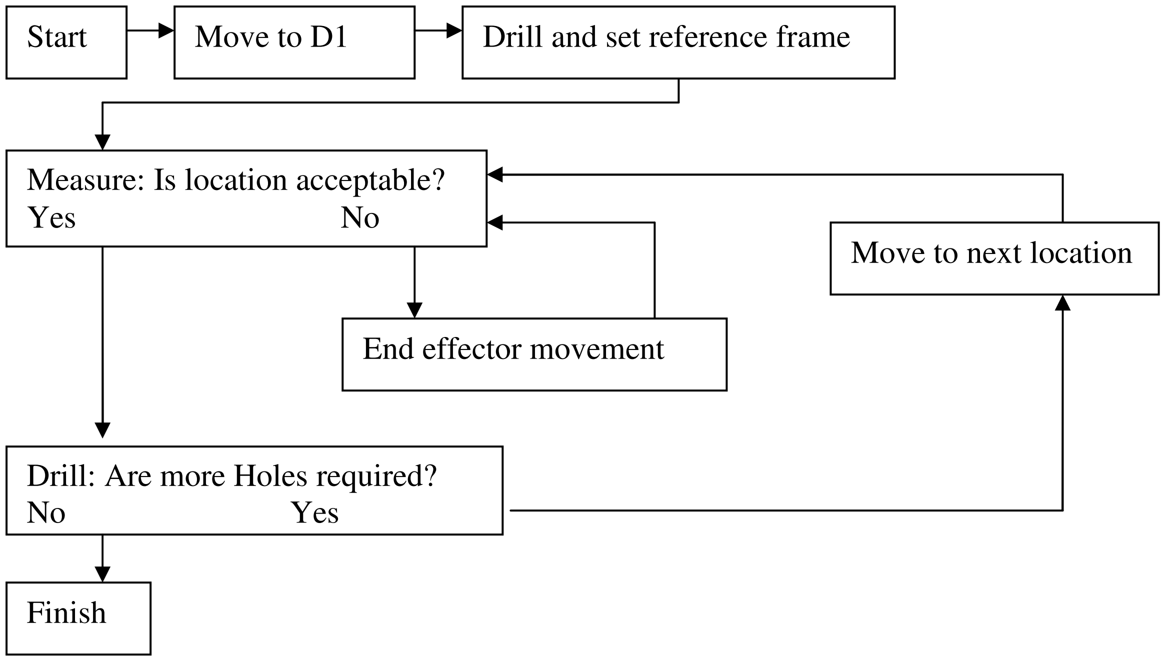

Figure 8.52 - Feedback loop Stage 2

8.6.2 Measurement results

Table 8.22 presents the average error of this scheme compared to the CMM measurement. Note that an additional trial was completed employed precision point data discussed in previous chapters, with a sample size of 20 measurement. Expanded results are included in Appendix E.

Table 8.22 – Physical error of drilled holes: Test 2

Test 2: IPS positioning	
Trial	Mean Error (mm)
1	0.322099
2	0.250891
3	0.338152
4	0.389657
5	0.39133
6	0.327524
20 sample	0.322686
Average	0.33462

The results demonstrate that the IPS controlled drilling results in an accuracy of 0.33mm this suggests that the accuracy of the IPS when used as a means of control for the system is similar to the accuracy of the micro-positioning end effector itself demonstrating internal robot computational errors.

This also suggests that the use of Precision point data will not offer a substantial benefit in physical drilling trials.

8.6.3 Recommendations

- IPS control shows no improvement on the accuracy of the operation in excess of the inaccuracy of the end effector itself.

- A single sample with larger numbers of measurement points (20) demonstrated that this does not significantly alter the error of the IPS/robot system.

- Further testing must be completed to identify if the IPS system control is able to accurately place the TCP to where the robot is moved by an unknown distance.

8.7 Test 3 – "Bump 1": Movement of end effector

Previous testing involved drilling holes about a central reference point, but did not demonstrate the capability to re-locate the initial drilling location (D1), if moved unintentionally. Using IPS feedback the robot's end effector may be relocated if bumped and returned to the known global location of D1

Therefore, Test 3 consisted of drilling operations guided by IPS measurement, including movement of the robotic platform during this process. D1 and D2 were drilled under IPS control as per Test 2. The robot was then disturbed and the tool was required to find D3 under IPS control.

8.7.1 Feedback loop – Stage 3

The feedback loop described in section 8.6.1 was adjusted to include data on the new end effector location and adjustment. The feedback loop for this data analysis is depicted in Figure 8.53.

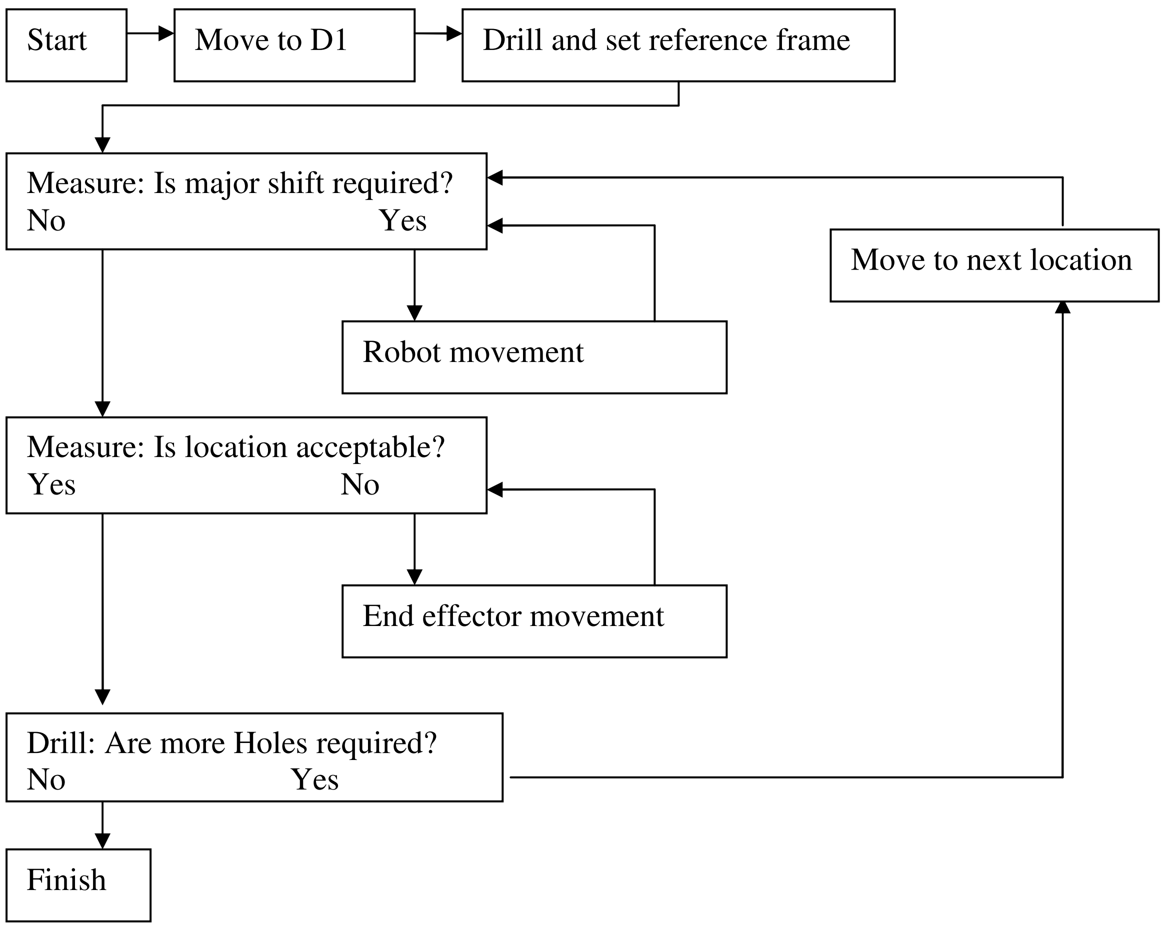

Figure 8.53 - Feedback loop Stage 3

8.7.2 Measurement results

Table 8.23 demonstrates that the average error of drilling trials is approximately 0.32mm. Expanded results are included in Appendix E. The important point is that the robot can relocate itself at the same inherent level of accuracy as its intended systems will allow if perturbed. This is significant as external controllers can now guide the robot with the same level of precision but over the range of the IPS workspace of a 35 meter square.

Table 8.23 – Physical error of drilled holes: Test 3

Test 3: Robot movement	
Trial	Mean Error (mm)
1	0.171324
2	0.197824
3	0.251859
4	0.460826
5	0.438082
6	0.423247
Average	0.32386

The results above demonstrate that the IPS controlled drilling resulted in an accuracy of 0.32mm while the system was compensating for movement of the robotic platform. This demonstrated that movement of the robotic platform and end effector has no significant impact on error.

8.7.3 Recommendations

- IPS may be used to cater for unintentional robotic platform movement.

- IPS control had no significant impact on the accuracy of the operation in excess of the inaccuracy of the end effector drilling trials. This suggested that the IPS is bounded most importantly by the repeatability of the robot, as demonstrated previously.

- Further testing must be completed to identify if the IPS system control was able to accurately place the TCP when the plate is moved by an unknown distance.

8.8 Test 4 – "Bump 2": Movement of drilling plate

Previous measurements consisted of drilling a set pattern of holes, this resembles the standard manufacturing process of robot operations on a pre-determined piece in a set location. Test 4 was designed to examine if the system was capable of accounting for movement of a workpiece, altering the actual process of operation. If successful true flexibility in manufacturing would be possible.

In Test 4, D1 and D2 only were drilled. The plate was now moved (rotated and translated).

The IPS was then used to calculate both degree of rotation and translation by measurement of 4 receivers on the plate.

D3 and D4 were drilled under IPS control as before but the test now incorporates rotated and translated entities of the plate.

8.8.1 Feedback loop – Stage 4

The feedback loop described in section 8.7.1 was adjusted to include movement of the plate and adjustment of the required location. The loop for data analysis is depicted in Figure 8.54.

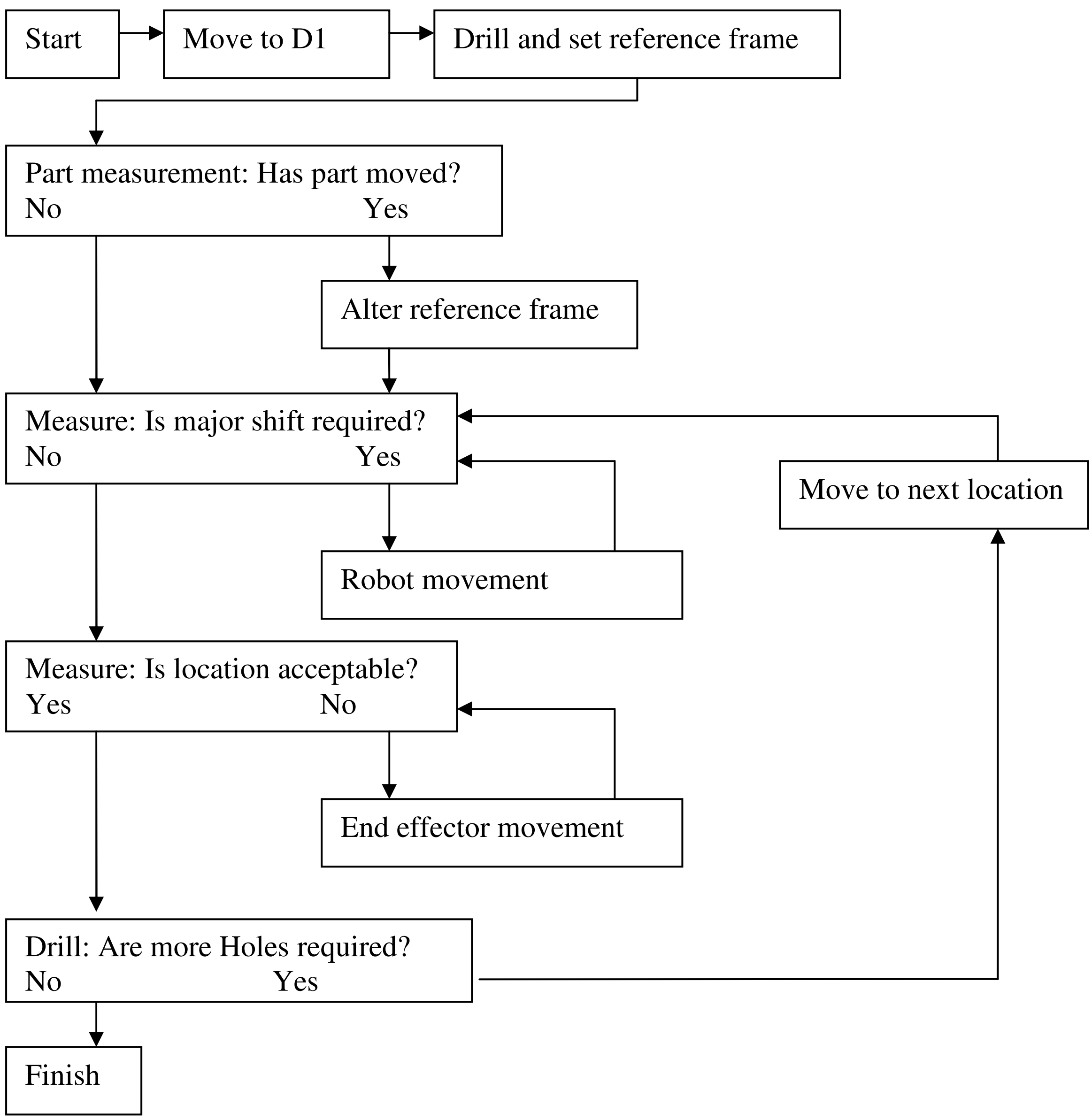

Figure 8.54 - Feedback loop Stage 4

8.8.2 Measurement results

Table 8.24 demonstrates the average error of drilling trials. Expanded results are included in Appendix E.

Table 8.24 – Physical error of drilled holes: Test 4

Test 4: Plate movement	
Trial	Mean error (mm)
1	0.469909
2	0.512868
3	0.314712
Mean	0.432496

The data in Table 8.24 demonstrate that the IPS controlled drilling results in an accuracy of 0.43mm, where the IPS is compensating for movement of the part. The level of accuracy is a 33% increase on the previous tests.

8.9 Summary of Results and Discussion

- Teach pendant positioning of the end effector gives an error of 0.34mm signifying the degree of computational internal error of a robot.
- An IPS guidance of end effectors provided an error of approximately 0.33mm. A maximum error of 0.43mm (approximately 0.5mm) was recorded for testing where both plate and end effector were perturbed.
- These errors were of the same order as teach pendant testing of the end effector itself, and therefore equivalent to the repeatability of the robot.
- When translated into practice, huge time savings may be evident where part and robot may be re-located by the IPS and re-positioned automatically if perturbed at any time to ensure correct operation.
- The flexibility of IPS guided robots has been therefore demonstrated.

8.10 Review of Key objectives

Phase Three testing has investigated the use of IPS for automated and machining tasks, Table 8.25 lists the achievements of the system compared to the original key attributes listed in Chapter 3.

Table 8.25 - Key attributes as of phase 3

Key	Attribute	Status
1	*System must be able to identify objects rapidly, including, but not restricted to, robotic tools, and workpieces.* • The system was proven capable of identifying position and posture of items, and developing adjustment data automatically.	*Substantially achieved*
2	*Measurement and control of systems must be capable using a minimum of workstations.* • Measurement was performed using a single portable computer, however due to the system robot controls were restricted to a control station.	*Achieved*
3	*Must be capable of micro-measurement, and micro-positioning of both end effectors and workpieces.* • Capable of fine measurement, and positioning below 0.5mm, restricted by the repeatability of the robotic tool.	*Substantially achieved*
4	*Must be capable of taking measurement in under 2 seconds.* • Measurement required approximately 5 seconds to complete accurately.	*Partially achieved*
5	*System must be capable of measuring and deploying multiple robots simultaneously, along with workpieces and additional requirements.* • Not yet demonstrated.	*Not yet demonstrated*
6	*System must be capable of adjusting tool centre point locations to allow for workpiece movement during the operation.* • Demonstrated accurately below 0.5mm.	*Demonstrated below 0.5mm.*
7	*Equipment must be readily portable and robust.* • All equipment readily moved by hand/vehicle with installation within an hour.	*Achieved*
8	*The system should be applicable to a number of different industries with minimal variation to the initial components.* • Tasks were not industry specific.	*Achieved*

8.11 Conclusions

The IPS was commissioned as a means for robotic control conducting successful dynamic testing and drilling operations. It was noted that:

- The system is capable of identifying part locations and robot end effector posture simultaneously in a short time period.

- The system is capable of identifying and adjusting for perturbation of both part and robot throughout machining process with the same level of accuracy as inherently possessed by the robot.

- Incorporation of an IPS guidance system gives the overall system a degree of stability if either or both part and system are pertubated.

- The degree of accuracy is the same as though the robotic end-effector was under its own program control without the added safeguard of being able to automatically relocate to a global location.

- The placement of robotic end effectors where deployed from a mobile platform is applicable over the entire IPS workspace, which is approximately a square of 35 meters.

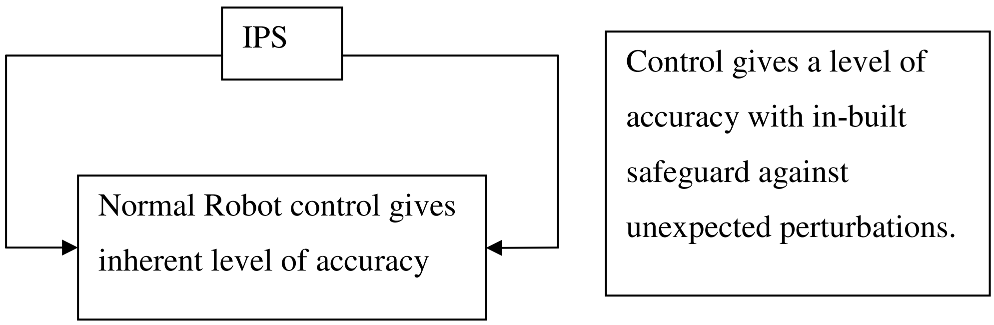

Figure 8.55 - IPS control

9 Chapter 9: Employing IPS – future developments

9.1 Introduction

This chapter describes several concepts for further development of the use of IPS in manufacturing of precision components. Due to restrictions throughout this research these could not be fully explored and may form the basis of future research into this area of manufacturing.

9.2 Automated robot control

This research has demonstrated IPS positional feedback used for control of drilling trials as an example of guiding precision manufacturing tasks. The research was reduced to the basic concept of application of a TCP to a location on a part, where both robot tool and part location are known to be unstable. This concept was intentionally generic so as to be readily utilised by a variety of tools, robotic systems and manufacturing tasks.

As discussed in previous chapters, the process may be improved by permanent location of transmitters and updated receivers and software. The experimentation in Chapter 7 demonstrated control of a single robotic system as this was limited by equipment available. The use of greater numbers of receivers and robotic systems will allow a number of concurrent operations within the workspace.. Additionally, area not dedicated to robotic manufacturing tasks surrounding the workspace may be used for other tasks, including quality assurance. An example IPS working area is depicted in Figure 9.56.

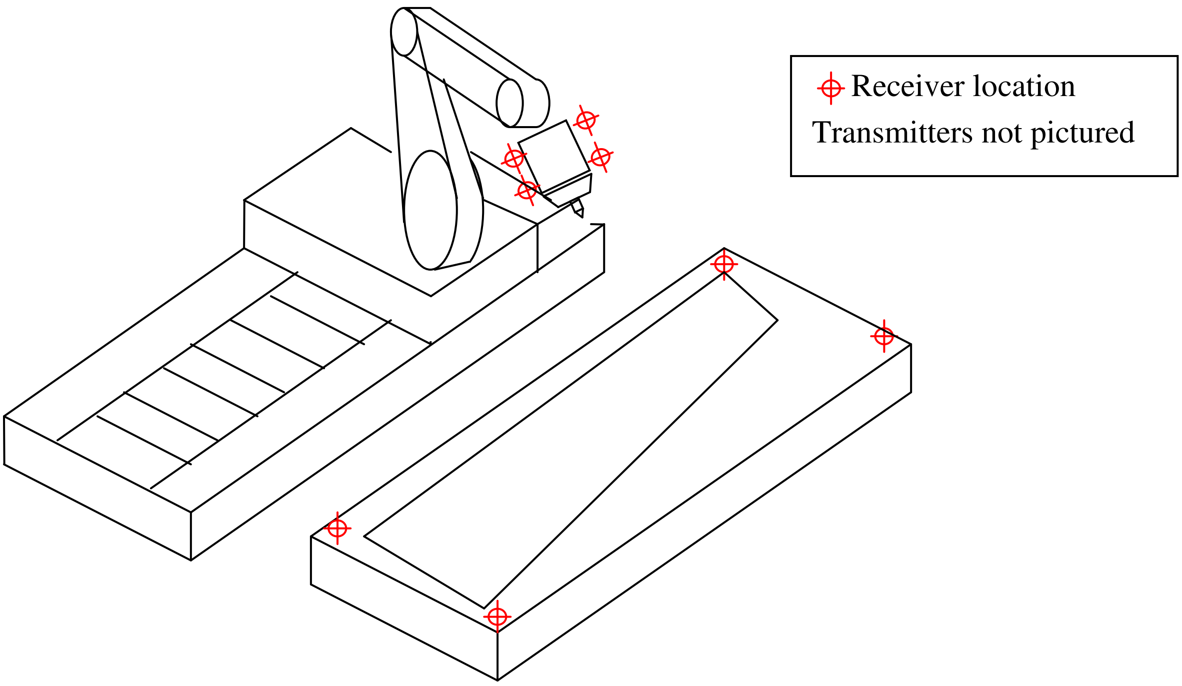

Figure 9.56 - Example IPS controlled working cell

9.3 Flexible manufacturing

Chapter 8 examined the use of IPS for controlling robotic movement of an end effector, including "Bump 1" and "Bump 2" demonstrating effective control of the manufacturing task where there is relative movement of the robot platform and part. This relied on accurate identification of movement and re-application of the drilling pattern in the updated location.

By alteration of the drilling pattern during or between drilling trials it is possible to manufacture alternate versions of the article in the machining process without increase in operating time or robot downtime. This concept is depicted in Figure 9.57.

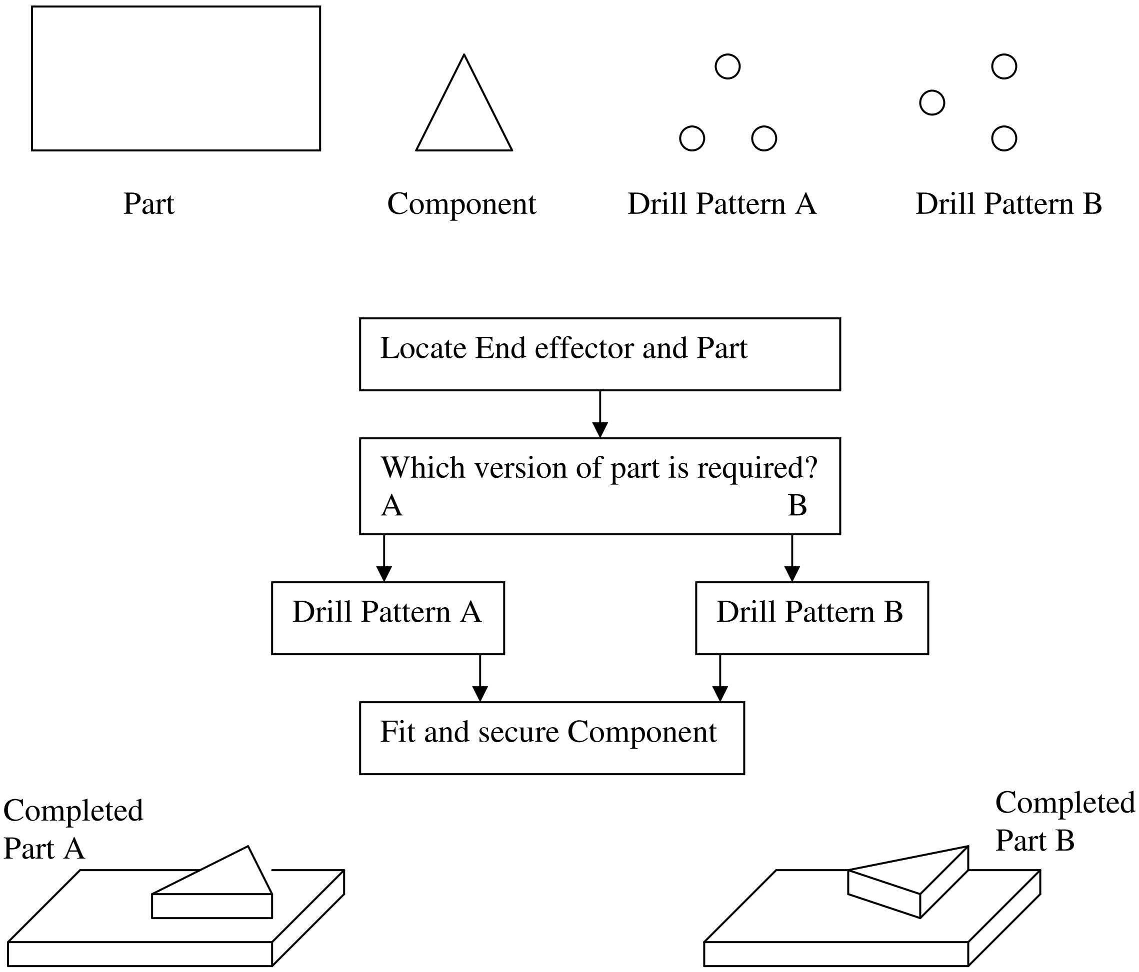

Figure 9.57 - Flexible drilling process

An extension of this is the use of a variety of robotic tools with an interchangeable end effector. This concept may allow real flexibility in the precision robotic manufacturing process.

9.4 Moving assembly line concept

An extension of the mobile robotic platform concept is the use of mobile platforms for mounting of parts. Receivers would be mounted on platforms providing positional data of the part allowing manufacturing tasks to be performed on the part in any location.

9.5 Conclusion

Testing described in this dissertation is restricted to simple items and robots. The extension of this process to develop may be achieved by the following:

- Increased/improved equipment (system and receivers) – This would allow for the commissioning of an IPS guided autonomous robotic cell.

- Variation of pattern and positional data between trials – This would allow for flexible operations on the part.

- End effector tool changer – This would allow flexible manufacturing with a minimum of different systems.

- Mobile part platforms – This would allow for the development of a moving assembly line.

Due to the generic nature of experimentation described in this dissertation these concepts would require little further development to achieve.

10 Chapter 10: Research conclusions and recommendations

10.1 Introduction

This dissertation has provided a thorough examination of research into identification of the IPS system as an option to provide positional information to control automated manufacturing systems. The adaptation of current robotic systems to advanced control techniques such as IPS is envisaged to provide a step change in the field of automated manufacturing. It also demonstrated that the system is readily capable of dealing with flexibility of both the robotic tools, and parts. The system would also be applicable to mobile platforms during the manufacturing process.

In this research, the development of control systems for manufacturing tasks on large components typical to that of the aerospace industry has been focused however the systems are by no means restricted to only a single field of manufacture, and would be equally applicable with a variety of processes and tools.

10.2 Review of Key attributes developed by the research

The Key attributes developed in Chapter 4 are reproduced in Table 10.26.

Table 10.26 - Key attributes

Key	Attribute
1	*System must be able to identify objects rapidly, including, but not restricted to, robotic tools, and workpieces.*
2	*Measurement and control of systems must be capable using a minimum of workstations.*
3	*Must be capable of micro-measurement, and micro-positioning of both end effectors and large workpieces to an accuracy of less than 0.1mm.*
4	*Must be capable of taking measurement in under 2 seconds.*
5	*System must be capable of measuring and deploying multiple robots simultaneously, along with workpieces and additional requirements.*
6	*System must be capable of adjusting tool centre point locations to allow for workpiece movement during the operation.*
7	*Equipment must be readily portable and robust.*
8	*The system should be applicable to a number of different industries with minimal variation to the initial components.*

10.2.1 Key attribute 1 – System must be able to identify objects rapidly, including, but not restricted to, robotic tools, and workpieces

The system has demonstrated its capacity to identify positional information at a rate of 10Hz for single point data and 0.5Hz for 20 point data. Precision point data and therefore data quality, are inverse to the data acquisition rate.

Experimentation in Chapter 8 employed only single data point measurements, suggesting that positional data may be obtained at a rate of 10Hz resulting in a reliable error below 0.5mm over a working area of approximately 30 square meters. The calculation of position and orientation from this data presented in Chapter 8 relied on manual operation of excel functions, this may be programmed to reduce calculation time to insignificant.

This measurement included workpiece and tool measurements, however is not restricted to these. Additional items may be measured simultaneously by employing a greater quantity of IPS receivers.

Substantially achieved.

10.2.2 Key attribute 2 – Measurement and control of systems must be capable using a minimum of workstations

All measurement is achieved using a single portable PC operating at 2Ghz. The IPS software is windows based and readily installed into other workstations allowing robot controllers to measure IPS targets in parallel with operation of their dedicated systems. This method allows data feedback to automatically control robot movement.

Substantially achieved.

10.2.3 Key attribute 3 – Must be capable of micro-measurement, and micro-positioning of both end effectors and large workpieces to an accuracy of less than 0.1mm

The system has demonstrated the capability to place an end effector with an absolute accuracy of below 0.5mm in Chapter 8. Chapters 6 and 7 demonstrated that the IPS measurement accuracy may be below 0.1mm given ample setup, testing and adjustment time for equipment. It can be suggested that with similar test time and redundant data (receivers) for robotic trials the accuracy of an absolutely placed TCP should be equivalent to the accuracy of the IPS system.

Achieved.

10.2.4 Key attribute 4 - Must be capable of taking measurement in under 2 seconds

Chapter 3 demonstrated that data for positional measurement may be acquired at a frequency of 10Hz, however employing precision point data values this may be reduced to 0.2Hz or lower. Testing in Chapter 8 demonstrated that precision point data was unnecessary for accurate tool placement.

Substantially achieved.

10.2.5 Key attribute 5 – System must be capable of measuring and deploying multiple robots simultaneously, along with workpieces and additional requirements

Chapter 8 demonstrated that a workpiece and end effector may be measured simultaneously. The number of concurrent measurements was restricted only by the available equipment.

Discussion in Chapter 3 indicated that the IPS is theoretically capable of measuring an unlimited number of receivers within a working area. This indicates that where position and orientation calculations are readily achieved a large number of concurrent measurements will allow for identification of a number of tools and workpieces simultaneously.

Not achieved, suggested by analysis.

10.2.6 Key attribute 6 – System must be capable of adjusting tool centre point locations to allow for workpiece movement during the

operation

Adjustment for both robot platform and part movement was positively demonstrated in Chapter 8, Section 8.7 and 8.8. Accuracy of the continued drilling operation was superior to 0.5mm.

Substantially achieved.

10.2.7 Key attribute 7 – Equipment must be readily portable and robust

Equipment packs into three cases each one weighing less than 100kg, measuring less than 1mx0.5mx0.5m in the largest dimensions. These are designed to carry all required equipment and protect from damage. During operation the metric value discussed in Chapter 6 is used as a means of identifying when system operation has been interrupted and a transmitter may be out of position. Recalibration allows system to continue measurement readily, ensuring that the process is not sensitive to interruption.

Substantially achieved.

10.2.8 Key attribute 8 – The system should be applicable to a number of different industries with minimal variation to the initial components

Experimentation as part of this research has been performed in a generic manner. While the research is aimed at aerospace manufacturing tasks, processes are not restricted to aerospace components.

Chapters 6 and 7 aimed at assessment of the system as a position server, and the data is used for analysis of the system only. Chapter 8 performed drilling on a composite panel, although the process included a robotic tool and material specific to aerospace manufacture the process of identification and adjustment is designed to be part independent and thus applicable to other industries.

Substantially achieved.

10.3 Conclusion

The key attributes for this research have been fulfilled, as noted in Table 10.27.

Table 10.27 - Revision of key attributes

Key	Attribute	Comment	Notes
1	*System must be able to identify objects rapidly, including, but not restricted to, robotic tools, and workpieces.*	*Substantially achieved*	
2	*Measurement and control of systems must be capable using a minimum of workstations.*	*Substantially achieved*	
3	*Must be capable of micro-measurement, and micro-positioning of both end effectors and workpieces.*	*Achieved*	*Measurement accuracy below 0.5mm, however analysis suggests that this may go below 0.1mm with more access to robotic tools and IPS equipment.*
4	*Must be capable of taking measurement in under 2 seconds.*	*Substantially achieved*	
5	*System must be capable of measuring and deploying multiple robots simultaneously, along with workpieces and additional requirements.*	*Considered and is regarded as an extension to the work specified herein.*	
6	*System must be capable of adjusting tool centre point locations to allow for workpiece movement during the operation.*	*Substantially achieved*	
7	*Equipment must be readily portable and robust.*	*Substantially achieved*	
8	*The system should be applicable to a number of different industries with minimal variation to the initial components.*	*Substantially achieved*	

This dissertation has demonstrated the capability of the IPS as a tool for the control of robotic manufacturing operations. The use of this equipment allows for control of robotic systems and adjustment for interruptions to the manufacturing process. Further development will offer this process as a means of reducing the costs and risks of robotic manufacturing.

Future development in this area will allow for a realistic means of controlling flexible manufacturing operations, and the development of moving assembly line processes with multiple robots and micro-precision machining. It is expected that this would offer a step change in the automated manufacturing of precision parts within, but not restricted to, the aerospace sector.

In conclusion the research has demonstrated that the IPS feedback used to control manufacturing operations on flexible structures or machines is limited to 0.5mm over a working range of 30 square meters. The accuracy of the IPS for manufacturing tasks was within the sub-millimetre region (0.3mm was achieved) when both robot and workpiece were moved by an unknown quantity over a working area of 30 square meters.

The candidate has demonstrated that the IPS system can effectively control manufacturing operations on large, flexible objects typically encountered in aerospace structures to tolerances that are acceptable by this important industry.

11 Chapter 11: References

Aoyama, H. Iwata, F. Sasaki, A. [1995] *Desktop flexible manufacturing system by multiple robots*, Proc. Of Int. Conf. on Robotics and Automation. pp. 660 – 665

ArcSecond Inc. [2002] "Constellation 3Di Error Budget and Specifications" <http://www.indoorgps.com/PDFs/wp_Eroor_Budget.pdf>, last accessed 12 April 2006.

ArcSecond Inc. [2003] *Indoor GPS users guide, ArcSecond*, U.S.A.

Atkinson, K. B. [1997] *Close Range Photogrammetry and Machine Vision*, Whittles Publishing, Caithness, Scotland.

Bonghetti, A. [2005], Personal communication.

Burner, A. W. Liu, T. [2001]Videogrammetric model deformation measurement technique, *Journal of Aircraft*, Vol 38 no. 4, July-August 2001, pp. 745-754.

Choi, H. S. Han, C. S. Kim, S. S. Kim, E. Z. Choi, T. H. Na, K. H., [2003] *A study on the development of a micro-positioning device for forming milli-structures*, SICE 2003 Annual Conference, 2003.

Clarke, T. Wang, X. Forbes, A. Cross, N. [2000] "The case for a consistent method of verifying the performance of large volume metrology systems." Co-ordinate Measurement Committee Conference, August 2000.

Constant, T. Mothe, F. Badia, M. Saint-Andre, L. [2002] "How to relate the standing tree shape to internal wood characteristics: Proposal of an experimental method applied to poplar trees." Wood quality Research Team, Research centre of Nancy, 54280 Champenoux, France.

Davidson, K. [1985] *Robots and Screw Theory: Application of Kinematics and Static to Robotics*, Oxford University Press, U.S.A.

Eos systems Inc [2000] *PhotoModeler Pro 4.0 users manual*, Vancouver, B. C. Canada.

Geodetic Services Inc.(GSI) [2006] <http://www.geodetic.com/vstars.htm> last accessed 12 April 2006.

Gruen, A. ([997] Fundamentals of videogrammetry – A review, *Human Movement Science*, Iss. 16, pp.155-187.

Heath, L. [1985] *Fundamentals of Robotics: Theory and applications*, Prentice Hall, Virginia.

Hefele, J. Brenner, C. [2000] *Robot Pose Correction using Photogrammetric Tracking*, In: Machine vision and three dimensional imaging systems for inspection and metrology, Photonics East, Boston.

Hohn, M. Robl, C. [1999] *Qualification of standard industrial robots for micro-assembly*, Proceedings of 1999 IEEE International Conference on Robotics and Automation, Detroit, MI.

Huang, W. H. [2000] *A tapping micropositioning cell*, Proceedings of ICRA '00. IEEE International Conference on Robotics and Automation, 2000., San Francisco, CA.

Kyle, S. Loser, R. Warren, D. [1997], "Automated part positioning with the laser tracker", Proceedings of the Fifth International Workshop on Accelerator Alignment, ANL/FNAL, Argonne, IL.

LaBrooy, R. [1991] *The kinematics of Robots*, RMIT University, Melbourne.

Leica Geosystems [2006] <http://www.leica-geosystems.com/metrology/en/products/laser_tracker/lgs35317.htm> last accessed 12 April 2006

Martin, A. Gilbert, P. Lee, E. [2001], *Measurement of Structural Deflection in a Training Aircraft under Manoeuvring Loading conditions*, Unpublished report.

McKerrow, P. [1991] *Introduction to Robotics*, Addison-Wesley, U.S.A.

Pappa, R. Giersch, L. Quagliaroli, J. (2001), Photogrammetry of a 5m inflatable space antenna with consumer-grade digital cameras, *Experimental techniques*, Vol 25, no 6, pp. 1033-1040.

Paul, R. [1981] *Robot Manipulatiors: Mathematics, programming and control*, MIT press, Cambridge.

Roskam, J. [1995] *Airplane flight dynamics and automatic flight controls*, DARcorporation, Kansas, U.S.A.

Steele, P. [2005], Personal communication.

Yi, B. Na, H. Chung, G. B. Whee Kuk Kim, W. K. Suh, I. H. [2002] *Design and experiment of a 3 DOF parallel micro-mechanism utilizing flexure hinges*, Proceedings of IEEE International Conference on Robotics and Automation, 2002, Washington DC.

Van Duin, S. [2001] Unpublished report.

Van Duin, S. [2006], Personal communication.

Young, J. [1973] *Robotics*, The Butterworth Group, London

Appendix A: IK solution set for a typical robot

Example summary of an inverse kinematic solution set for a typical robot.

$\Phi_1 = \tan^{-1}(p_y/p_x)$ or $\Phi_1 = \Phi_1+180°$ $\Phi_{234} = \tan^{-1}[(C_1 a_x + S_1 a_y)/(-a_z)]$ $\Phi_3 = \tan^{-1}(S_3/C_3)$ Where $C_3 = [(C_1p_x+S_1p_y)^2+p_z^2-a_2^2-a_3^2]/(2a_2a_3)$ $S_3 = \pm\sqrt{(1- C_3^2)}$ $\Phi_{n45} = \tan^{-1}[(S_1n_x-C_1n_y)(S_1o_x-C_1o_y)]$ $\Phi_2 = \tan^{-1}[(ea-db)/(da+eb)]$	Where $a = p_x$ $b = C_1p_x+S_1p_y$ $c = S_3a_3$ $d = C_3a_3+a_2$ Also $\Phi_4 = \Phi_{234}- \Phi_2- \Phi_3$ $\Phi_4' = \Phi_{n4}=n^* \Phi_4$ $\Phi_5 = \Phi_{n45}- \Phi_{n4}$

Appendix B: IPS, setup and operation

B.1 Basics of metrology

Metrology is the basis for many measurement systems, IPS included. Although this is of great importance to this area of study, an extensive discussion is of little relevance to this dissertation. Therefore only a brief discussion of the applicable metrology principles is be presented here. This analysis is based entirely on the work of Atkinson [1996], ArcSecond Inc. [2003], Eos Systems Inc. [2000] and Geodetic Services Inc [2006]

B.1.1 Basic Metrology Principles

The principles of metrology are employed in many different applications, including navigation, photogrammetry and operation of the IPS. To demonstrate the concept of metrology the example of photogrammetry is to be employed here.

Photogrammetry involves the taking of a number of images of an object from a variety of angles surrounding the object. At this point it can be considered that the images consist of a "snapshot in time" as movement of the item between images cannot be allowed. (Atkinson [1996])

B.1.2 Use of Triangulation

The analysis of metrology data is based on the concept of Triangulation. A series of "rays" are projected from the camera locations to each target location. The intersection of these "rays" determines the object's absolute location. This concept is depicted in Figure B.58.

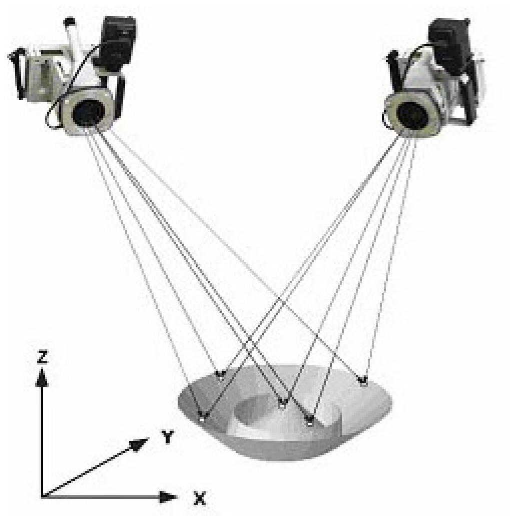

Figure B.58 – Photogrammetric "rays" to an object

(Geodetic Services Inc [2006])

These “rays” are lines projected to infinity in space. It is the convergence of these lines that is used to calculate the positional information. If the camera locations are known, the positional data of each target can then be calculated.

If the parameters of the system are not known a calibration is required. This process is based on a mathematical algorithm referred to as “bundle adjustment” (so called because the procedure examines the “bundles” of rays in space at each location. (Atkinson [1996], ArcSecond Inc. [2003] and Geodetic Services Inc [2006])

B.1.3 Metrology preparation

There are several factors that metrologists need to consider common to any survey, and form the basis for planning projects. (Atkinson [1996])

B.1.3.1 Four factors of accuracy

The following sections outline the four major aspects to consider when performing a survey, as discussed in Geodetic Services Inc (2002).

B.1.3.1.1 Number of intersecting "rays"

The principle of triangulation used for metrology surveys suggests that the maximum base stations possible should be used for a survey that requires high accuracy. As additional data can serve to improve the accuracy of each measured point as well as assess the degree of error for marked points within the survey.

Whilst large data sets involve more complex calculations, there is little variation on the basic concept. Indeed, most metrology surveys will use many data sets, such as in the photogrammetry work discussed by Martin, Gilbert and Lee [2001], where approximately 100 images are used in measuring displacements of the PC-9 fatigue test aircraft. Pappa, Giersch and Quagliaroli [2001] used only four digital cameras for their survey of an inflatable space antenna.

B.1.3.1.2 Resolution

Atkinson [1997] suggests that resolution of an objects' image is limited by the image capture area sensor's sensitivity. At the limit, this will be 1 pixel. It is important to distinguish between adjacent positions using this criteria.

Resolution is more commonly associated with camera quality, as the size of the numbers of pixels available in a digitized image. Geodetic Services Inc [2002] discusses this in terms of the accuracy available in an image and the capability to separate points on an image. This suggests that increasing the resolution is likely to improve the accuracy of a survey by allowing more detail of its' features to be distinguished on the sensor.

B.1.3.1.3 Geometry

Another consideration is geometry, which relates to intersection angles of the measured points. Gruen [1997] suggests that generally it is ideal to have projected ray angles intersecting at, or as close to, 90 degrees as possible. Figure B.59 demonstrates this concept.

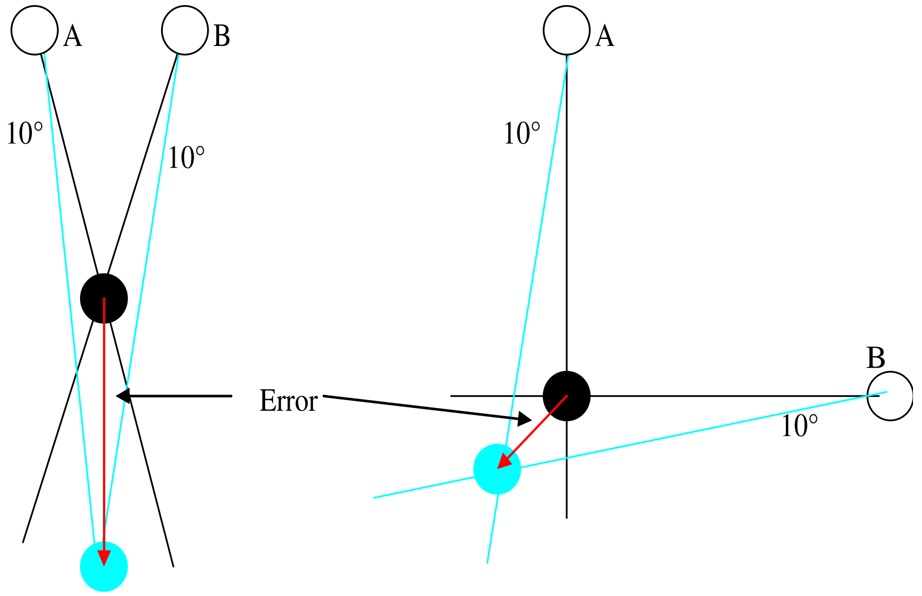

Using rays emanating from two base stations, the black lines indicate the actual location of a point and the blue lines indicate inaccurate measurement, 10° from the correct direction. Note that the image with poor measurement accuracy shows far greater error for the same 10° error.

Figure B.59 - Intersection rays and error

B.1.3.1.4 Complexity of object

The final factor discussed here is the complexity of the survey. Geodetic Services Inc (2002) suggests that the more complex an item, the more difficult it becomes to perform an adequate location survey. This may be considered in reference to other factors where a difficult survey may not allow for images to be taken from ideal locations or only allow few useful images.

B.2 IPS

The IPS transmitter can be likened to two fan-shaped laser beams (LB1 and LB2) coupled to each other and rotating in synchronisation about axis Z.

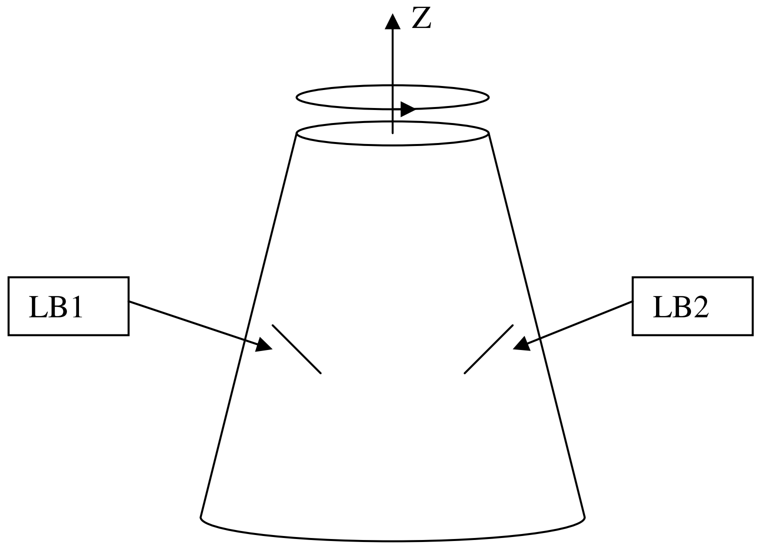

Figure B.60 - Physicality of IPS transmitter head

The fan-shaped beams are in a fixed geometric relationship to each other at 90° apart on the vertical (Z) axis, where their apertures can produce fan-shaped beams. The beams are projected at +/-30° from the horizontal plane The beam can be mapped to produce data resulting in timing pulses which in turn can be mapped to produce elevation and azimuth data relating to the location of measured points.

Figure B.61 demonstrates how geometric data is processed to produce information regarding the location of receivers located on a part.

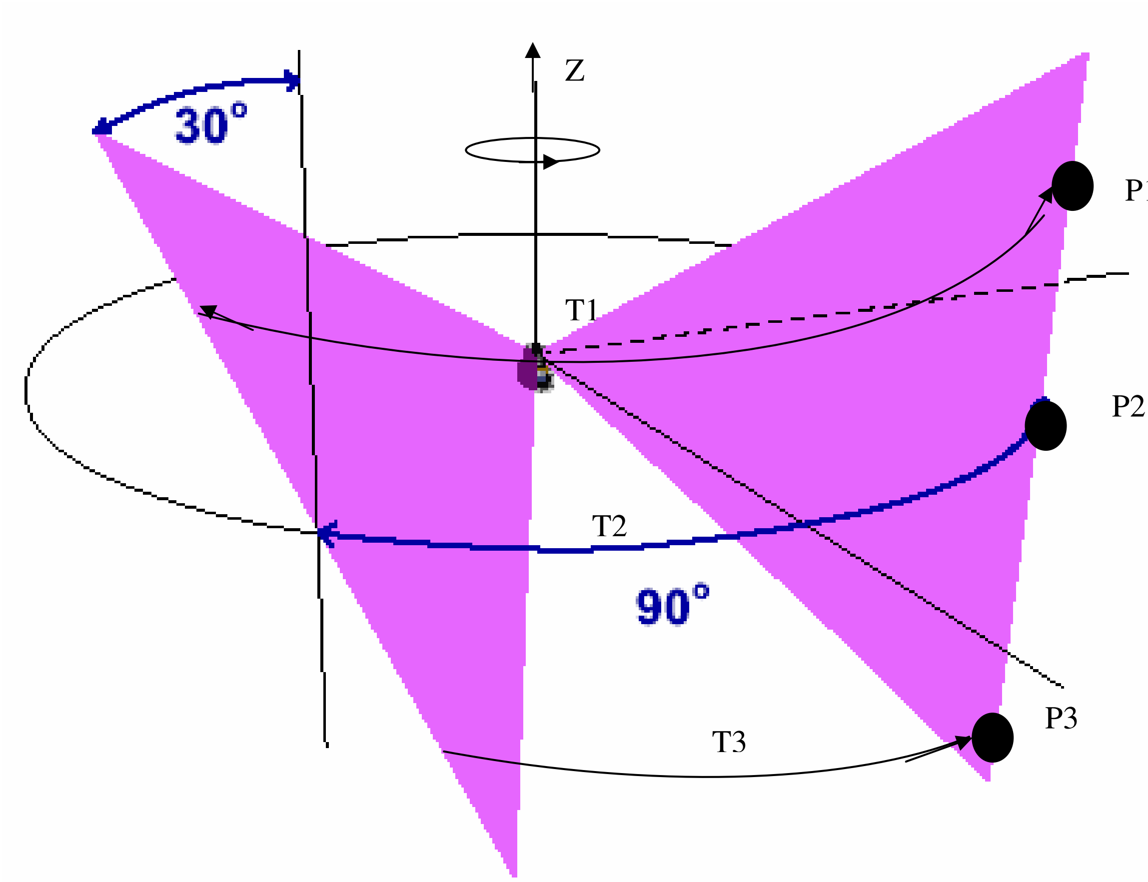

Figure B.61 - Calculation of positional data

(Adapted from ArcSecond Inc [2003])

P1, P2 and P3 are as detected by fan 1, and T1, T2 and T3 are the time it takes respectively for fan 2 to reach these locations. This timing data is then analysed to determine vertical angle. A strobe once every two cycles is used as a reference to identify the azimuth angles. These angles are then employed using triangulation methods to provide positional data, Figure B.62 graphically describes an example of timing data as recorded by a receiver.

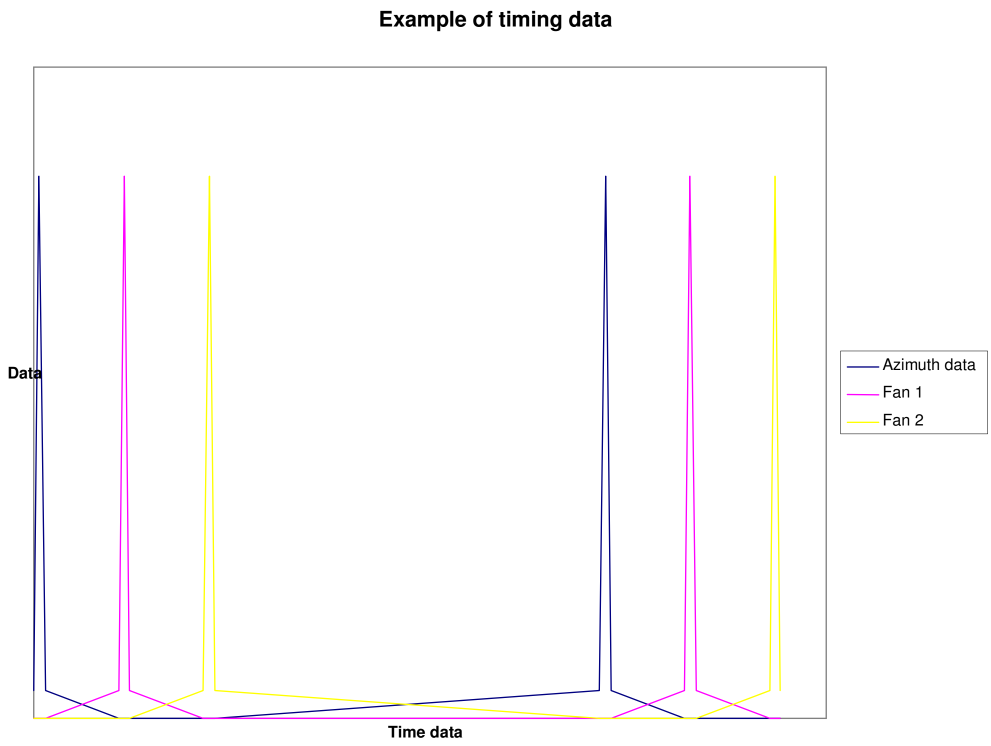

Figure B.62 - Figure of measurement example

When a receiver “sees” the signal from two or more transmitters, the position of that receiver may then be calculated using triangulation assuming that transmitter locations are known. The location of transmitters is determined through a calibration process discussed later. This calibration sequence identifies the position and orientation of each transmitter, establishing the required reference stations. With streaming data, a rate of up to 20Hz may be achieved, however testing for this dissertation found that this resulted in poor data resolution and 10Hz was the effective maximum.

B.2.1 Setup or Calibration

To determine a location the receiver must correctly convert the intervals described above, the transmitter location and orientation need to be known relative to the system. The 6 degrees of freedom of each transmitter are precisely determined during the setup process. This is critically important as the quality of all position data is heavily dependant on the quality of setup data. (ArcSecond Inc. [2003])

The method of determining transmitter location uses the "Bundle Adjustment" method. The three stages of bundle adjustment are as follows:

a) Collect observations

At each observation point the system measures a "ray" (azimuth and elevation angle) from each transmitter to receiver. These rays are at this stage lines projected into space, with no information to bound the line by transmitters or receivers.

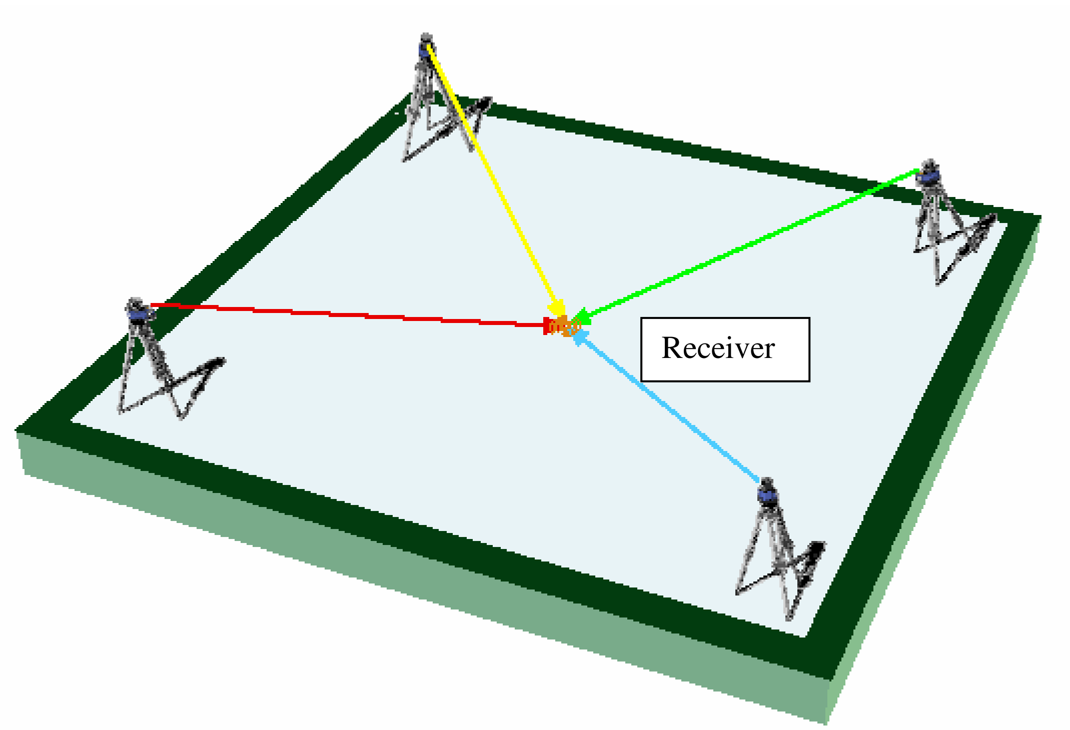

Figure B.63 – Single IPS observation

(ArcSecond Inc. [2003])

b) Apply scale

At this stage there is no data referring to the size or location of components in the system. This means that the data is ill defined, and the application of a scale between two known points will indicate the magnitude of measurement. The scale is often set using “scale bars”.

c) Calculate a solution

Finally, calculation of the data relies on analysis of “bundles” of ray converging on each location. (It is this process that provides the term “bundle adjustment”.) The Bundle adjustment algorithm requires that each of these rays converges at the given location, where mapping interpretation provides position and orientation of respective transmitters.

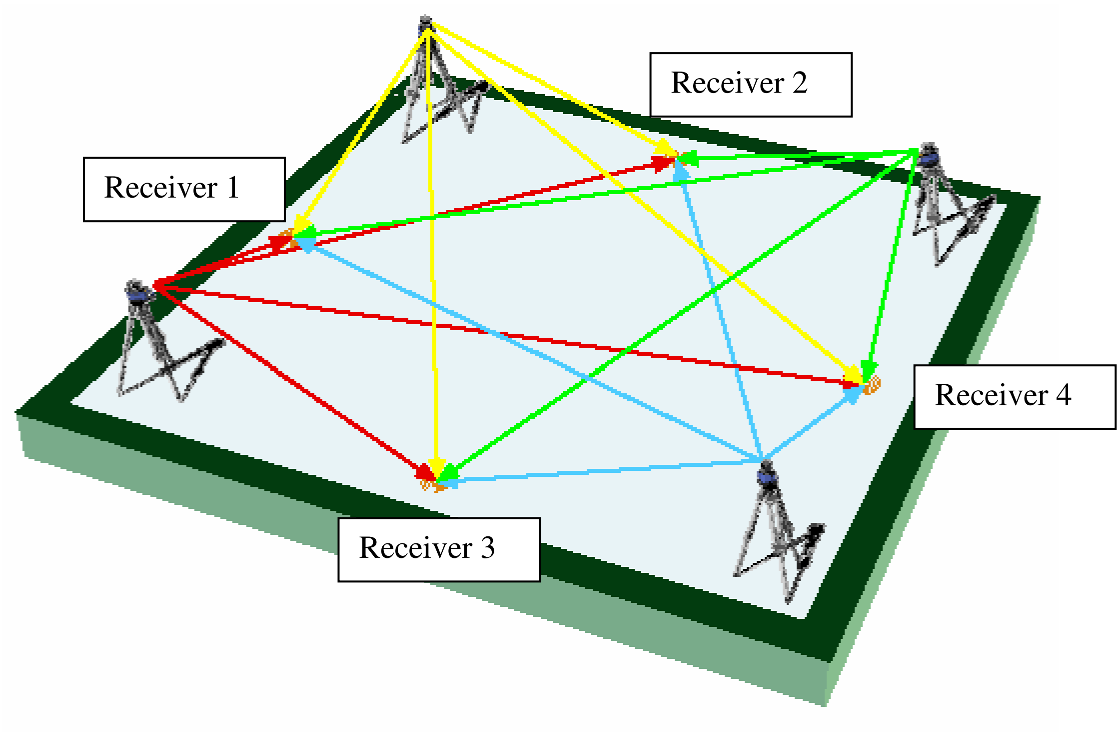

Figure B.64 – Multiple IPS observations

(ArcSecond Inc. [2003])

B.2.2 M-value (metric)

The metric (or M-value) is a representative of the “best closure” of ray bundles, which means the shortest distance form the calculated position to the closest ray. This M-value will be very large unless the setup is accurate. The M-value should not be taken to be a direct indication of error, however if offers an indication of error.

The M value is the minimum distance perpendicular to a ray from the location of a receiver. The M-values are shown below for 3 Rays ($R_1 - R_3$).

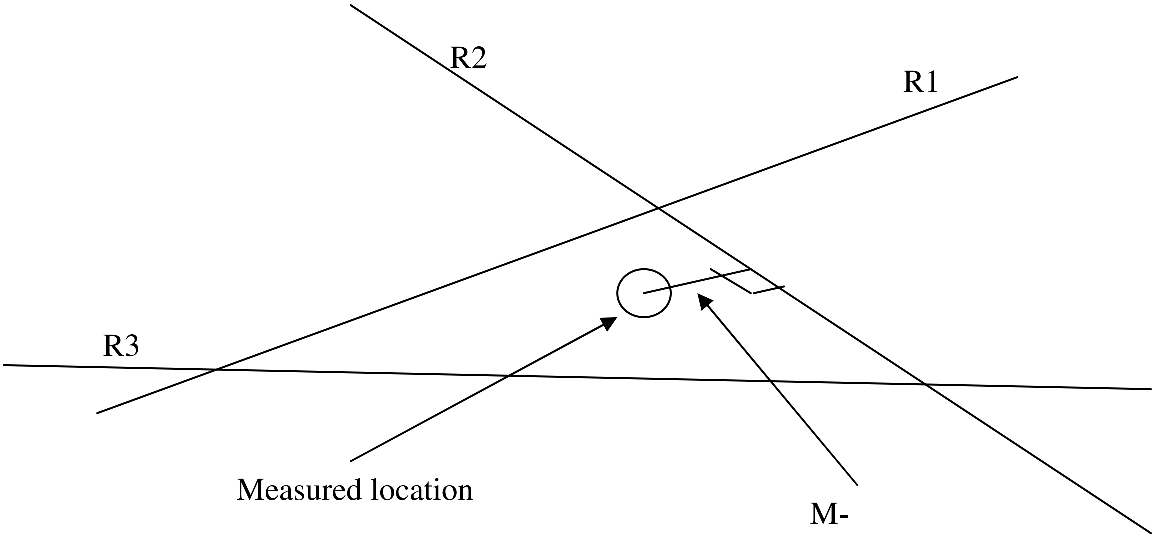

Figure B.65 - Example of M-value

B.2.3 Precision point data

A development in IPS measurement was the use of the "Precision Point" function. This allows an operator to set an interval based on time or number of measurements, all data collected during this time is analysed as a bundle to produce a single precise measurement. This has been employed throughout testing during this research.

B.3 Components

This section is a summary of equipment discussed in ArcSecond Inc. [2003]

B.3.1 Hardware

Figure B.66 - IPS hardware

(ArcSecond Inc. [2003])

B.3.1.1 Transmitters

The system consists of 2 to 6 transmitters, which come in two grades, industrial and metrology grades depending on the requirements of the user. Generally, industrial requirements offer accuracy of 1mm or less, while metrology purposes offer sub-millimetre accuracy.

The transmitters require rechargeable batteries.

Figure B.67 - IPS transmitter

(ArcSecond Inc. [2003])

B.3.1.2 Sensors

The IPS receiver consists of a sensor (photodiode detector) and it's associated digital signal processor. This generally consists of a receiver, amplifier and PCE (position calculation engine). The receivers PCE requires a rechargeable battery.

B.3.1.2.1 Types of sensors

- Vector bar

Two receivers in a bar, amplifier included.

Figure B.68 - Vector bar

(ArcSecond Inc. [2003])

- Receiver

Basic receiver offers 360 degree by 120 degree coverage. 8 or 32 planar surfaces.

Figure B.69 - Cylindrical receiver

(ArcSecond Inc. [2003])

- Planar receiver

Flat receiver, allows approximately 170 degree cone angle.

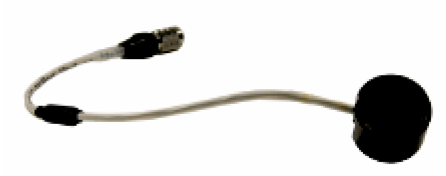

Figure B.70 - Planar receiver

(ArcSecond Inc. [2003])

- Measurement tools.

Consist of a set of receivers in a mechanical arrangement to identify an unknown point. A single receiver might be used if its centre is unknown.

- Arrangement of a receiver

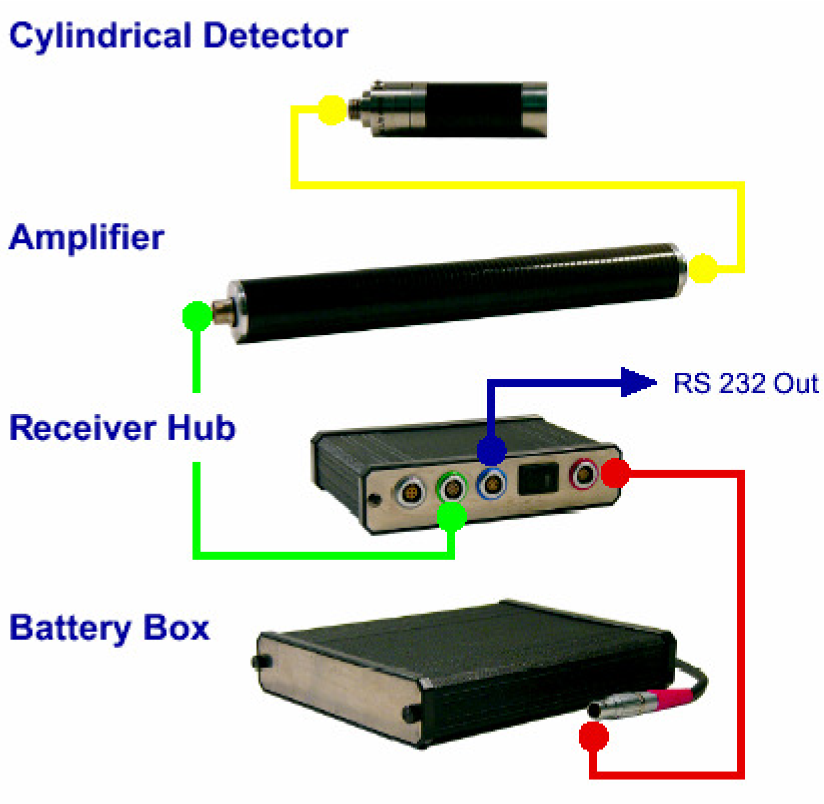

Figure B.71 - Receiver and PCE setup

(ArcSecond Inc. [2003])

B.3.2 Software functions

The series of angles (azimuth and elevation) are then calculated by the position server and provided to the system. The basic functions included by the Position Network Server include the following:

- Create and perform setups on transmitter configurations.
- Setup and control receiver hubs
- Setup multiple types of concurrent Position Servers to process, display, and distribute Indoor GPS data.
- Provide for remote device connection which can supply data to Position Servers.

- Control the display of data so that it can be represented in different units with different levels of precision and data rates.

- Save settings and setups for later reuse.

While the data is available through the Position Network Sever, it is more commonly provided to third party software as positional information. Such software packages include CAD/CAM software, modelling software, and most frequently software developed through programming languages such as visual basic.

B.4 Setup arrangement of IPS

The operation of IPS is dictated by the process for which the IPS is used. The receivers must be capable of taking a measurement from each to the transmitters initially through setup of the system, and be capable of taking effective measurement throughout operation.

To cater for varying measurement subjects, different methods of measurement must be undertaken. These are reflected in the arrangement of the IPS system.

B.4.1 "Square" configuration

The Square configuration is a typical configuration where items within the working area do not interfere with lines of sight between transmitters and receivers. In this arrangement the transmitters are set in a spare pattern as depicted in Figure B.72.

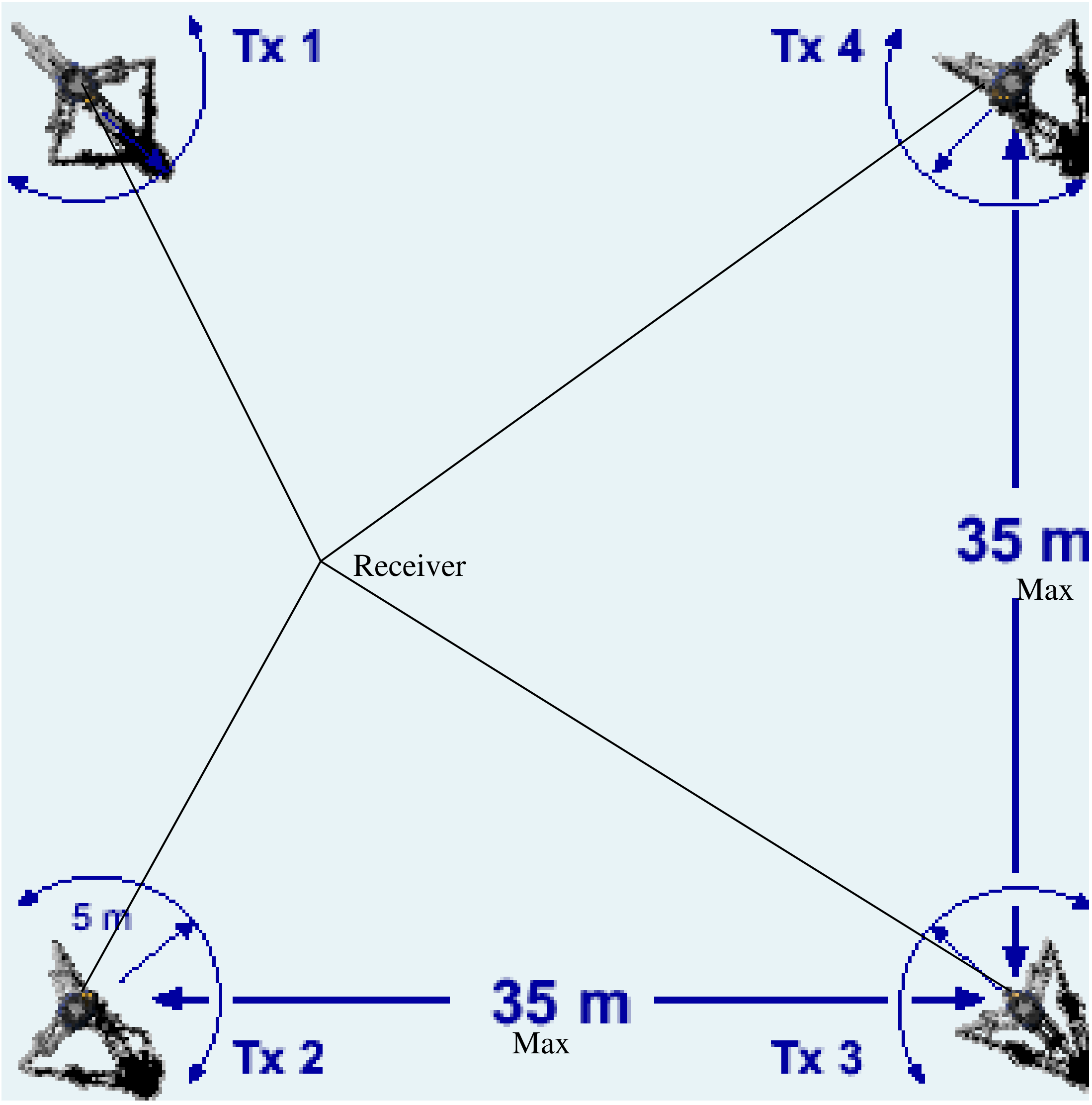

Figure B.72 - "Square" configuration

(ArcSecond Inc. [2003])

This configuration is an ideal arrangement as it allows for some ray intersection angles to approach 90˚ within the working area offering the best accuracy at any target location. Logically this allows for the highest accuracy to be at the centre of the working area, and the lowest accuracy towards the edge of the working area. The manufacturer suggests a spacing of 35m between transmitters, however a transmitter spacing of approximately 10 meters has provided excellent measurement accuracy.

B.4.2 “C” configurations

The “C” configuration is demonstrated in Figure B.73. This arrangement allows transmitters to be located along a single side of a survey item or where a square configuration cannot be achieved. It should be noted that the error will increase along the “major axis” (Noted in Figure B.73 as the x-axis) as the target location is brought further from the transmitters as the intersection angles reduce.

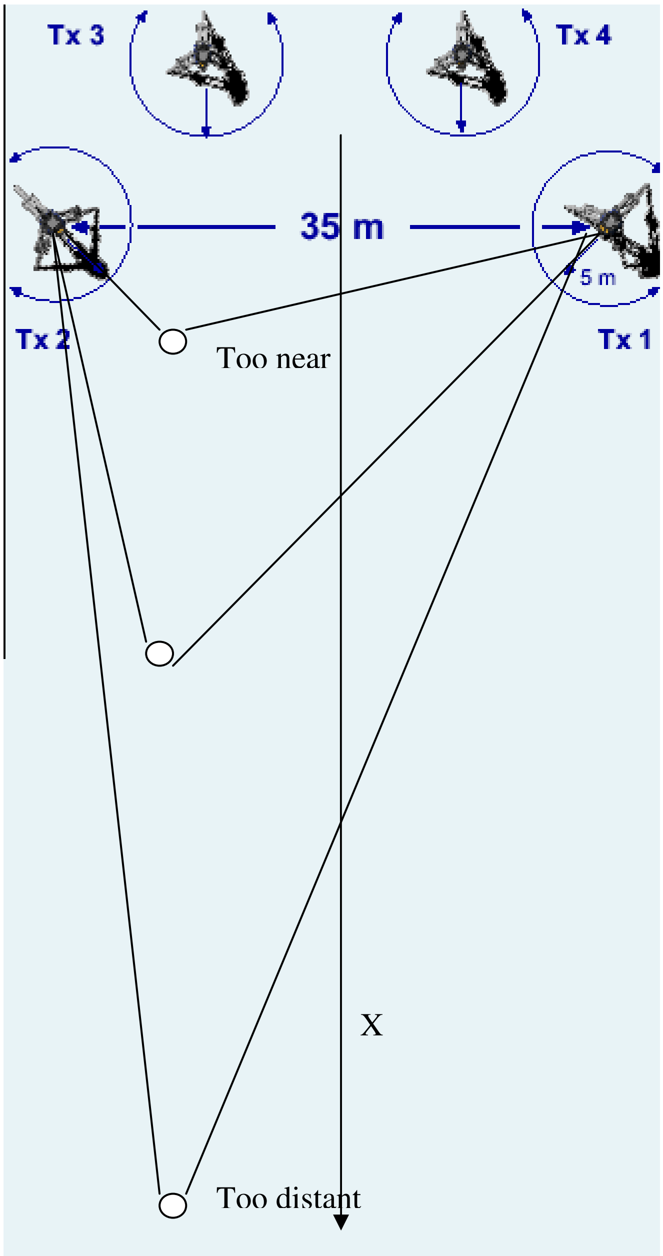

Figure B.73 - "C" configuration

(ArcSecond Inc. [2003])

Appendix C: Phase One testing

C.1 Extended results of area testing

Table C.28 – Extended results for area testing error – Day 1 (mm)

		Day 1																			
		1 point				5 point				10 point				15 point				20 point			
X (m)	Y (m)	st-x	st-y	st-z	st-3	st-x	St-y	St-z	st-3	st-x	st-y	st-z	st-3	st-x	st-y	st-z	st-3	st-x	st-y	st-z	st-3
0	0	0.179	0.231	0.047	0.296	0.091	0.109	0.025	0.145	0.068	0.078	0.016	0.104	0.073	0.063	0.015	0.098	0.062	0.073	0.015	0.097
0	2	0.263	0.191	0.042	0.328	0.112	0.099	0.027	0.152	0.053	0.105	0.021	0.12	0.077	0.089	0.014	0.119	0.066	0.071	0.013	0.098
0	4	0.176	0.129	0.036	0.221	0.105	0.086	0.017	0.137	0.085	0.065	0.014	0.108	0.084	0.053	0.013	0.1	0.073	0.049	0.007	0.088
0	6	0.278	0.158	0.047	0.323	0.134	0.089	0.021	0.162	0.079	0.078	0.011	0.112	0.067	0.075	0.011	0.101	0.063	0.081	0.01	0.102
0	8	0.202	0.13	0.057	0.247	0.116	0.077	0.046	0.147	0.076	0.062	0.018	0.1	0.079	0.07	0.026	0.108	0.094	0.066	0.024	0.117
0.74	0	0.163	0.233	0.069	0.293	0.095	0.187	0.036	0.212	0.083	0.178	0.021	0.198	0.076	0.152	0.026	0.172	0.066	0.141	0.021	0.157
0.74	2	0.184	0.193	0.089	0.281	0.092	0.112	0.039	0.15	0.066	0.074	0.021	0.101	0.054	0.053	0.024	0.08	0.055	0.072	0.023	0.094
0.74	4	0.214	0.152	0.04	0.266	0.12	0.084	0.022	0.148	0.083	0.081	0.014	0.117	0.082	0.074	0.011	0.112	0.068	0.066	0.012	0.095
0.74	6	0.24	0.153	0.039	0.288	0.12	0.097	0.018	0.156	0.085	0.066	0.019	0.109	0.063	0.066	0.012	0.093	0.057	0.057	0.012	0.082
0.74	8	0.196	0.161	0.049	0.259	0.117	0.074	0.024	0.14	0.066	0.058	0.014	0.089	0.084	0.07	0.012	0.11	0.075	0.07	0.01	0.103
3.43	0	0.154	0.278	0.041	0.321	0.116	0.146	0.018	0.187	0.094	0.104	0.015	0.141	0.084	0.094	0.015	0.127	0.074	0.069	0.011	0.102
3.43	2	0.147	0.184	0.038	0.239	0.128	0.127	0.02	0.181	0.108	0.091	0.014	0.141	0.092	0.101	0.012	0.137	0.09	0.086	0.013	0.125
3.43	4	0.168	0.199	0.04	0.263	0.095	0.137	0.017	0.167	0.069	0.123	0.015	0.142	0.062	0.127	0.012	0.142	0.06	0.132	0.018	0.146
3.43	6	0.146	0.144	0.106	0.231	0.073	0.08	0.056	0.122	0.052	0.1	0.025	0.115	0.06	0.11	0.023	0.128	0.063	0.101	0.024	0.121
3.43	8	0.152	0.181	0.044	0.241	0.09	0.128	0.024	0.158	0.07	0.102	0.016	0.125	0.066	0.092	0.014	0.114	0.063	0.102	0.013	0.12
5.02	0	0.162	0.407	0.039	0.44	0.095	0.198	0.017	0.22	0.056	0.111	0.014	0.125	0.053	0.117	0.011	0.129	0.055	0.119	0.01	0.132
5.02	2	0.135	0.256	0.037	0.292	0.073	0.123	0.016	0.144	0.055	0.113	0.016	0.127	0.056	0.113	0.011	0.127	0.051	0.096	0.009	0.109
5.02	4	0.201	0.205	0.04	0.29	0.119	0.108	0.018	0.162	0.092	0.12	0.012	0.152	0.087	0.123	0.009	0.151	0.074	0.12	0.008	0.141
5.02	6	0.157	0.192	0.039	0.251	0.085	0.129	0.023	0.156	0.084	0.097	0.019	0.13	0.08	0.094	0.014	0.124	0.06	0.083	0.007	0.103
5.02	8	0.134	0.181	0.037	0.228	0.093	0.106	0.026	0.144	0.094	0.15	0.017	0.178	0.111	0.154	0.013	0.19	0.092	0.147	0.013	0.174
6.77	0	0.113	0.224	0.048	0.255	0.077	0.148	0.016	0.167	0.086	0.11	0.013	0.14	0.073	0.093	0.011	0.119	0.06	0.095	0.009	0.113
6.77	2	0.171	0.224	0.034	0.283	0.081	0.141	0.02	0.164	0.06	0.099	0.014	0.116	0.059	0.059	0.011	0.084	0.055	0.063	0.012	0.084

6.77	4	0.17	0.201	0.029	0.265	0.093	0.122	0.015	0.154	0.093	0.095	0.01	0.133	0.098	0.076	0.012	0.125	0.076	0.078	0.008	0.109
6.77	6	0.198	0.265	0.041	0.333	0.093	0.146	0.018	0.174	0.066	0.115	0.01	0.133	0.054	0.101	0.009	0.115	0.063	0.097	0.007	0.116
6.77	8	0.144	0.211	0.036	0.258	0.104	0.15	0.023	0.184	0.075	0.157	0.016	0.175	0.053	0.138	0.013	0.149	0.066	0.12	0.014	0.138
10	0	0.247	0.372	0.047	0.449	0.189	0.241	0.026	0.307	0.171	0.231	0.014	0.288	0.16	0.154	0.015	0.223	0.166	0.145	0.008	0.22
10	2	0.253	0.259	0.045	0.365	0.135	0.153	0.028	0.205	0.091	0.118	0.023	0.151	0.162	0.142	0.019	0.216	0.151	0.131	0.017	0.201
10	4	0.24	0.186	0.042	0.307	0.182	0.119	0.025	0.219	0.14	0.088	0.016	0.166	0.116	0.096	0.015	0.152	0.14	0.087	0.009	0.165
10	6	0.187	0.181	0.038	0.263	0.096	0.106	0.02	0.145	0.124	0.089	0.015	0.153	0.125	0.075	0.019	0.147	0.092	0.094	0.017	0.132
10	8	0.184	0.292	0.038	0.347	0.094	0.225	0.019	0.245	0.08	0.165	0.015	0.184	0.07	0.164	0.012	0.179	0.067	0.143	0.01	0.159

Table C.29 - Extended results for area testing error – Day 2 (mm)

		Day 2																			
		1 point				5 point				10 point				15 point				20 point			
x (m)	y (m)	st-x	st-y	st-z	st-3	st-x	st-y	st-z	st-3	st-x	st-y	st-z	st-3	St-x	st-y	st-z	st-3	st-x	st-y	st-z	st-3
0	0	0.164	0.203	0.052	0.266	0.09	0.113	0.024	0.146	0.055	0.104	0.02	0.12	0.036	0.08	0.016	0.09	0.036	0.073	0.011	0.082
0	2	0.278	0.163	0.035	0.324	0.16	0.095	0.023	0.187	0.174	0.057	0.018	0.184	0.126	0.061	0.015	0.141	0.109	0.034	0.014	0.115
0	4	0.21	0.132	0.042	0.251	0.135	0.068	0.023	0.152	0.08	0.063	0.015	0.103	0.055	0.059	0.009	0.081	0.053	0.047	0.01	0.071
0	6	0.191	0.125	0.041	0.232	0.129	0.081	0.016	0.153	0.103	0.054	0.012	0.117	0.105	0.061	0.013	0.122	0.09	0.06	0.014	0.11
0	8	0.27	0.149	0.05	0.313	0.088	0.098	0.02	0.133	0.09	0.057	0.016	0.108	0.074	0.062	0.015	0.098	0.072	0.048	0.012	0.088
0.74	0	0.144	0.214	0.048	0.263	0.099	0.121	0.021	0.157	0.088	0.101	0.013	0.134	0.088	0.081	0.011	0.12	0.066	0.054	0.012	0.086
0.74	2	0.193	0.14	0.051	0.244	0.079	0.08	0.021	0.114	0.083	0.052	0.018	0.1	0.078	0.05	0.015	0.094	0.087	0.044	0.013	0.099
0.74	4	0.145	0.102	0.044	0.183	0.08	0.08	0.023	0.115	0.062	0.062	0.023	0.091	0.061	0.046	0.017	0.079	0.039	0.049	0.014	0.064
0.74	6	0.15	0.105	0.05	0.19	0.113	0.068	0.023	0.134	0.072	0.059	0.014	0.094	0.074	0.043	0.016	0.087	0.065	0.058	0.011	0.088
0.74	8	0.172	0.166	0.037	0.242	0.121	0.088	0.021	0.151	0.081	0.058	0.017	0.101	0.069	0.076	0.014	0.104	0.066	0.089	0.014	0.111
3.43	0	0.15	0.26	0.046	0.303	0.066	0.139	0.02	0.155	0.049	0.102	0.01	0.114	0.039	0.082	0.011	0.092	0.032	0.087	0.008	0.093
3.43	2	0.133	0.194	0.041	0.239	0.069	0.126	0.018	0.145	0.043	0.084	0.011	0.095	0.033	0.074	0.01	0.082	0.046	0.063	0.009	0.078
3.43	4	0.128	0.134	0.035	0.189	0.099	0.11	0.02	0.149	0.065	0.081	0.012	0.104	0.057	0.091	0.011	0.108	0.06	0.081	0.01	0.101
3.43	6	0.134	0.14	0.042	0.199	0.094	0.106	0.021	0.144	0.065	0.076	0.014	0.101	0.056	0.045	0.007	0.072	0.037	0.048	0.011	0.062
3.43	8	0.163	0.18	0.056	0.249	0.049	0.11	0.021	0.122	0.049	0.116	0.018	0.127	0.068	0.126	0.013	0.144	0.049	0.142	0.012	0.151
5.02	0	0.115	0.204	0.048	0.239	0.054	0.131	0.02	0.143	0.041	0.078	0.014	0.09	0.039	0.063	0.016	0.076	0.039	0.038	0.013	0.056
5.02	2	0.135	0.181	0.037	0.228	0.08	0.1	0.016	0.129	0.052	0.07	0.014	0.089	0.056	0.056	0.011	0.079	0.056	0.058	0.009	0.081
5.02	4	0.151	0.184	0.036	0.24	0.074	0.096	0.017	0.122	0.068	0.065	0.014	0.095	0.045	0.07	0.01	0.084	0.047	0.049	0.007	0.068
5.02	6	0.13	0.144	0.031	0.197	0.054	0.07	0.014	0.09	0.057	0.05	0.012	0.077	0.039	0.042	0.008	0.058	0.032	0.039	0.007	0.051
5.02	8	0.122	0.188	0.037	0.227	0.067	0.077	0.016	0.104	0.05	0.089	0.012	0.103	0.052	0.074	0.011	0.091	0.072	0.105	0.009	0.128
6.77	0	0.122	0.225	0.043	0.259	0.083	0.169	0.017	0.19	0.08	0.135	0.015	0.158	0.076	0.082	0.011	0.113	0.09	0.094	0.014	0.131
6.77	2	0.162	0.168	0.052	0.239	0.11	0.12	0.017	0.163	0.115	0.105	0.012	0.156	0.1	0.1	0.009	0.142	0.079	0.094	0.009	0.124
6.77	4	0.206	0.202	0.025	0.29	0.098	0.116	0.016	0.153	0.099	0.079	0.01	0.127	0.088	0.076	0.007	0.117	0.083	0.071	0.008	0.109
6.77	6	0.144	0.189	0.035	0.24	0.076	0.102	0.018	0.129	0.058	0.098	0.011	0.115	0.067	0.069	0.008	0.096	0.066	0.077	0.007	0.102
6.77	8	0.135	0.183	0.037	0.23	0.081	0.109	0.022	0.138	0.069	0.082	0.019	0.109	0.064	0.131	0.011	0.146	0.071	0.14	0.011	0.157
10	0	0.182	0.183	0.049	0.263	0.112	0.099	0.028	0.153	0.1	0.083	0.014	0.13	0.09	0.063	0.011	0.111	0.075	0.06	0.009	0.096
10	2	0.255	0.143	0.045	0.296	0.107	0.072	0.02	0.131	0.092	0.046	0.014	0.104	0.064	0.044	0.012	0.079	0.06	0.055	0.01	0.082
10	4	0.259	0.142	0.041	0.298	0.154	0.09	0.017	0.179	0.133	0.092	0.011	0.162	0.115	0.068	0.013	0.135	0.106	0.063	0.012	0.124
10	6	0.232	0.138	0.039	0.273	0.126	0.082	0.022	0.152	0.117	0.065	0.016	0.135	0.096	0.062	0.013	0.115	0.089	0.058	0.009	0.107
10	8	0.146	0.215	0.046	0.264	0.07	0.077	0.023	0.106	0.078	0.069	0.018	0.105	0.061	0.072	0.014	0.096	0.057	0.064	0.013	0.087

Table C.30 - Extended results for area testing error – Day 3 (mm)

		Day 3																			
		1 point				5 point				10 point				15 point				20 point			
x (m)	y (m)	st-x	st-y	st-z	st-3	st-x	st-y	st-z	st-3	st-x	st-y	st-z	st-3	St-x	st-y	st-z	st-3	st-x	st-y	st-z	st-3
0	0	0.345	0.317	0.065	0.473	0.15	0.129	0.025	0.199	0.111	0.116	0.018	0.161	0.129	0.085	0.014	0.155	0.098	0.095	0.014	0.137
0	2	0.255	0.174	0.04	0.311	0.144	0.067	0.017	0.159	0.094	0.061	0.015	0.113	0.089	0.041	0.011	0.098	0.081	0.027	0.008	0.086
0	4	0.231	0.131	0.041	0.269	0.112	0.097	0.023	0.15	0.072	0.085	0.016	0.113	0.054	0.056	0.018	0.08	0.059	0.043	0.012	0.074
0	6	0.19	0.144	0.044	0.242	0.083	0.079	0.022	0.116	0.063	0.063	0.022	0.091	0.053	0.052	0.014	0.076	0.062	0.054	0.009	0.083
0	8	0.258	0.167	0.04	0.31	0.245	0.108	0.024	0.269	0.203	0.077	0.016	0.218	0.169	0.071	0.011	0.183	0.142	0.073	0.009	0.16
0.74	0	0.201	0.299	0.041	0.363	0.13	0.182	0.029	0.225	0.124	0.163	0.018	0.205	0.095	0.086	0.014	0.129	0.078	0.061	0.013	0.1
0.74	2	0.188	0.221	0.045	0.294	0.094	0.061	0.02	0.114	0.116	0.1	0.016	0.154	0.114	0.073	0.013	0.136	0.101	0.05	0.011	0.114
0.74	4	0.167	0.141	0.042	0.223	0.094	0.061	0.02	0.114	0.075	0.049	0.015	0.091	0.08	0.063	0.013	0.103	0.073	0.051	0.013	0.09
0.74	6	0.18	0.11	0.036	0.214	0.116	0.075	0.023	0.14	0.063	0.083	0.019	0.106	0.072	0.108	0.017	0.131	0.039	0.085	0.013	0.095
0.74	8	0.168	0.132	0.042	0.218	0.092	0.067	0.028	0.117	0.101	0.052	0.021	0.116	0.083	0.067	0.014	0.107	0.1	0.056	0.008	0.115
3.43	0	0.151	0.293	0.038	0.332	0.078	0.174	0.02	0.192	0.053	0.154	0.015	0.164	0.05	0.082	0.011	0.097	0.038	0.093	0.01	0.101
3.43	2	0.2	0.354	0.034	0.408	0.096	0.106	0.016	0.144	0.07	0.088	0.021	0.114	0.059	0.08	0.016	0.101	0.053	0.079	0.012	0.096
3.43	4	0.228	0.171	0.039	0.288	0.134	0.099	0.014	0.167	0.125	0.077	0.017	0.148	0.1	0.05	0.011	0.113	0.088	0.059	0.011	0.106
3.43	6	0.126	0.197	0.057	0.241	0.066	0.156	0.017	0.171	0.041	0.14	0.016	0.147	0.064	0.12	0.016	0.137	0.053	0.091	0.013	0.106
3.43	8	0.189	0.288	0.045	0.347	0.077	0.135	0.021	0.157	0.056	0.084	0.015	0.102	0.045	0.093	0.012	0.104	0.049	0.078	0.01	0.092
5.02	0	0.124	0.311	0.05	0.339	0.076	0.202	0.026	0.218	0.056	0.103	0.014	0.118	0.055	0.112	0.014	0.125	0.043	0.093	0.016	0.103
5.02	2	0.128	0.237	0.035	0.272	0.082	0.104	0.025	0.135	0.083	0.08	0.015	0.116	0.063	0.042	0.01	0.077	0.073	0.06	0.012	0.095
5.02	4	0.137	0.153	0.037	0.208	0.09	0.109	0.016	0.142	0.065	0.093	0.013	0.114	0.061	0.095	0.012	0.113	0.075	0.077	0.008	0.107
5.02	6	0.126	0.149	0.034	0.198	0.063	0.078	0.019	0.103	0.047	0.078	0.017	0.092	0.03	0.064	0.012	0.072	0.038	0.066	0.013	0.077
5.02	8	0.156	0.22	0.043	0.273	0.108	0.178	0.02	0.209	0.103	0.148	0.021	0.181	0.08	0.14	0.011	0.161	0.091	0.134	0.013	0.163
6.77	0	0.202	0.352	0.04	0.408	0.113	0.303	0.016	0.323	0.076	0.287	0.01	0.297	0.087	0.207	0.013	0.225	0.063	0.134	0.009	0.149
6.77	2	0.187	0.226	0.038	0.296	0.111	0.144	0.018	0.183	0.076	0.139	0.015	0.159	0.084	0.103	0.011	0.133	0.072	0.088	0.009	0.114
6.77	4	0.123	0.167	0.033	0.21	0.088	0.095	0.012	0.13	0.072	0.091	0.012	0.117	0.043	0.062	0.01	0.076	0.053	0.047	0.008	0.071
6.77	6	0.156	0.168	0.037	0.233	0.098	0.09	0.024	0.135	0.081	0.105	0.015	0.133	0.064	0.072	0.013	0.097	0.069	0.092	0.012	0.116
6.77	8	0.148	0.226	0.035	0.273	0.089	0.134	0.017	0.162	0.062	0.112	0.012	0.129	0.061	0.082	0.006	0.103	0.043	0.078	0.007	0.089
10	0	0.187	0.297	0.05	0.354	0.126	0.183	0.022	0.223	0.147	0.157	0.017	0.216	0.137	0.116	0.019	0.181	0.119	0.104	0.015	0.159
10	2	0.189	0.157	0.059	0.252	0.122	0.113	0.02	0.167	0.135	0.077	0.014	0.156	0.107	0.056	0.012	0.121	0.104	0.061	0.013	0.121
10	4	0.294	0.187	0.037	0.351	0.155	0.097	0.019	0.184	0.155	0.065	0.016	0.169	0.097	0.058	0.016	0.114	0.092	0.049	0.016	0.106
10	6	0.164	0.15	0.04	0.226	0.101	0.079	0.022	0.13	0.088	0.054	0.017	0.104	0.074	0.043	0.012	0.087	0.072	0.043	0.014	0.085

10	8	0.149	0.177	0.058	0.239	0.128	0.099	0.027	0.164	0.072	0.091	0.018	0.118	0.076	0.07	0.01	0.104	0.069	0.072	0.013	0.101

Table C.31 - Extended results for area testing error – Day 4 (mm)

x (m)	y (m)	Day 4 1 point st-x	st-y	st-z	st-3	5 point st-x	st-y	st-z	st-3	10 point st-x	st-y	st-z	st-3	15 point st-x	st-y	st-z	st-3	20 point st-x	st-y	st-z	st-3
0	0	0.24	0.248	0.063	0.35	0.131	0.112	0.029	0.175	0.104	0.097	0.015	0.143	0.072	0.073	0.018	0.104	0.081	0.073	0.015	0.11
0	2	0.181	0.167	0.035	0.249	0.078	0.084	0.02	0.116	0.104	0.08	0.012	0.131	0.118	0.073	0.01	0.139	0.106	0.061	0.013	0.123
0	4	0.2	0.138	0.079	0.256	0.117	0.07	0.042	0.143	0.085	0.081	0.033	0.122	0.072	0.042	0.027	0.087	0.081	0.066	0.028	0.108
0	6	0.214	0.136	0.06	0.26	0.146	0.139	0.023	0.202	0.099	0.129	0.021	0.164	0.109	0.098	0.011	0.147	0.111	0.103	0.01	0.152
0	8	0.188	0.196	0.056	0.277	0.123	0.132	0.026	0.182	0.099	0.101	0.013	0.142	0.085	0.099	0.012	0.131	0.099	0.084	0.01	0.13
0.74	0	0.176	0.207	0.045	0.275	0.116	0.105	0.029	0.159	0.091	0.13	0.024	0.16	0.081	0.108	0.017	0.136	0.07	0.085	0.019	0.112
0.74	2	0.154	0.161	0.05	0.228	0.134	0.099	0.022	0.168	0.131	0.091	0.02	0.161	0.111	0.057	0.018	0.126	0.07	0.089	0.014	0.114
0.74	4	0.24	0.117	0.033	0.269	0.193	0.08	0.019	0.21	0.155	0.091	0.014	0.18	0.141	0.062	0.011	0.154	0.125	0.048	0.012	0.134
0.74	6	0.168	0.128	0.028	0.213	0.18	0.074	0.017	0.196	0.14	0.058	0.016	0.153	0.14	0.074	0.015	0.159	0.127	0.074	0.011	0.147
0.74	8	0.213	0.172	0.05	0.279	0.123	0.111	0.017	0.167	0.077	0.099	0.013	0.126	0.088	0.093	0.009	0.129	0.073	0.092	0.009	0.118
3.43	0	0.199	0.206	0.041	0.289	0.132	0.119	0.024	0.179	0.098	0.113	0.016	0.15	0.093	0.089	0.017	0.13	0.078	0.098	0.014	0.126
3.43	2	0.12	0.163	0.053	0.209	0.11	0.129	0.014	0.17	0.11	0.108	0.013	0.154	0.096	0.107	0.008	0.144	0.076	0.09	0.008	0.118
3.43	4	0.161	0.163	0.033	0.231	0.111	0.076	0.017	0.135	0.091	0.082	0.012	0.123	0.091	0.081	0.015	0.123	0.078	0.076	0.015	0.11
3.43	6	0.157	0.139	0.043	0.215	0.093	0.086	0.02	0.128	0.086	0.055	0.013	0.103	0.074	0.074	0.009	0.106	0.077	0.092	0.011	0.121
3.43	8	0.195	0.241	0.04	0.312	0.101	0.129	0.019	0.165	0.079	0.145	0.012	0.166	0.087	0.128	0.02	0.156	0.075	0.123	0.017	0.145
5.02	0	0.145	0.284	0.034	0.321	0.09	0.123	0.026	0.155	0.065	0.108	0.016	0.127	0.07	0.065	0.01	0.096	0.062	0.072	0.011	0.095
5.02	2	0.143	0.227	0.029	0.269	0.058	0.149	0.013	0.16	0.046	0.102	0.015	0.113	0.045	0.085	0.011	0.097	0.052	0.085	0.011	0.1
5.02	4	0.097	0.139	0.043	0.175	0.047	0.088	0.017	0.101	0.045	0.062	0.013	0.078	0.037	0.075	0.011	0.084	0.03	0.071	0.009	0.078
5.02	6	0.154	0.157	0.028	0.222	0.109	0.125	0.016	0.167	0.074	0.084	0.013	0.113	0.075	0.079	0.014	0.109	0.065	0.071	0.01	0.097
5.02	8	0.106	0.196	0.044	0.227	0.08	0.074	0.026	0.112	0.056	0.05	0.021	0.078	0.057	0.06	0.019	0.086	0.049	0.076	0.016	0.092
6.77	0	0.119	0.197	0.035	0.232	0.081	0.093	0.022	0.125	0.069	0.092	0.018	0.116	0.067	0.085	0.013	0.109	0.074	0.088	0.009	0.115
6.77	2	0.123	0.137	0.034	0.187	0.04	0.077	0.018	0.089	0.048	0.085	0.015	0.099	0.039	0.043	0.013	0.059	0.048	0.043	0.013	0.066
6.77	4	0.115	0.18	0.034	0.216	0.079	0.104	0.026	0.133	0.084	0.083	0.017	0.119	0.071	0.081	0.014	0.109	0.057	0.073	0.013	0.093
6.77	6	0.141	0.174	0.04	0.228	0.089	0.104	0.026	0.139	0.078	0.108	0.018	0.135	0.078	0.098	0.014	0.126	0.071	0.086	0.011	0.112
6.77	8	0.12	0.184	0.041	0.224	0.088	0.098	0.019	0.133	0.085	0.086	0.014	0.122	0.065	0.072	0.012	0.098	0.061	0.068	0.009	0.092
10	0	0.194	0.181	0.042	0.268	0.145	0.1	0.024	0.177	0.154	0.068	0.018	0.169	0.141	0.072	0.011	0.159	0.12	0.073	0.012	0.141
10	2	0.202	0.135	0.06	0.25	0.127	0.101	0.019	0.163	0.107	0.094	0.015	0.144	0.142	0.074	0.017	0.161	0.126	0.065	0.015	0.142
10	4	0.174	0.125	0.04	0.218	0.079	0.076	0.022	0.112	0.125	0.075	0.015	0.147	0.119	0.067	0.012	0.137	0.095	0.057	0.012	0.111

10	6	0.259	0.191	0.039	0.324	0.109	0.106	0.017	0.153	0.071	0.078	0.012	0.106	0.062	0.054	0.013	0.083	0.111	0.047	0.014	0.122
10	8	0.207	0.203	0.045	0.294	0.079	0.119	0.022	0.145	0.078	.138	0.015	0.159	0.083	0.092	0.009	0.124	0.09	0.085	0.015	0.125

Figure C.74 - Extended results for area testing error – average (mm)

		Average																			
		1 point				5 point				10 point				15 point				20 point			
x (m)	y (m)	st-x	st-y	st-z	st-3	st-x	st-y	st-z	st-3	st-x	st-y	st-z	st-3	st-x	st-y	st-z	st-3	st-x	st-y	st-z	st-3
0	0	0.232	0.249	0.057	0.346	0.116	0.116	0.026	0.166	0.084	0.099	0.017	0.132	0.078	0.075	0.016	0.112	0.069	0.078	0.014	0.106
0	2	0.244	0.174	0.038	0.303	0.123	0.086	0.022	0.154	0.106	0.076	0.017	0.137	0.102	0.066	0.013	0.124	0.09	0.048	0.012	0.105
0	4	0.204	0.133	0.05	0.249	0.117	0.08	0.026	0.146	0.081	0.074	0.02	0.111	0.066	0.052	0.017	0.087	0.066	0.051	0.014	0.085
0	6	0.218	0.141	0.048	0.264	0.123	0.097	0.02	0.159	0.086	0.081	0.016	0.121	0.083	0.072	0.012	0.112	0.082	0.075	0.011	0.112
0	8	0.23	0.16	0.051	0.287	0.143	0.104	0.029	0.183	0.117	0.074	0.016	0.142	0.102	0.075	0.016	0.13	0.102	0.068	0.014	0.124
0.74	0	0.171	0.238	0.051	0.298	0.11	0.148	0.029	0.188	0.096	0.143	0.019	0.174	0.085	0.107	0.017	0.139	0.07	0.085	0.016	0.114
0.74	2	0.18	0.179	0.059	0.262	0.1	0.088	0.026	0.137	0.099	0.079	0.019	0.129	0.089	0.058	0.018	0.109	0.079	0.064	0.015	0.105
0.74	4	0.191	0.128	0.04	0.235	0.122	0.076	0.021	0.147	0.094	0.071	0.017	0.12	0.091	0.061	0.013	0.112	0.076	0.054	0.013	0.096
0.74	6	0.185	0.124	0.039	0.226	0.132	0.079	0.02	0.156	0.09	0.067	0.017	0.116	0.087	0.073	0.015	0.117	0.072	0.069	0.012	0.103
0.74	8	0.187	0.158	0.045	0.249	0.113	0.085	0.022	0.144	0.081	0.067	0.016	0.108	0.081	0.077	0.012	0.112	0.079	0.077	0.01	0.112
3.43	0	0.163	0.259	0.042	0.311	0.098	0.144	0.02	0.178	0.074	0.118	0.014	0.142	0.067	0.087	0.013	0.111	0.056	0.087	0.011	0.106
3.43	2	0.15	0.224	0.041	0.273	0.101	0.122	0.017	0.16	0.083	0.093	0.015	0.126	0.07	0.091	0.011	0.116	0.066	0.08	0.01	0.104
3.43	4	0.171	0.167	0.037	0.243	0.109	0.105	0.017	0.154	0.087	0.091	0.014	0.129	0.078	0.087	0.012	0.121	0.071	0.087	0.014	0.116
3.43	6	0.141	0.155	0.062	0.221	0.081	0.107	0.028	0.141	0.061	0.093	0.017	0.116	0.063	0.088	0.014	0.111	0.057	0.083	0.015	0.102
3.43	8	0.175	0.223	0.046	0.288	0.079	0.125	0.021	0.151	0.064	0.112	0.015	0.13	0.067	0.11	0.014	0.129	0.059	0.111	0.013	0.127
5.02	0	0.136	0.302	0.043	0.335	0.079	0.164	0.022	0.184	0.054	0.1	0.015	0.115	0.054	0.089	0.013	0.106	0.05	0.08	0.012	0.097
5.02	2	0.135	0.225	0.035	0.265	0.073	0.119	0.017	0.142	0.059	0.091	0.015	0.111	0.055	0.074	0.011	0.095	0.058	0.075	0.01	0.096
5.02	4	0.147	0.17	0.039	0.229	0.082	0.1	0.017	0.132	0.068	0.085	0.013	0.11	0.058	0.091	0.011	0.108	0.056	0.079	0.008	0.099
5.02	6	0.142	0.16	0.033	0.217	0.078	0.101	0.018	0.129	0.066	0.077	0.015	0.103	0.056	0.07	0.012	0.091	0.049	0.065	0.009	0.082
5.02	8	0.129	0.196	0.04	0.239	0.087	0.109	0.022	0.142	0.076	0.109	0.018	0.135	0.075	0.107	0.014	0.132	0.076	0.115	0.013	0.139
6.77	0	0.139	0.249	0.041	0.289	0.088	0.178	0.018	0.201	0.078	0.156	0.014	0.178	0.076	0.117	0.012	0.141	0.072	0.103	0.01	0.127
6.77	2	0.161	0.189	0.04	0.251	0.085	0.121	0.018	0.15	0.075	0.107	0.014	0.133	0.07	0.076	0.011	0.105	0.064	0.072	0.011	0.097
6.77	4	0.154	0.188	0.03	0.245	0.09	0.109	0.017	0.142	0.087	0.087	0.012	0.124	0.075	0.074	0.011	0.107	0.067	0.067	0.009	0.096
6.77	6	0.16	0.199	0.038	0.259	0.089	0.111	0.021	0.144	0.071	0.106	0.014	0.129	0.066	0.085	0.011	0.109	0.067	0.088	0.009	0.111
6.77	8	0.137	0.201	0.037	0.246	0.09	0.123	0.02	0.154	0.073	0.109	0.015	0.134	0.061	0.106	0.011	0.124	0.06	0.101	0.01	0.119
10	0	0.202	0.258	0.047	0.333	0.143	0.156	0.025	0.215	0.143	0.135	0.016	0.201	0.132	0.101	0.014	0.168	0.12	0.095	0.011	0.154
10	2	0.225	0.173	0.053	0.291	0.123	0.11	0.022	0.167	0.106	0.084	0.016	0.139	0.119	0.079	0.015	0.144	0.11	0.078	0.014	0.136
10	4	0.242	0.16	0.04	0.294	0.143	0.095	0.021	0.174	0.138	0.08	0.015	0.161	0.112	0.072	0.014	0.134	0.108	0.064	0.012	0.126
10	6	0.211	0.165	0.039	0.272	0.108	0.093	0.02	0.145	0.1	0.072	0.015	0.125	0.089	0.058	0.015	0.108	0.091	0.061	0.013	0.111
10	8	0.171	0.222	0.047	0.286	0.093	0.13	0.023	0.165	0.077	0.116	0.017	0.142	0.072	0.1	0.011	0.126	0.071	0.091	0.013	0.118

C.2 Precision point testing

Table C.32 - Precision point Error (mm)

test 1					test 2				
PP	X	Y	Z	Absolute	PP	X	Y	Z	3
1	0.406629	0.354137	0.176824	0.539221	1	0.372231	0.329301	0.15946	0.496986
5	0.216964	0.208359	0.079796	0.300811	5	0.215563	0.192315	0.074385	0.288882
10	0.175116	0.167309	0.062036	0.242194	10	0.173219	0.159535	0.057817	0.235492
15	0.158287	0.151418	0.055421	0.219048	15	0.150426	0.136576	0.050876	0.203177
20	0.140605	0.130109	0.054531	0.191567	20	0.133525	0.119085	0.045578	0.178914
30	0.141352	0.130957	0.050194	0.192692	30	0.141201	0.115216	0.043894	0.182243
40	0.104674	0.099327	0.042443	0.144301	40	0.1135	0.076973	0.037268	0.137138
50	0.084257	0.089495	0.041901	0.122917	50	0.104578	0.068966	0.034701	0.125271
60	0.078588	0.087693	0.037056	0.117755	60	0.096571	0.056062	0.031999	0.111665
80	0.073544	0.078667	0.034587	0.10769	80	0.087333	0.04874	0.030202	0.100014
100	0.066752	0.068918	0.036738	0.095946	100	0.067394	0.048659	0.029089	0.083124
test 3									
PP	X	Y	Z	3					
1	0.35539	0.362298	0.151547	0.507506					
5	0.200722	0.179006	0.068817	0.268947					
10	0.164461	0.147378	0.054514	0.220835					
15	0.152461	0.130577	0.046621	0.200735					
20	0.12261	0.127107	0.037283	0.176606					
30	0.133008	0.121011	0.039944	0.179819					
40	0.096823	0.094872	0.029581	0.135556					
50	0.08227	0.082278	0.027892	0.116353					
60	0.070377	0.073525	0.026067	0.101778					
80	0.071265	0.059128	0.022491	0.0926					
100	0.067466	0.049689	0.022875	0.083789					

Table C.33 - Precision point comparison data

Samples	rate (Hz)	X	Y	Z	Absolute	Error (mm)
1	10	100.00%	100.00%	100.00%	100.00%	0.385928
5	2	56.35%	55.49%	46.35%	55.64%	0.21466
10	1	44.91%	44.25%	35.64%	44.35%	0.17463
15	0.666667	40.01%	39.52%	31.37%	39.67%	0.15574
20	0.5	34.94%	35.55%	28.15%	35.17%	0.136772
30	0.333333	36.08%	35.09%	27.66%	35.61%	0.138689
40	0.25	27.83%	26.28%	22.26%	27.21%	0.104249
50	0.2	24.25%	23.34%	20.91%	23.91%	0.091135
60	0.166667	22.03%	21.47%	19.31%	22.01%	0.0828
80	0.125	19.86%	17.90%	17.76%	19.16%	0.075076
100	0.1	17.54%	16.36%	17.79%	17.11%	0.065715

C.3 Dynamic data

The following data represents the errors developed using InnovMetric's Polyworks inspector.

Table C.34 - Error data at 2.5RPM

	Precision points							
	1		10			20		
	Radius	2σ	Radius	2σ	% increase	Radius	2σ	% increase
spot 1	549.04	1.978	548.849	9.36	373.21%	550.863	11.878	218.27%
spot 2	548.495	2.072	548.256	14.214	586.00%	546.242	34.92	495.90%
spot 3	548.792	2.706	548.516	11.924	340.65%	547.827	15.294	348.96%
spot 4	548.946	2.142	548.296	14.99	599.81%	552.363	32.168	436.30%
spot 5	548.67	3.146	549.469	14.042	346.34%	548.069	31.366	805.63%
average	548.7886	2.43	548.6772	12.862	429.30%	549.0728	26.536	518.12%

Table C.35 - Error data at 5RPM

	Precision points							
	1		10			20		
	Radius	2σ	Radius	2σ	% increase	radius	2σ	% increase
spot 1	548.899	2.206	548.663	17.014	671.26%	544.4	35.892	434.70%
spot 2	548.475	3.162	547.889	18.542	486.40%	548.133	27.706	469.61%
spot 3	548.924	3.266	547.926	12.116	270.97%	548.64	19.946	636.09%
spot 4	548.767	2.852	548.06	19.72	591.44%	548.649	31.656	435.23%
spot 5	548.512	3.59	547.608	19.06	430.92%	554.206	34.572	702.28%
average	548.7154	3.062	548.0292	17.478	470.80%	548.8056	30.682	551.69%

Table C.36 - Error data at 10RPM

	Precision points							
	1		10			20		
	Radius	2σ	Radius	2σ	% increase	Radius	2σ	% increase
spot 1	548.869	4.514	547.274	28.248	525.79%	547.981	64.766	1131.79%
spot 2	548.487	7.516	548.651	33.242	342.28%	513.263	72.094	2006.27%
spot 3	548.808	3.784	548.594	29.776	686.89%	525.108	54.904	699.31%
spot 4	548.655	3.508	547.695	29.666	745.67%	520.845	51.952	596.72%
spot 5	548.545	4.482	545.683	26.964	501.61%	486.137	111.374	2120.35%
average	548.6728	5.028	547.5794	29.496	486.63%	518.6668	79.486	1533.38%

Table C.37 - Summary of dynamic data

		Precision points					
		1		10		20	
speed	Rpm	Radius	2σ	Radius	2σ	radius	2σ
1	2.5	548.973	1.994	549.145	9.054	549.54	11.738
2	3	548.973	7.14	549.145	9.178	549.54	12.666
3	5	548.973	2.23	549.145	15.94	549.54	34.52
4	7.5	548.973	3.052	549.145	18.538	549.54	100.668
5	10	548.973	4.56	549.145	25.622	549.54	63.118
Average		548.973	4.29	549.145	16.736	549.54	54.058

C.4 Drift

Table C.38 - Extended drift data

Location 1							
day	test	x (mm)	x drift (mm)	y (mm)	d drift (mm)	z (mm)	z drift (mm)
7	1	1246.571	0	4276.406	-94.2636	-950.44	4.368262
7	2	1217.997	-28.5742	4182.143	-89.0389	-946.07	314.0375
7	3	1219.575	-26.996	4187.367	-93.1129	-636.40	4.062511
7	4	1218.561	-28.0106	4183.293	0.909258	-946.38	179.3225
8	1	1247.758	1.186467	4277.316	-88.548	-771.12	3.643463
8	2	1221.261	-25.3106	4187.858	0.458704	-946.80	312.8431
8	3	1246.248	-0.32349	4276.865	-85.4682	-637.60	3.226576
8	4	1220.101	-26.4703	4190.938	1.154654	-947.21	-1.05762
8	5	1245.54	-1.03088	4277.561	-89.357	-951.50	3.0672
8	6	1218.065	-28.5068	4187.049	-84.1598	-947.37	2.753582
8	7	1219.22	-27.3515	4192.247	29.88579	-947.69	-6.04757
9	1	1228.683	-17.888	4306.292	-89.8015	-956.49	3.194137
9	2	1218.469	-28.1019	4186.605	-95.9778	-947.25	313.0557
9	3	1218.013	-28.5583	4180.429	-88.5567	-637.39	3.77518
9	4	1218.616	-27.9552	4187.85	-91.0681	-946.67	3.929456
9	5	1218.383	-28.1884	4185.338	-82.2791	-946.51	3.141693
9	6	1219.065	-27.5066	4194.127	-93.4012	-947.30	4.018942
9	7	1218.146	-28.4258	4183.005	-87.735	-946.42	3.328705
9	8	1218.558	-28.0129	4188.671	0	-947.11	0

Location 2							
day	test	x (mm)	x drift (mm)	y (mm)	d drift (mm)	z (mm)	z drift (mm)
7	1	8642.407	0	4555.071	0.1202	-770.89	-0.07687
7	2	8642.67	0.262598	4555.192	0.195037	-770.97	134.4878
7	3	8642.731	0.324034	4555.266	5.47596	-636.40	-0.24788
7	4	8609.298	-33.1089	4560.547	4.443993	-771.14	-0.22721
8	1	8615.731	-26.6757	4559.515	0.034257	-771.12	-0.12222
8	2	8642.571	0.16377	4555.106	0.057252	-771.01	133.2935
8	3	8642.77	0.362524	4555.129	-0.14218	-637.60	-0.39347
8	4	8643.517	1.10997	4554.929	-0.01106	-771.28	-0.53958
8	5	8643.48	1.072744	4555.06	0.109294	-771.43	-0.56405
8	6	8643.711	1.303833	4555.181	0.294357	-771.4	-0.7178
8	7	8643.59	1.182508	4555.366	0.158369	-771.61	-0.21752
9	1	8642.947	0.539981	4555.23	0.240718	-771.11	-0.33946
9	2	8642.715	0.308019	4555.312	0.14655	-771.23	133.506
9	3	8643.052	0.644605	4555.218	4.78752	-637.39	-0.46937
9	4	8613.54	-28.8666	4559.859	0.227616	-771.36	-0.28818
9	5	8643.18	0.772484	4555.299	0.273398	-771.18	-0.48653
9	6	8643.171	0.763567	4555.345	4.678776	-771.38	-0.51448
9	7	8615.435	-26.9717	4559.75	0.308684	-771.41	-0.5015
9	8	8642.737	0.330132	4555.38	0	-771.39	0

Location 3							
day	test	x (mm)	x drift (mm)	y (mm)	d drift (mm)	z (mm)	z drift (mm)
7	1	3792.442	0	7280.878	0.134919	-636.32	-0.03033
7	2	3792.271	-0.17061	7281.013	0.215298	-636.35	-0.0843
7	3	3792.033	-0.40879	7281.093	0.472915	-636.40	-0.14228
7	4	3792.084	-0.35778	7281.351	0.863086	-636.46	-1.06185
8	1	3791.005	-1.43673	7281.741	0.95932	-637.38	-1.14569
8	2	3790.99	-1.45215	7281.837	1.254518	-637.46	-1.27863
8	3	3790.828	-1.61447	7282.133	1.539416	-637.60	-1.4092
8	4	3790.796	-1.64617	7282.418	1.830395	-637.73	-1.46969
8	5	3790.37	-2.07212	7282.709	2.238089	-637.79	-1.49794
8	6	3790.37	-2.07212	7283.116	2.579578	-637.82	-1.61779
8	7	3790.204	-2.23762	7283.458	17.48876	-637.94	-3.63469
9	1	3780.282	-12.1606	7298.367	0.102845	-639.95	-1.0422
9	2	3791.636	-0.80581	7280.981	0.316067	-637.36	-1.06611
9	3	3791.62	-0.82194	7281.194	0.47649	-637.3	-1.09392
9	4	3791.662	-0.78017	7281.355	0.569131	-637.41	-1.12986
9	5	3791.586	-0.85565	7281.447	0.628166	-637.45	-1.15813
9	6	3791.586	-0.85565	7281.506	0.555096	-637.48	-1.183
9	7	3791.688	-0.7539	7281.433	0.620487	-637.50	-1.21526
9	8	3791.617	-0.8247	7281.499	0	-637.53	0

The following diagrams demonstrate the drift over 3 days.

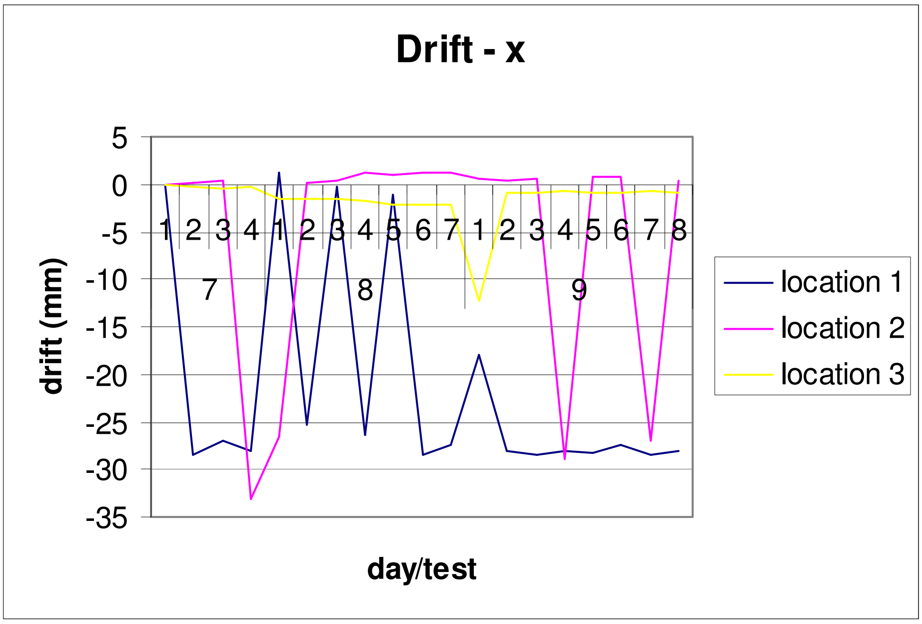

Figure C.75 - Drift, 3 day in x axis

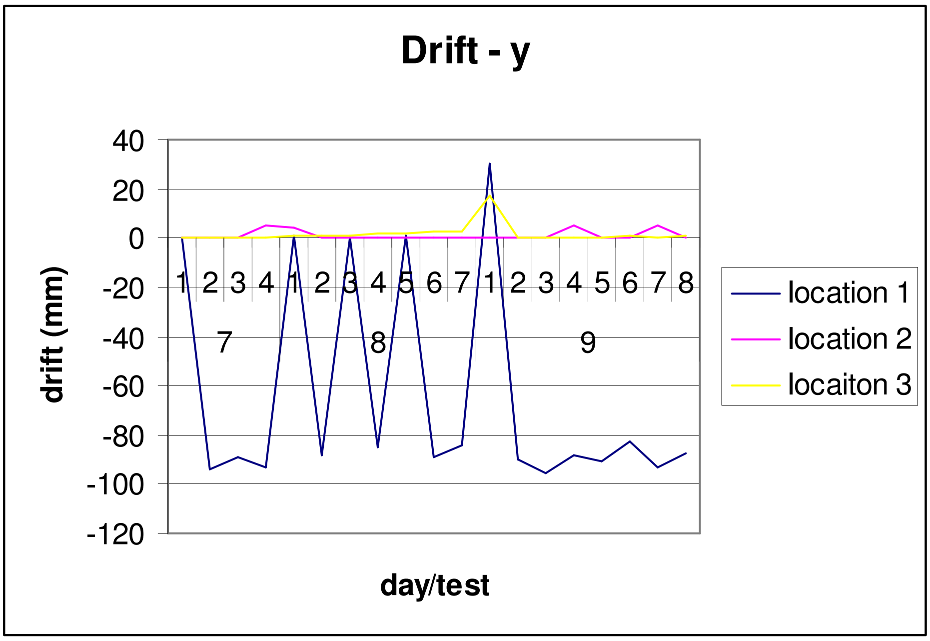

Figure C.76 - Drift, 3 day in y axis

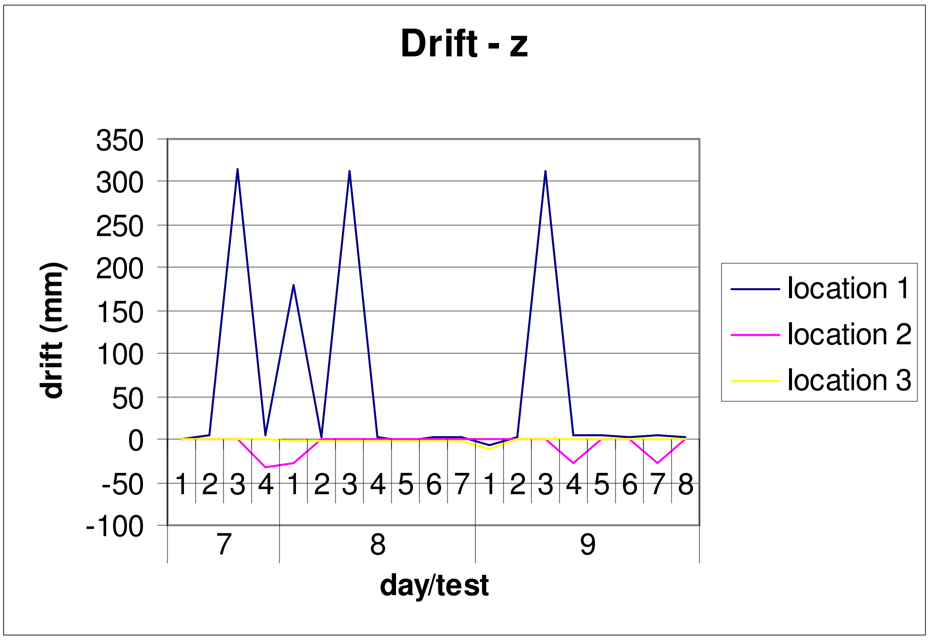

Figure C.77 - Drift, 3 day in z axis

Table C.39 - Drift data single day

x	y	Z	Abs
0	0	0	0
-0.17061	0.134919	-0.0303	0.219615
-0.40879	0.215298	-0.0843	0.469645
-0.35778	0.472915	-0.1422	0.609832

x	y	Z	
0	0	0	0
-0.01613	0.213222	-0.0239	0.215164
0.025647	0.373645	-0.0517	0.378078
-0.04983	0.466286	-0.0876	0.477065
-0.04983	0.525321	-0.1159	0.540265
0.051918	0.452252	-0.140	0.476499
-0.01889	0.517642	-0.1730	0.546133

x	y	Z	
0	0	0	0
-0.01542	0.096235	-0.0838	0.128565
-0.17774	0.391433	-0.2167	0.481463
-0.20945	0.67633	-0.3473	0.788631
-0.63539	0.96731	-0.4078	1.227089
-0.63539	1.375003	-0.4360	1.576241
-0.80089	1.716493	-0.5559	1.974042

The following diagrams demonstrate the drift over 1 day.

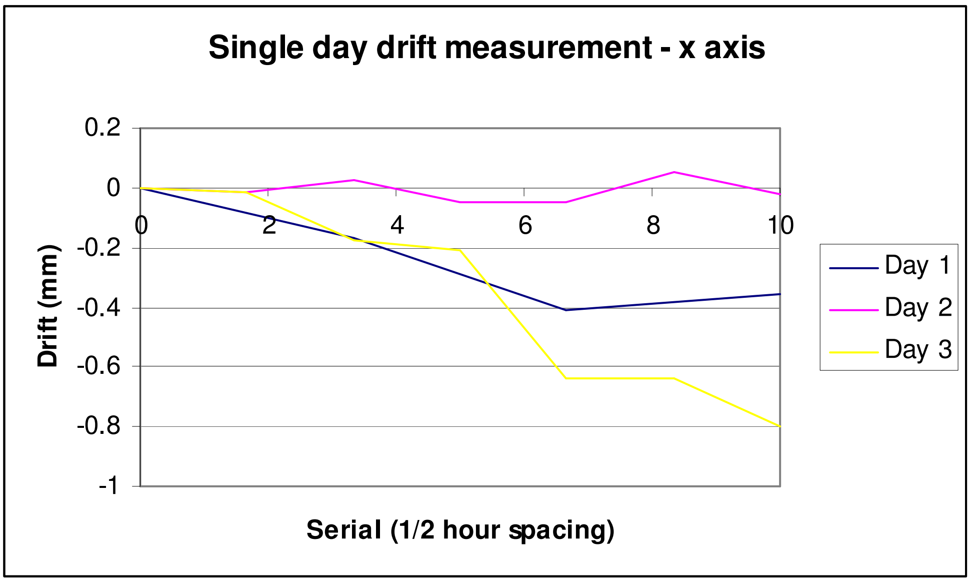

Figure C.78 - Drift, 1 day in x axis

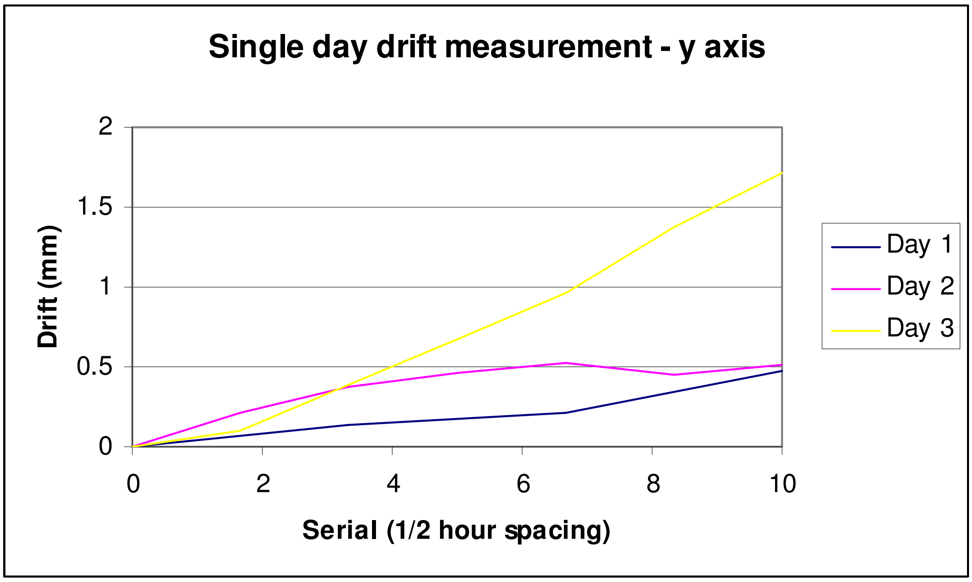

Figure C.79 - Drift, 1 day in y axis

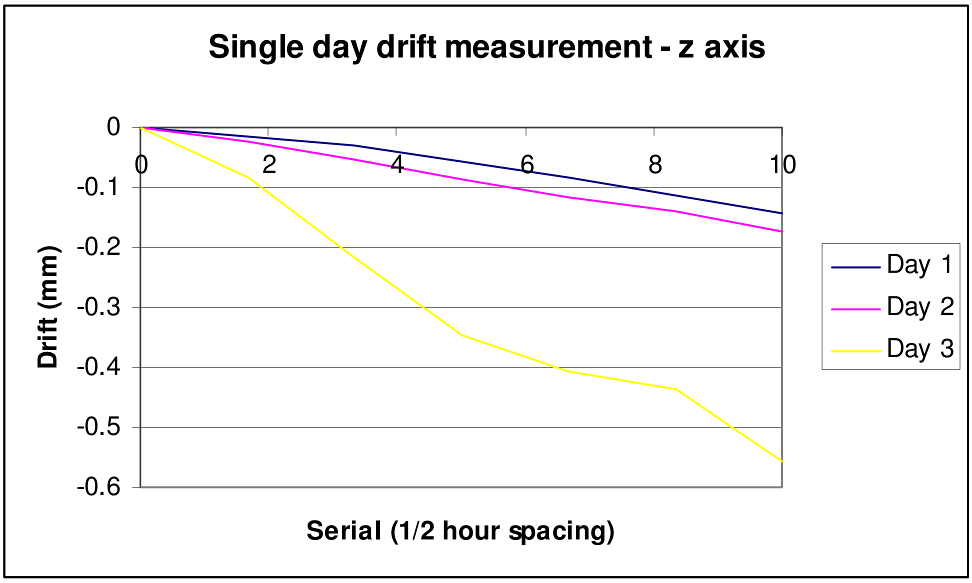

Figure C.80 - Drift, 1 day in z axis

Appendix D: Phase two testing

D.1 Krueger flap measurement data

The Krueger flap assembly jig is depicted below in Figure D.81.

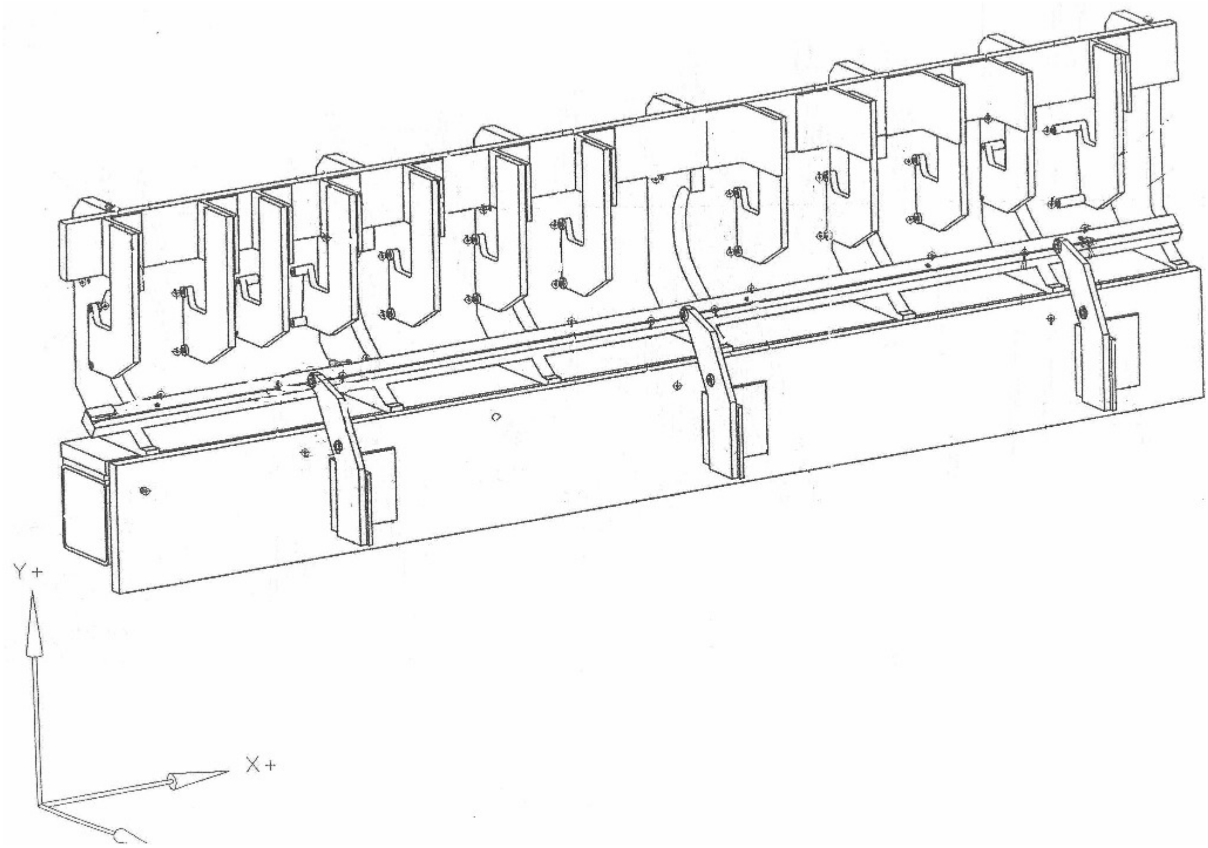

Figure D.81 - Krueger flap assembly jig diagram

Approximately 5000 samples were taken for each point, reference (EHi) and OTPi, using the IPS system. It should be noted that each of these points represents a point on the jig. When conjoined they represent vectors on a 3D rigid body. As IPS data varied for each sample point laser tracker data was taken to be absolute. Laser tracker data for the jig is presented in Table D.40.

Table D.40 - Laser tracker data (inches)

	Theoretical location		
Target	X (inch)	Y (inch)	Z (inch)
OTP 511	10.97078	-7.5552	3.21
OTP 512	17.06278	-7.5552	3.21
OTP 514	40.31738	-7.5552	3.21
OTP 515	46.40938	-7.5552	3.21
OTP 517	69.73608	-7.5552	3.21
OTP 518	75.82808	-7.5552	3.21
OTP 513	10.97078	-11.4052	6.61
OTP 516	40.31738	-11.4052	6.61
OTP 519	69.73608	-11.4052	6.61
eh1	1.5307	7.635344	-3.1273
eh2	46.7344	7.637444	-3.262
eh3	83.0347	7.642544	-2.9339
eh4	83.2332	-16.953	6.593744
eh5	55.548	-12.3913	6.674444
eh6	30.95	-12.2198	6.667844
eh7	-0.482	-16.8226	6.602944
SP501	0.0179	-12.6758	6.512844

A first best fit was calculated using laser tracker determined points as a reference. It was presumed that the IPSE Hi data would be more accurate because the mounting arrangement was less prone to parallax error as described in Section 7.2.2.

A transformation was determined between the IPS EHi point data and the laser tracker points corresponding to the EHi data points. The translation was then applied to all points in the IPSE Hi and OTPi data sets. Errors were then calculated as below:

$$\Delta X = X_{LT} - X_{IPS}$$
$$\Delta Y = Y_{LT} - Y_{IPS}$$
$$\Delta Z = Z_{LT} - Z_{IPS}$$
$$Error = \sqrt{\Sigma(\Delta X + \Delta Y + \Delta Z)}$$

The data for this scheme is presented in Table D.41.

Table D.41 - Krueger IPS data oriented by reference (EH) locations (inch)

	oriented by reference (EH) locations			Difference			Error	
	X	Y	Z	ΔX	ΔY	ΔZ		
eh1	1.55243	7.648943	-3.04984	-0.02173	-0.0136	-0.07746	0.081593	max
eh2	46.76942	7.656261	-3.33804	-0.03502	-0.01882	0.076039	0.085806	0.191819
eh3	83.0327	7.65778	-2.98573	0.002005	-0.01524	0.051828	0.054058	
eh4	83.26892	-16.9151	6.778361	-0.03572	-0.03788	-0.18462	0.191819	min
eh5	55.61539	-12.4259	6.596859	-0.06739	0.034574	0.077585	0.108425	0.054058
eh6	30.91938	-12.2802	6.534098	0.030618	0.060423	0.133746	0.149921	
eh7	-0.51118	-16.7795	6.669114	0.029181	-0.04313	-0.06617	0.084204	mean
SP501	-0.10189	-12.7231	6.446329	0.119789	0.047266	0.066515	0.14494	0.112596
OTP 511	11.03362	-7.64234	3.661999	-0.06283	0.087142	-0.452	0.464591	max
OTP 512	17.12676	-7.64665	3.647798	-0.06397	0.091445	-0.4378	0.451799	0.486737
OTP 514	40.37867	-7.64643	3.585784	-0.06129	0.091232	-0.37578	0.391526	
OTP 515	46.46944	-7.65263	3.594967	-0.06005	0.097425	-0.38497	0.401618	min
OTP 517	69.7996	-7.64431	3.662622	-0.06351	0.089106	-0.45262	0.465661	0.391526
OTP 518	75.89138	-7.65429	3.669232	-0.06329	0.099086	-0.45923	0.474044	
OTP 513	11.03429	-11.4361	7.091585	-0.0635	0.030919	-0.48159	0.486737	mean
OTP 516	40.3772	-11.4226	7.032285	-0.05982	0.017448	-0.42229	0.426857	0.446974
OTP 519	69.80139	-11.3732	7.064152	-0.06531	-0.03197	-0.45415	0.459936	

When the mean data was examined in Table D.41 it was clear that the mean error of 0.112596 inch applying to points EHi was smaller than the error of 0.44674 inch that applied to the points OTPi. This was now a measure of what was summarized in earlier chapters. Ie. That parallax error errors resulting from horizontally mounted receivers were of the order of 0.4 inch. Hence for the first time a measure of parallax error could be defined for a real jig.

This procedure was then repeated by comparing the OHi data sets between the IPS and laser tracker measurements, the results are presented in Table D.42.

Table D.42 - Krueger IPS data oriented by OTP locations (inch)

	oriented by OTP locations			Difference			Error	
	X	Y	Z	ΔX	ΔY	ΔZ		
eh1	1.493787	7.83962	-3.23229	0.036913	-0.20428	0.104989	0.232624	max
eh2	46.71078	7.840251	-3.52097	0.023622	-0.20281	0.258971	0.32978	0.628176
eh3	82.97405	7.827536	-3.16918	0.060647	-0.18499	0.235279	0.305379	
eh4	83.20436	-16.8911	6.220113	0.028841	-0.06194	0.373631	0.379828	min
eh5	55.55192	-12.3928	6.10728	-0.00392	0.0015	0.567164	0.56718	0.232624
eh6	30.85595	-12.2402	6.047082	0.094047	0.020367	0.620762	0.628176	
eh7	-0.57571	-16.7333	6.1141	0.093709	-0.08935	0.488844	0.505701	mean
SP501	-0.16543	-12.674	5.953018	0.183326	-0.00177	0.559826	0.589081	0.442219

OTP 511	10.9713	-7.55428	3.246116	-0.00051	-0.00092	-0.03612	0.036131	max
OTP 512	17.06444	-7.55986	3.231766	-0.00165	0.004658	-0.02177	0.02232	0.057837
OTP 514	40.31635	-7.56439	3.169441	0.001037	0.009194	0.040559	0.041601	
OTP 515	46.40711	-7.57222	3.178445	0.002275	0.017017	0.031555	0.035923	min
OTP 517	69.73727	-7.57064	3.245896	-0.00119	0.015438	-0.0359	0.039093	0.009357
OTP 518	75.82905	-7.58221	3.252269	-0.00096	0.027009	-0.04227	0.050171	
OTP 513	10.97107	-11.3998	6.617615	-0.00029	-0.00543	-0.00761	0.009357	mean
OTP 516	40.31399	-11.3926	6.558122	0.003396	-0.01262	0.051878	0.053498	0.038437
OTP 519	69.73819	-11.3509	6.590329	-0.0021	-0.05435	0.019671	0.057837	

The condensed data set is as shown below in Table D.43, this is presented in millimeters as appropriate for this thesis and employed in Chapter 5.

Table D.43 - Condensed Krueger data set (mm)

Oriented by data set	OTP		Reference	
	OTP	reference	OTP	Reference
Errors				
Maximum	0.057837	0.628176	0.486737	0.191819
Average	0.038437	0.442219	0.446974	0.112596
Minimum	0.009357	0.232624	0.391526	0.054058

This demonstrates that parallax error was dominant and is again quantified by the difference between accuracy of EHi and OTPi data sets.

Table D.44 - Krueger data accuracy (inch)

	Variation (inch)			
	1	10	20	50
eh1	0.011731	0.003948	0.003348	0.002596
eh2	0.011254	0.003384	0.002673	0.001877
eh3	0.009345	0.003348	0.002871	0.002133
eh4	0.009754	0.003528	0.002851	0.002009
eh5	8.168311	0.013558	0.009451	0.007796
eh6	28.57035	9.816874	0.113605	0.115899
eh7	0.157643	0.004161	0.003183	0.002364
SP501	0.026927	0.003415	0.00255	0.001918
OTP 511	0.006598	0.0026	0.002019	0.001243
OTP 512	4.151065	0.004567	0.003714	0.002785
OTP 514	0.008024	0.002561	0.001942	0.001093
OTP 515	0.010489	0.003232	0.00278	0.001696
OTP 517	0.014633	0.0037	0.002915	0.002366
OTP 518	0.008597	0.002605	0.00178	0.001215
OTP 513	0.009184	0.0033	0.002274	0.001565
OTP 516	0.020884	0.005099	0.004533	0.003176
OTP 519	0.009464	0.002797	0.002088	0.001214

D.2 757 spar section data

Table D.45 - 757 front spar data, day 1

Single sample	X		y		z		Tot		
	Avg	stdev	avg	Stdev	avg	Stdev	Stdev	error	
1a	767.1929	0.122862	3655.603	0.590272	-689.18	0.057427	0.605652	1.211304	
1b	1021.775	0.290898	3651.016	0.223042	-680.17	0.073447	0.37385	0.7477	
3a	2241.786	0.193988	3628.514	0.493179	-636.93	0.106189	0.540494	1.080987	
3b	2503.497	0.175045	3623.108	0.248395	-627.65	0.056811	0.309141	0.618282	
4a	3526.866	0.160105	3611.676	0.225483	-591.9	0.047863	0.280655	0.56131	
5a	4159.531	0.16527	3603.628	0.227082	-570.02	0.049796	0.285237	0.570473	
5b	4418.602	0.174014	3600.434	0.208947	-561.55	0.049565	0.276399	0.552798	
6a	6055.252	0.238735	3575.381	0.2917	-504.38	0.114962	0.394081	0.788161	
6b	6319.163	0.14041	3574.863	0.235068	-494.81	0.048927	0.278147	0.556293	
7a	7960.347	0.120961	3553.834	0.205851	-438.00	0.042254	0.24247	0.48494	average error
7b	8222.745	0.134849	3542.571	0.316777	-428.75	0.042445	0.346891	0.693782	0.715094

10 sample	X		y		Z		Tot		
	Avg	stdev	avg	Stdev	Avg	Stdev	Stdev	error	
1a	767.2077	0.063939	3655.664	0.231486	-689.18	0.021786	0.24114	0.48228	
1b	1021.782	0.142412	3651.024	0.114765	-680.17	0.028343	0.185083	0.370165	
3a	2241.796	0.068093	3628.516	0.115563	-636.93	0.020021	0.135618	0.271236	
3b	2503.523	0.058642	3623.12	0.125695	-627.64	0.024224	0.140801	0.281602	
4a	3526.881	0.069662	3611.691	0.105952	-591.89	0.016491	0.127869	0.255738	
5a	4159.55	0.076292	3603.639	0.093824	-570.01	0.021	0.122737	0.245475	
5b	4418.624	0.074097	3600.465	0.071544	-561.54	0.019421	0.104815	0.209629	
6a	6055.252	0.094761	3575.415	0.124186	-504.38	0.017883	0.157231	0.314461	
6b	6319.183	0.055939	3574.888	0.108425	-494.80	0.018593	0.123414	0.246827	
7a	7960.362	0.053273	3553.864	0.087198	-437.99	0.013243	0.103038	0.206076	average error
7b	8222.766	0.066603	3542.606	0.158755	-428.74	0.018175	0.173117	0.346233	0.293611

20 sample	X		y		Z		Tot	
	Avg	stdev	avg	Stdev	Avg	Stdev	Stdev	error
1a	767.1995	0.058235	3655.65	0.173904	-689.18	0.0169	0.184173	0.368346
1b	1021.756	0.116637	3650.991	0.092824	-680.17	0.027906	0.151655	0.30331
3a	2241.785	0.053775	3628.484	0.094489	-636.93	0.014006	0.109618	0.219236
3b	2503.513	0.045596	3623.092	0.115401	-627.64	0.017755	0.125346	0.250692
4a	3526.869	0.066317	3611.696	0.091988	-591.89	0.011524	0.113985	0.227969
5a	4159.541	0.062857	3603.616	0.079278	-570.02	0.014343	0.102185	0.20437
5b	4418.608	0.054783	3600.445	0.045263	-561.55	0.009028	0.071634	0.143267
6a	6055.246	0.073714	3575.399	0.096885	-504.38	0.010915	0.122227	0.244455
6b	6319.177	0.040951	3574.872	0.064544	-494.80	0.011791	0.077343	0.154686

7a	7960.36	0.046565	3553.845	0.060359	-437.99	0.009934	0.076878	0.153755	average error
7b	8222.756	0.058726	3542.572	0.136106	-428.74	0.011829	0.148706	0.297411	0.233409

50 sample	X Avg	stdev	y avg	Stdev	Z Avg	Stdev	Tot Stdev	error	
1a	767.2047	0.037532	3655.651	0.116995	-689.18	0.013167	0.123571	0.247142	
1b	1021.732	0.10514	3650.968	0.063967	-680.17	0.016526	0.124175	0.24835	
3a	2241.772	0.049976	3628.493	0.068544	-636.93	0.008721	0.085276	0.170553	
3b	2503.485	0.047883	3623.08	0.074456	-627.65	0.015762	0.089916	0.179833	
5a	3526.873	0.043236	3611.679	0.069797	-591.89	0.007086	0.082409	0.164818	
6a	4159.537	0.046615	3603.627	0.055426	-570.02	0.009812	0.073084	0.146168	
6b	4418.596	0.041954	3600.443	0.025194	-561.55	0.007935	0.049577	0.099154	
7a	6055.229	0.030488	3575.389	0.053599	-504.38	0.006482	0.062003	0.124005	
7b	6319.167	0.017925	3574.863	0.04482	-494.80	0.010089	0.049314	0.098629	
8a	7960.358	0.025794	3553.832	0.031611	-438.00	0.006742	0.041352	0.082704	average error
8b	8222.749	0.035091	3542.573	0.094238	-428.74	0.008247	0.100896	0.201793	0.160286

Table D.46 - 757 rear spar data, day 1

single sample	X Avg	stdev	y avg	Stdev	z avg	Stdev	Tot Stdev	error	
1s	1799.497	0.131852	6126.564	0.189823	-736.48	0.077756	0.243852	0.487704	
1l	1736.681	0.314096	6130.843	1.58093	-739.12	0.123527	1.616556	3.233113	
3s	3068.349	0.519183	6109.914	0.262967	-692.01	0.189853	0.612166	1.224332	
3l	3001.467	0.30952	6112.31	0.447479	-694.35	0.12885	0.559144	1.118289	
5s	6018.765	1.149884	6065.414	2.256992	-589.50	0.106801	2.535282	5.070563	
5l	5956.276	0.142113	6072.488	0.161801	-592.18	0.04176	0.219361	0.438723	
6s	7919.829	0.157764	6032.927	0.648827	-522.83	0.052807	0.669817	1.339634	average error
6l	7854.861	0.257847	6046.773	0.556249	-526.01	0.04606	0.614833	1.229667	1.767753

10 sample	X Avg	stdev	y avg	Stdev	Z Avg	Stdev	Tot Stdev	error	
1s	1799.517	0.054226	6126.577	0.091116	-736.48	0.020014	0.107904	0.215808	
1l	1736.631	0.273608	6131.301	1.538192	-739.14	0.079624	1.564364	3.128728	
3s	3068.388	0.456746	6109.937	0.171436	-692.01	0.148515	0.509965	1.01993	
3l	3001.405	0.478764	6112.433	0.309663	-694.36	0.040273	0.571602	1.143203	
5s	6018.845	1.082302	6065.559	2.15053	-589.49	0.090557	2.409223	4.818447	
5l	5956.288	0.048444	6072.524	0.06492	-592.17	0.020036	0.083444	0.166888	
6s	7919.852	0.064785	6032.92	0.135245	-522.83	0.019998	0.151289	0.302578	average error
6l	7854.891	0.075874	6046.83	0.085913	-526.00	0.019549	0.116276	0.232552	1.378517

20 sample	X		y		Z		Tot		
	Avg	stdev	avg	Stdev	Avg	Stdev	Stdev	error	
1s	1799.515	0.045418	6126.567	0.059204	-736.49	0.012288	0.075624	0.151248	
1l	1736.588	0.256863	6131.395	1.481545	-739.14	0.077439	1.50564	3.011279	
3s	3068.374	0.449661	6109.924	0.151	-692.01	0.131947	0.492348	0.984695	
3l	3001.329	0.640914	6112.451	0.415707	-694.36	0.049945	0.765557	1.531115	
5s	6018.813	1.116243	6065.486	2.216637	-589.49	0.090769	2.483488	4.966977	
5l	5956.275	0.033775	6072.516	0.046384	-592.18	0.01435	0.059145	0.11829	
6s	7919.841	0.052527	6032.9	0.109109	-522.83	0.016294	0.122186	0.244371	average error
6l	7854.885	0.069933	6046.824	0.080343	-526.01	0.013638	0.107385	0.21477	1.402843

50 sample	X		y		Z		Tot		
	Avg	stdev	avg	Stdev	Avg	Stdev	Stdev	error	
1s	1799.494	0.036419	6126.586	0.037591	-736.49	0.006587	0.052753	0.105505	
1l	1736.561	0.262542	6131.634	1.485662	-739.16	0.074861	1.510538	3.021076	
3s	3068.46	0.064981	6109.892	0.035826	-692.05	0.012712	0.075284	0.150568	
3l	3001.471	0.068555	6112.372	0.068897	-694.36	0.019282	0.099088	0.198176	
5s	6018.761	1.153958	6065.367	2.331321	-589.49	0.085876	2.602701	5.205402	
5l	5956.282	0.036865	6072.503	0.023218	-592.18	0.0099	0.044678	0.089356	
6s	7919.833	0.023507	6032.888	0.082839	-522.84	0.010699	0.086772	0.173544	average error
6l	7854.879	0.042703	6046.813	0.043885	-526.01	0.008146	0.061772	0.123544	1.133396

Table D.47 - 757 front spar data, day 2

Single sample	X		Y		Z		Tot		
	Avg	stdev	Avg	Stdev	Avg	Stdev	Stdev	error	
1a	766.3195	0.115582	3648.068	0.39204	-688.25	0.071037	0.41485	0.8297	
1b	1022.695	0.270677	3649.393	0.204156	-679.44	0.083902	0.349265	0.698529	
3a	2241.464	0.144084	3627.746	0.293337	-636.28	0.072413	0.33474	0.66948	
3b	2503.236	0.164004	3623.301	0.232919	-627.08	0.068695	0.293031	0.586062	
4a	3526.498	0.169384	3611.494	0.219399	-591.51	0.064508	0.284584	0.569169	
4b	3789.08	0.183168	3600.168	0.247961	-581.61	0.0816	0.318894	0.637789	
5a	4158.948	0.186999	3603.059	0.236075	-570.08	0.065563	0.308218	0.616436	
5b	4418.614	0.144131	3600.946	0.177079	-560.54	0.051693	0.2341	0.468201	
6a	6055.052	0.135244	3575.656	0.246902	-504.37	0.052951	0.286453	0.572906	
6b	6349.418	407.8708	4147.699	1439.987	-504.06	39.95972	1497.17		
7a	7959.315	0.785624	3552.903	0.502323	-437.08	0.75585	1.200351	2.400703	average error
7b	8223.292	0.168935	3543.204	0.347093	-427.42	0.085777	0.395437	0.790874	0.803623

10 sample	X		Y		Z		Tot	

	Avg	stdev	Avg	Stdev	Avg	Stdev	Stdev	error	
1a	766.3039	0.044605	3647.97	0.278412	-688.26	0.030741	0.283633	0.567267	
1b	1022.66	0.109119	3649.359	0.085079	-679.45	0.024475	0.140515	0.281029	
3a	2241.437	0.053283	3627.705	0.120256	-636.29	0.02103	0.133202	0.266404	
3b	2503.211	0.054705	3623.252	0.091844	-627.09	0.024166	0.109599	0.219198	
4a	3526.468	0.098354	3611.467	0.113004	-591.52	0.02162	0.151364	0.302727	
4b	3789.054	0.077356	3600.129	0.10143	-581.62	0.025676	0.13012	0.26024	
5a	4158.927	0.117974	3603.012	0.142061	-570.09	0.022301	0.186002	0.372004	
5b	4418.595	0.050837	3600.914	0.065681	-560.55	0.014149	0.084253	0.168506	
6a	6055.023	0.059165	3575.637	0.131916	-504.38	0.018462	0.14575	0.291501	
6b	6326.114	69.9326	3984.936	729.7247	-505.59	16.73202	733.2589		
7a	7959.297	0.485553	3552.859	0.213211	-437.13	0.381356	0.653186	1.306373	average error
7b	8223.261	0.073775	3543.165	0.183961	-427.43	0.036581	0.201551	0.403102	0.403486

20 sample	X		Y		Z		Tot		
	Avg	stdev	Avg	Stdev	Avg	Stdev	Stdev	error	
1a	766.3187	0.036375	3648.012	0.253262	-688.25	0.025723	0.257151	0.514302	
1b	1022.702	0.073505	3649.397	0.05519	-679.44	0.01846	0.093753	0.187506	
3a	2241.466	0.044995	3627.751	0.068992	-636.28	0.017442	0.084194	0.168389	
3b	2503.241	0.040199	3623.29	0.071229	-627.08	0.0153	0.083209	0.166417	
4a	3526.494	0.074208	3611.5	0.093732	-591.51	0.014013	0.12037	0.24074	
4b	3789.08	0.064567	3600.172	0.07675	-581.61	0.018039	0.101906	0.203812	
5a	4158.963	0.110312	3603.031	0.129932	-570.08	0.013852	0.171006	0.342012	
5b	4418.619	0.033209	3600.94	0.04917	-560.54	0.012269	0.060589	0.121179	
6a	6055.042	0.044431	3575.675	0.114846	-504.37	0.014677	0.124013	0.248026	
6b	6334.994	24.6861	4019.023	562.81	-502.79	10.18259	563.4432		
7a	7959.356	0.246222	3552.901	0.153182	-437.12	0.249873	0.382788	0.765576	average error
7b	8223.288	0.056848	3543.218	0.143548	-427.42	0.027996	0.156912	0.313825	0.297435

50 sample	X		Y		Z		Tot		
	Avg	stdev	Avg	Stdev	Avg	Stdev	Stdev	error	
1a	766.3124	0.031939	3648.002	0.208828	-688.25	0.020362	0.212235	0.42447	
1b	1022.69	0.042047	3649.386	0.027101	-679.44	0.013065	0.051702	0.103404	
3a	2241.455	0.033154	3627.747	0.056731	-636.29	0.010447	0.066534	0.133067	
3b	2503.235	0.030936	3623.276	0.060808	-627.08	0.010635	0.069049	0.138098	
4a	3526.477	0.080143	3611.501	0.084168	-591.51	0.010203	0.116668	0.233335	
4b	3789.075	0.050028	3600.161	0.067699	-581.61	0.013892	0.085317	0.170634	
5a	4158.945	0.093595	3603.039	0.108392	-570.08	0.013752	0.143868	0.287737	
5b	4418.613	0.022202	3600.937	0.032315	-560.54	0.00657	0.039754	0.079507	
6a	6055.038	0.039491	3575.664	0.097688	-504.38	0.009288	0.105777	0.211554	
6b	6327.56	7.492178	3875.068	259.11	-502.84	4.056073	259.25		
7a	7959.377	0.121776	3552.88	0.074418	-437.16	0.054324	0.152704	0.305408	average error
7b	8223.29	0.049034	3543.193	0.13184	-427.42	0.020863	0.142201	0.284403	0.215601

Table D.48 - 757 rear spar data, day 2

single sample	X		Y		Z		Tot		
	Avg	stdev	avg	stdev	Avg	Stdev	Stdev	error	
1s	1798.44	0.135308	6124.29	0.180885	-736.75	0.063567	0.234666	0.469333	
1l	1731.796	0.200782	6126.921	0.380303	-738.72	0.06425	0.434824	0.869648	
3s	3067.386	0.189499	6108.17	0.184198	-691.54	0.053363	0.269604	0.539207	
3l	3000.732	0.433198	6110.418	0.913795	-694.25	0.786158	1.280908	2.561816	
5s	6035.535	136.7142	6073.649	54.95961	-579.69	75.06205	165.3652		
5l	5952.358	0.150893	6073.544	0.14386	-591.24	0.071866	0.22052	0.441041	
6s	7922.392	0.170581	6040.893	0.253177	-522.56	0.063158	0.311745	0.62349	average error
6l	7852.605	0.142805	6046.412	0.184584	-525.59	0.084539	0.248216	0.496433	0.857281

10 sample	X		Y		Z		Tot		
	Avg	stdev	avg	stdev	Avg	Stdev	Stdev	error	
1s	1798.425	0.066745	6124.261	0.061349	-736.76	0.023409	0.09363	0.18726	
1l	1731.777	0.068083	6126.881	0.162619	-738.73	0.026235	0.178237	0.356474	
3s	3067.358	0.116197	6108.144	0.09376	-691.55	0.017895	0.150376	0.300752	
3l	3000.704	0.259571	6110.377	0.444236	-694.26	0.504101	0.720306	1.440612	
5s	6031.985	67.94327	6072.132	27.35551	-581.97	38.01256	82.5201		
5l	5952.335	0.052475	6073.521	0.046454	-591.25	0.023461	0.073906	0.147812	
6s	7922.376	0.083988	6040.851	0.131841	-522.57	0.018127	0.157368	0.314736	average error
6l	7852.585	0.042932	6046.374	0.061067	-525.60	0.020419	0.07739	0.154781	0.414632

20 sample	X		Y		Z		Tot		
	Avg	stdev	avg	stdev	Avg	Stdev	Stdev	error	
1s	1798.456	0.056679	6124.288	0.039947	-736.75	0.01997	0.07216	0.14432	
1l	1731.795	0.059048	6126.915	0.09592	-738.71	0.04327	0.120663	0.241325	
3s	3067.385	0.106374	6108.174	0.082745	-691.54	0.016032	0.135717	0.271434	
3l	3000.731	0.12892	6110.404	0.286779	-694.23	0.25154	0.40266	0.805319	
5s	6028.289	30.42559	6070.635	12.33442	-584.08	18.34235	37.60713		
5l	5952.368	0.065009	6073.548	0.040533	-591.23	0.015944	0.078252	0.156504	
6s	7922.401	0.068772	6040.874	0.112383	-522.56	0.013724	0.132468	0.264937	average error
6l	7852.609	0.035193	6046.406	0.04152	-525.59	0.016724	0.05694	0.113879	0.285388

50 sample	X		Y		Z		Tot	
	Avg	stdev	avg	stdev	Avg	Stdev	Stdev	error
1s	1798.448	0.049346	6124.283	0.019501	-736.75	0.011046	0.054197	0.108394
1l	1731.794	0.06216	6126.89	0.136419	-738.78	0.023029	0.151672	0.303344
3s	3067.393	0.098013	6108.159	0.052415	-691.55	0.011137	0.111705	0.223409
3l	3000.723	0.082826	6110.374	0.074219	-694.21	0.100442	0.149857	0.299714
5s	6024.83	8.870751	6069.119	3.611369	-586.77	5.268709	10.93122	

5l	5952.543	0.544401	6073.605	0.193438	-591.23	0.028064	0.578428	1.156856	
6s	7922.398	0.056793	6040.877	0.098264	-522.56	0.011723	0.114099	0.228199	average error
6l	7852.604	0.029677	6046.401	0.028586	-525.59	0.009072	0.042192	0.084384	0.343471

Table D.49 - 757 rear spar data, day 3

Single sample	X		Y		Z		Tot		
	Avg	stdev	Avg	Stdev	Avg	Stdev	Stdev	error	
1a	761.3972	0.138936	3661.838	0.407252	-596.89	0.089945	0.4396	0.879199	
1b	1015.158	0.367408	3663.698	0.282037	-589.02	0.086119	0.471116	0.942232	
3a	2236.5	0.16824	3644.08	0.296372	-550.26	0.072981	0.348522	0.697044	
3b	2495.742	0.184494	3637.694	0.270035	-542.65	0.074366	0.335391	0.670783	
6a	4411.693	0.185429	3615.279	0.237156	-483.57	0.048325	0.304897	0.609794	
6b	4411.693	0.185429	3615.279	0.237156	-483.57	0.048325	0.304897	0.609794	
7a	6048.769	0.142987	3590.053	0.214704	-432.59	0.053188	0.263386	0.526772	
7b	6313.635	10.64403	3649.42	492.3935	-427.10	4.055226	492.5252		
8a	7970.801	177.8228	3583.226	137.7867	-370.05	38.98098	228.3104		average error
8b	8217.594	0.164388	3557.806	0.295815	-364.56	0.067287	0.345048	0.690095	0.703214

10 sample	X		Y		Z		Tot		
	Avg	stdev	Avg	Stdev	Avg	Stdev	Stdev	error	
1a	761.3799	0.056015	3661.831	0.221496	-596.92	0.029219	0.23033	0.460661	
1b	1015.108	0.203625	3663.659	0.144359	-589.04	0.025699	0.250924	0.501848	
3a	2236.475	0.070323	3644.039	0.114994	-550.27	0.019927	0.136257	0.272514	
3b	2495.71	0.067881	3637.666	0.121936	-542.66	0.024867	0.141755	0.283511	
6a	4411.671	0.080998	3615.248	0.10938	-483.58	0.013856	0.136809	0.273618	
6b	4411.671	0.080998	3615.248	0.10938	-483.58	0.013856	0.136809	0.273618	
7a	6048.745	0.057165	3590.018	0.085962	-432.60	0.015495	0.104391	0.208782	
7b	6313.127	4.475438	3629.542	199.5147	-427.31	2.218738	199.5772		
8a	7970.12	74.79	3548.498	181.741	-370.22	17.38948	197.2961		average error
8b	8217.571	0.0663	3557.765	0.136879	-364.57	0.018812	0.15325	0.3065	0.322631

20 sample	X		Y		Z		Tot	
	Avg	stdev	Avg	Stdev	Avg	Stdev	Stdev	error
1a	761.3919	0.04198	3661.913	0.200797	-596.90	0.023419	0.206471	0.412942
1b	1015.179	0.170899	3663.696	0.104222	-589.02	0.02172	0.201347	0.402694
3a	2236.503	0.058217	3644.104	0.096433	-550.26	0.014604	0.113586	0.227173
3b	2495.743	0.061009	3637.716	0.100852	-542.65	0.016677	0.119043	0.238087
6a	4411.701	0.067422	3615.285	0.092221	-483.57	0.010872	0.114755	0.22951
6b	4411.701	0.067422	3615.285	0.092221	-483.57	0.010872	0.114755	0.22951
7a	6048.77	0.045341	3590.055	0.05341	-432.59	0.010815	0.07089	0.141779
7b	6313.394	2.975228	3625.556	132.3583	-426.75	1.558179	132.4009	

8a	7972.108	63.58401	3562.283	94.06194	-369.06	17.43505	114.8676		average error
8b	8217.593	0.053023	3557.822	0.121517	-364.56	0.014992	0.133427	0.266853	0.268568

50 sample	X		Y		Z		Tot		
	Avg	stdev	Avg	Stdev	Avg	Stdev	Stdev	error	
1a	761.3905	0.042263	3661.904	0.137421	-596.91	0.015254	0.14458	0.289161	
1b	1015.165	0.148156	3663.689	0.076439	-589.03	0.018445	0.16773	0.335459	
3a	2236.5	0.048703	3644.097	0.081132	-550.26	0.011118	0.095278	0.190557	
3b	2495.741	0.04813	3637.715	0.090236	-542.65	0.010049	0.102762	0.205524	
6a	4411.678	0.070048	3615.292	0.073569	-483.58	0.011841	0.102271	0.204542	
6b	4411.678	0.070048	3615.292	0.073569	-483.58	0.011841	0.102271	0.204542	
7a	6048.765	0.030943	3590.047	0.026595	-432.59	0.009062	0.041796	0.083592	
7b	6312.823	0.755954	3594.545	23.99256	-426.75	0.990772	24.0249		
8a	7957.54	6.696696	3567.511	22.6872	-372.84	2.467828	23.78329		average error
8b	8217.593	0.042567	3557.808	0.103929	-364.56	0.008995	0.112668	0.225337	0.217339

single sample	X		Y		Z		Tot		
	Avg	stdev	Avg	Stdev	Avg	Stdev	Stdev	error	
1s	1777.377	0.131225	6143.195	0.204177	-617.53	0.082238	0.256265	0.512529	
1l	1712.866	0.732181	6143.568	0.636181	-619.46	0.129931	0.978621	1.957241	
3s	3061.063	0.355979	6126.41	0.407941	-576.52	0.32998	0.634054	1.268107	
3l	2991.434	0.168549	6128.147	0.181301	-578.98	0.05759	0.254157	0.508313	
5s	6027.861	61.05366	6093.14	24.76673	-486.25	77.38013	101.6298		
5l	5948.944	0.169897	6090.281	0.176327	-487.24	0.054817	0.25092	0.501841	
6s	7906.896	0.493936	6062.52	0.35032	-426.98	0.36467	0.706881	1.413762	average error
6l	7845.104	0.17235	6067.593	0.2446	-428.88	0.0816	0.310149	0.620298	0.96887

10 sample	X		Y		Z		Tot		
	Avg	stdev	Avg	Stdev	Avg	Stdev	Stdev	error	
1s	1777.356	0.035906	6143.168	0.098738	-617.54	0.029104	0.10902	0.218041	
1l	1712.74	0.645935	6143.448	0.56118	-619.48	0.082002	0.859581	1.719162	
3s	3064.874	28.19624	6131.798	39.74111	-571.92	34.01519	59.42573		
3l	2991.407	0.071611	6128.12	0.075452	-578.99	0.020268	0.105981	0.211962	
5s	6024.099	26.5564	6091.466	11.2029	-488.68	39.27193	48.71378		
5l	5948.922	0.078766	6090.249	0.076787	-487.25	0.016705	0.111263	0.222526	
6s	7906.861	0.160818	6062.463	0.122883	-427.00	0.113664	0.232126	0.464252	average error
6l	7845.074	0.099099	6067.57	0.133815	-428.89	0.02355	0.168171	0.336343	0.528714

20 sample	X		Y		Z		Tot	

	Avg	stdev	Avg	Stdev	Avg	Stdev	Stdev	error	
1s	1777.374	0.038385	6143.199	0.099527	-617.54	0.021789	0.108875	0.217751	
1l	1712.691	0.629686	6143.43	0.535075	-619.48	0.077147	0.829917	1.659834	
3s	3064.533	18.80245	6131.294	26.53176	-572.38	22.95307	39.80339		
3l	2991.436	0.062685	6128.153	0.063061	-578.98	0.012729	0.089822	0.179645	
5s	6024.489	22.67522	6091.691	10.22992	-485.54	18.73688	31.14302		
5l	5948.953	0.067303	6090.269	0.055926	-487.24	0.011517	0.088261	0.176523	
6s	7906.888	0.185331	6062.492	0.128328	-426.98	0.11048	0.25104	0.502081	average error
6l	7845.093	0.088572	6067.613	0.118934	-428.88	0.017589	0.149331	0.298662	0.505749

50 sample	X		Y		Z		Tot		
	Avg	stdev	Avg	Stdev	Avg	Stdev	Stdev	error	
1s	1777.371	0.029428	6143.184	0.059398	-617.54	0.011461	0.067272	0.134544	
1l	1712.631	0.612223	6143.373	0.521927	-619.49	0.071496	0.807673	1.615346	
3s	3066.24	19.29834	6133.747	27.32	-570.34	23.24033	40.72986		
3l	2991.43	0.058601	6128.144	0.043835	-578.98	0.008405	0.073663	0.147327	
5s	6020.681	6.738122	6090.103	3.763391	-486.24	5.024979	9.20955		
5l	5948.974	0.104328	6090.283	0.084065	-487.24	0.007345	0.134183	0.268367	
6s	7906.866	0.071893	6062.479	0.048578	-427.00	0.022071	0.08953	0.17906	average error
6l	7845.093	0.06327	6067.604	0.074963	-428.88	0.014391	0.099145	0.198289	0.423822

Table D.50 - Summary of 757 spar data

Samples	Test 1		Test 2		Test 3		Average	
	front	Back	Front	Back	front	back	Front	back
1	0.71509	1.76775	0.80362	0.857281	0.703214	0.96887	0.740643	1.197968
10	0.29361	1.37851	0.40348	0.414632	0.322631	0.528714	0.33991	0.773954
20	0.23340	1.40284	0.29743	0.285388	0.268568	0.505749	0.266471	0.731327
50	0.16028	1.13339	0.21560	0.343471	0.217339	0.423822	0.197742	0.633563

D.3 757 main section data

Table D.51 - 757 main jig, single data point

location	X	st-x	Y	st-y	Z	St-z	St	err
1	11504.6	0.113244	4344.176	0.173991	-536.04	0.045447	0.212515	0.42503
2	13301.87	0.971376	5291.338	0.594722	-550.60	0.101634		
3	11080.03	792.521	5087.771	391.3186	-559.21	47.77004		
4	9698.556	0.14627	4599.278	0.223107	-571.78	0.079688	0.278427	0.556853
5	9147.669	0.14663	4883.37	0.220541	-586.21	0.059198	0.271372	0.542744
6	7311.645	0.127124	5749.33	0.214541	-654.68	0.097086	0.267608	0.535217
7	8103.213	0.176686	5036.177	0.206391	-609.87	0.065065	0.279372	0.558743
8	6214.349	0.140067	5779.157	0.187091	-677.23	0.114594	0.260295	0.52059
9	7040.943	0.120155	5221.029	0.17428	-636.76	0.04439	0.21629	0.43258
10	5120.05	0.159655	5883.122	0.308205	-701.18	0.087311	0.357915	0.71583
11	5581.507	0.200393	5405.133	0.234207	-668.94	0.100148	0.324099	0.648198
12	7595.327	0.150212	5661.183	0.203595	-648.62	0.050829	0.258066	0.516132
13	8867.248	0.162571	5386.122	0.211575	-612.70	0.104786	0.286659	0.573317
14	6860.139	0.135131	5095.049	0.25654	-634.36	0.063302	0.296783	0.593567
15	8395.465	0.168079	5109.579	0.192349	-605.67	0.054853	0.261261	0.522523
16	10424.42	0.149947	5037.661	0.246901	-583.66	0.088134	0.302013	0.604026
17	11460.63	0.124036	4528.047	0.184118	-543.53	0.064733	0.231246	0.462492
18	9594.358	0.149466	5330.045	0.195241	-605.86	0.047115	0.250358	0.500716
19	10526.57	0.12221	5406.91	0.206476	-595.12	0.048479	0.244781	0.489563
20	12242.6	0.11631	4325.769	0.245398	-523.42	0.054779	0.277036	0.554072
							max	0.71583
							average	0.541788
							min	0.42503

Table D.52 - 757 main jig, 10 data point

location	X	st-x	Y	st-y	Z	St-z	st	err
1	11504.58	0.055458	4344.149	0.07321	-536.05	0.014586	0.092995	0.185989
2	13301.78	0.509391	5291.272	0.312096	-550.62	0.054559		
3	11084.96	778.1166	5091.755	383.839	-561.22	43.03261		
4	9698.535	0.047383	4599.244	0.079737	-571.79	0.025669	0.09624	0.192479
5	9147.645	0.060115	4883.341	0.080986	-586.22	0.026754	0.104347	0.208694
6	7311.624	0.051944	5749.297	0.081464	-654.69	0.043087	0.105788	0.211576
7	8103.185	0.064771	5036.148	0.085731	-609.87	0.029914	0.111535	0.22307
8	6214.326	0.054563	5779.128	0.07441	-677.24	0.038661	0.100043	0.200086
9	7040.924	0.053907	5221.001	0.062664	-636.76	0.013843	0.083812	0.167623
10	5120.028	0.105203	5883.07	0.128915	-701.19	0.032166	0.169474	0.338948
11	5581.475	0.070067	5405.103	0.09173	-668.95	0.04763	0.12487	0.249739
12	7595.304	0.095353	5661.148	0.09363	-648.63	0.016829	0.134692	0.269384
13	8867.222	0.069841	5386.088	0.096398	-612.72	0.058969	0.132844	0.265688
14	6860.115	0.058098	5095.006	0.09528	-634.37	0.021929	0.11373	0.227461

15	8395.439	0.082488	5109.549	0.075005	-605.68	0.014874	0.112478	0.224955
16	10424.4	0.056772	5037.63	0.125851	-583.67	0.060824	0.150868	0.301736
17	11460.61	0.054008	4528.013	0.052451	-543.54	0.025034	0.079339	0.158678
18	9594.333	0.059819	5330.015	0.089882	-605.87	0.011516	0.10858	0.217161
19	10526.54	0.04071	5406.879	0.087799	-595.13	0.012707	0.097608	0.195216
20	12242.58	0.056955	4325.727	0.091829	-523.43	0.015314	0.109138	0.218276
							max	0.338948
							average	0.225376
							min	0.158678

Table D.53 - 757 main jig, 20 data point

location	X	st-x	Y	st-y	Z	st-z	st	err
1	11504.6	0.044962	4344.179	0.059095	-536.04	0.011341	0.075116	0.150232
2	13301.88	0.318404	5291.337	0.209128	-550.60	0.058189		
3	11098.27	770.4684	5107.255	360.9208	-562.00	37.06567		
4	9698.56	0.02845	4599.273	0.051428	-571.78	0.019225	0.061838	0.123675
5	9147.665	0.04456	4883.376	0.051516	-586.21	0.017245	0.070263	0.140526
6	7311.643	0.035612	5749.33	0.060589	-654.68	0.019905	0.073044	0.146088
7	8103.214	0.04111	5036.181	0.060887	-609.86	0.018846	0.075844	0.151689
8	6214.349	0.028049	5779.157	0.046746	-677.23	0.024655	0.059831	0.119662
9	7040.945	0.047435	5221.029	0.050566	-636.76	0.011155	0.070224	0.140448
10	5120.05	0.091839	5883.124	0.10909	-701.17	0.016144	0.143512	0.287024
11	5581.495	0.065051	5405.139	0.076706	-668.93	0.03014	0.104995	0.209989
12	7595.324	0.082257	5661.183	0.084647	-648.62	0.011334	0.118574	0.237148
13	8867.246	0.051236	5386.117	0.084013	-612.70	0.053901	0.1122	0.224399
14	6860.139	0.043633	5095.052	0.06986	-634.36	0.018214	0.084356	0.168712
15	8395.46	0.061549	5109.581	0.063504	-605.67	0.007707	0.088772	0.177544
16	10424.42	0.04367	5037.663	0.101067	-583.66	0.056745	0.123861	0.247722
17	11460.63	0.045163	4528.041	0.040009	-543.53	0.010478	0.061239	0.122478
18	9594.356	0.046686	5330.048	0.068559	-605.86	0.006155	0.083174	0.166347
19	10526.56	0.031262	5406.912	0.053625	-595.13	0.010818	0.063008	0.126016
20	12242.6	0.041444	4325.761	0.059094	-523.42	0.013617	0.073451	0.146903
							max	0.287024
							average	0.171478
							min	0.119662

Table D.54 - 757 main jig, 50 data point

location	X	st-x	Y	st-y	Z	st-z	st	err
1	11504.59	0.028378	4344.172	0.053759	-536.04	0.008793	0.061422	0.122843
2	13301.86	0.302333	5291.319	0.213038	-550.60	0.048515		
3	11115.13	705.6862	5123.197	321.7345	-566.24	26.89094		
4	9698.559	0.022137	4599.264	0.027896	-571.79	0.00859	0.036634	0.073268
5	9147.658	0.024181	4883.378	0.02612	-586.21	0.008091	0.036503	0.073006
6	7311.638	0.018241	5749.313	0.025095	-654.68	0.009627	0.032484	0.064967
7	8103.208	0.010242	5036.173	0.016576	-609.87	0.011917	0.022841	0.045682
8	6214.347	0.015919	5779.151	0.028921	-677.23	0.007914	0.033948	0.067896

9	7040.941	0.026897	5221.024	0.026904	-636.76	0.006707	0.03863	0.07726
10	5120.039	0.047956	5883.109	0.075928	-701.17	0.008402	0.090197	0.180393
11	5581.489	0.043835	5405.134	0.048921	-668.94	0.019677	0.068571	0.137142
12	7595.33	0.054339	5661.169	0.050279	-648.62	0.005357	0.074225	0.148451
13	8867.244	0.02966	5386.11	0.051303	-612.71	0.037617	0.070191	0.140382
14	6860.136	0.026439	5095.045	0.02845	-634.37	0.009987	0.040102	0.080204
15	8395.452	0.030191	5109.569	0.032766	-605.67	0.003958	0.04473	0.08946
16	10424.41	0.025454	5037.663	0.069241	-583.66	0.053381	0.091059	0.182118
17	11460.62	0.025094	4528.033	0.023886	-543.53	0.003658	0.034837	0.069674
18	9594.352	0.029461	5330.041	0.048164	-605.86	0.004755	0.05666	0.11332
19	10526.56	0.02078	5406.908	0.038891	-595.13	0.006514	0.044573	0.089146
20	12242.6	0.022813	4325.75	0.028213	-523.42	0.010475	0.037764	0.075528
							max	0.182118
							average	0.101708
							min	0.045682

Table D.55 - Summary of 757 main assembly jig data

Location	Data points			
	1	10	20	50
1	0.42503	0.185989	0.150232	0.122843
2	NA	NA	NA	NA
3	NA	NA	NA	NA
4	0.556853	0.192479	0.123675	0.073268
5	0.542744	0.208694	0.140526	0.073006
6	0.535217	0.211576	0.146088	0.064967
7	0.558743	0.22307	0.151689	0.045682
8	0.52059	0.200086	0.119662	0.067896
9	0.43258	0.167623	0.140448	0.07726
10	0.71583	0.338948	0.287024	0.180393
11	0.648198	0.249739	0.209989	0.137142
12	0.516132	0.269384	0.237148	0.148451
13	0.573317	0.265688	0.224399	0.140382
14	0.593567	0.227461	0.168712	0.080204
15	0.522523	0.224955	0.177544	0.08946
16	0.604026	0.301736	0.247722	0.182118
17	0.462492	0.158678	0.122478	0.069674
18	0.500716	0.217161	0.166347	0.11332
19	0.489563	0.195216	0.126016	0.089146
20	0.554072	0.218276	0.146903	0.075528
Max	0.71583	0.338948	0.287024	0.182118
Average	0.541788	0.225376	0.171478	0.101708
Min	0.42503	0.158678	0.119662	0.045682

D.4 777 measurement data

Table D.56 - 777 main assembly jig trials

Trial 1

IPS points			LT points						difference
X	Y	z	x	Y	z	X	y	z	scalar
0	0	0	-1.21591	0.53365	1.022415	-1.21591	0.53365	1.022415	1.675875
336.8479	-159.56	3.289806	337.5213	-159.236	3.336041	0.673363	0.324746	0.046235	0.74901
865.4313	-899.37	951.4715							
1103.568	-1018.9	514.6293	1103.377	-1018.96	514.9835	-0.19074	-0.03393	0.354146	0.403675
1869.396	-1388.6	843.7518	1869.809	-1389.12	843.2989	0.413678	-0.46491	-0.45294	0.769692
3312.231	-2102.1	212.3049	3311.917	-2102.7	212.4024	-0.31332	-0.55819	0.097531	0.647501
3698.3	-2265.9	849.9926							
6820.674	-3760.0	1017.617	6821.735	-3761.22	1018.258	1.061123	-1.20238	0.641561	1.727226
7910.312	-4291.4	792.9766	7910.734	-4291.31	792.8546	0.422184	0.087186	-0.12195	0.44801
9039.399	-4841.4	550.9817	9038.992	-4840.65	550.7317	-0.40721	0.750571	-0.25	0.889764
9989.859	-5303.6	349.6275	9989.263	-5303.46	349.8023	-0.59577	0.146906	0.174758	0.638013
11065.73	-5813.1	115.6817	11065.73	-5813.4	115.8339	-0.00218	-0.25238	0.152222	0.294736

Trial 2

IPS data			Laser tracker data			Difference			difference
X	Y	z	X	Y	z	X	y	z	scalar
0	0	0	-1.24921	0.473852	0.600302	-1.24921	0.473852	0.600302	1.464725
336.8479	-159.56	3.289806	337.4875	-159.297	2.92065	0.639585	0.264024	-0.36916	0.784254
865.4313	-899.37	951.4715							NA
1103.568	-1018.9	514.6293	1103.413	-1018.85	514.7568	-0.15503	0.079593	0.127466	0.215912
1869.396	-1388.6	843.7518	1869.891	-1388.89	843.0904	0.494896	-0.24099	-0.66142	0.860511
3312.231	-2102.1	212.3049	3311.904	-2102.71	212.2342	-0.32682	-0.56128	-0.07066	0.653332
3698.3	-2265.9	849.9926							NA
6820.674	-3760.0	1017.617	6821.829	-3760.96	1018.161	1.155489	-0.94283	0.544016	1.587465
7910.312	-4291.4	792.9766	7910.793	-4291.14	792.7844	0.481302	0.262703	-0.19214	0.58102
9039.399	-4841.4	550.9817	9039.013	-4840.56	550.6899	-0.38585	0.836034	-0.29181	0.965914
9989.859	-5303.6	349.6275	9989.253	-5303.45	349.7844	-0.60578	0.157566	0.156903	0.6453
11065.73	-5813.1	115.6817	11065.68	-5813.48	115.8382	-0.04858	-0.32867	0.156512	0.367256

Appendix E: Phase Three testing

E.1 HdH CMM data – Plate 1

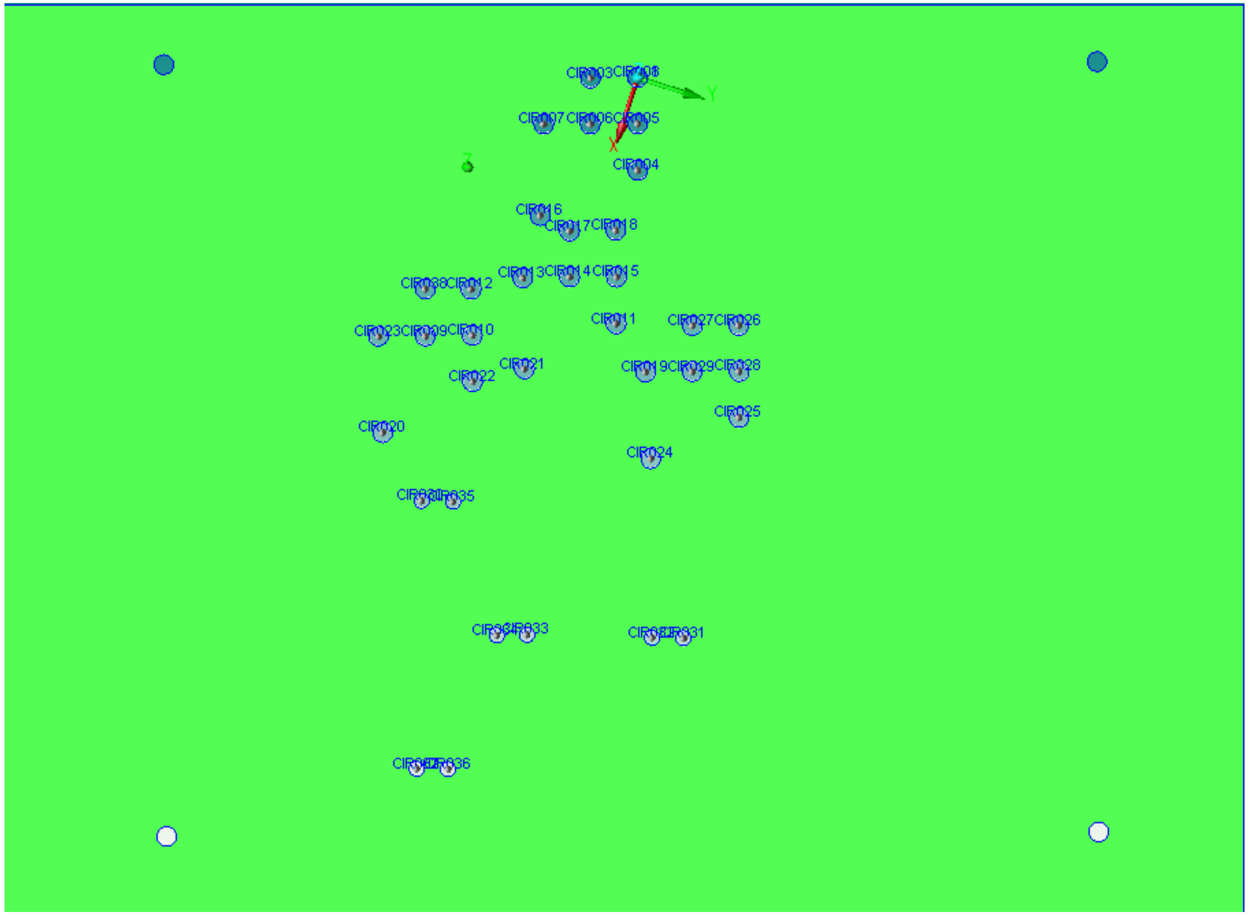

E.2 HdH CMM data – Plate 2

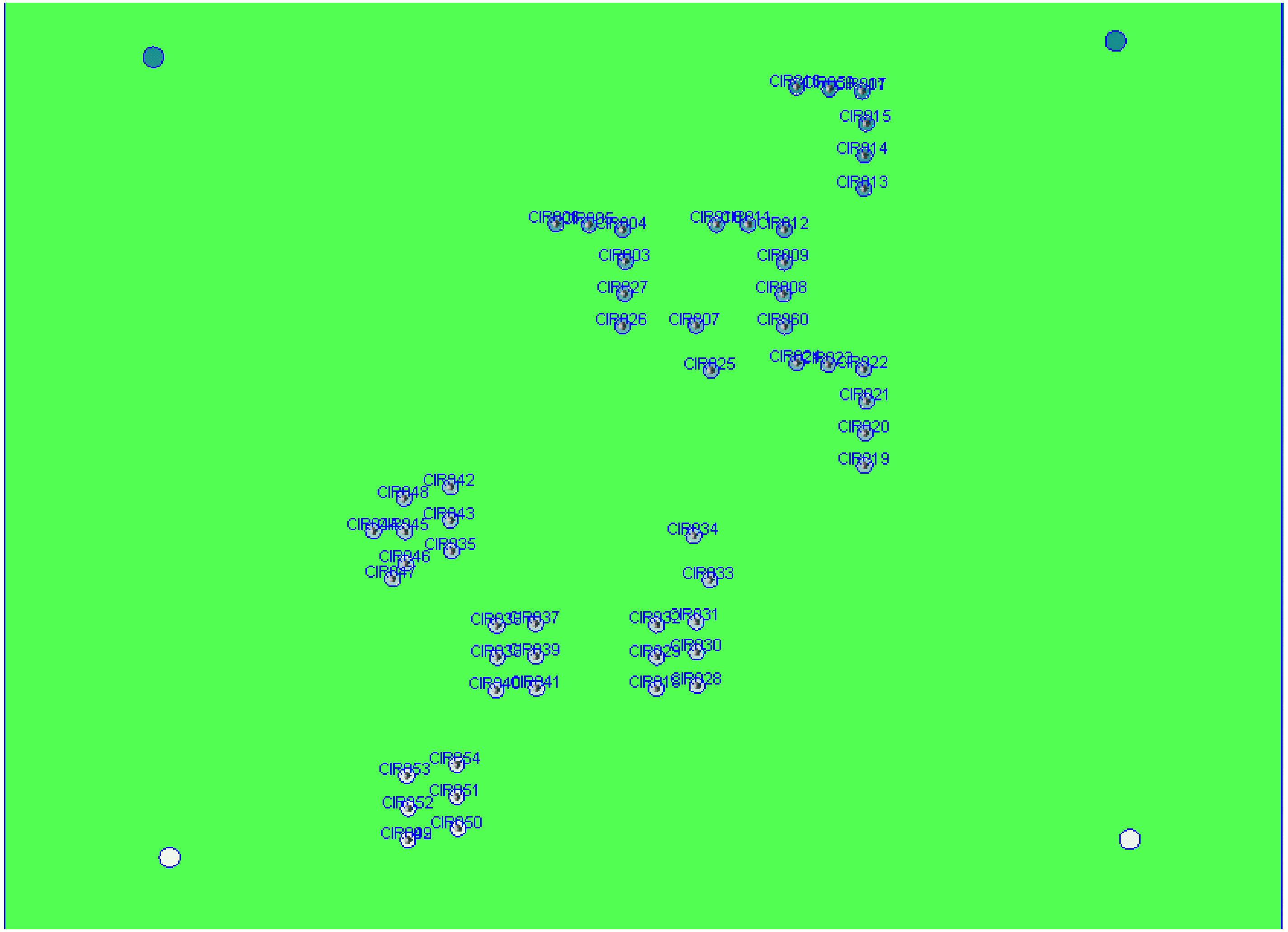

E.3 HdH CMM data – Plate 3

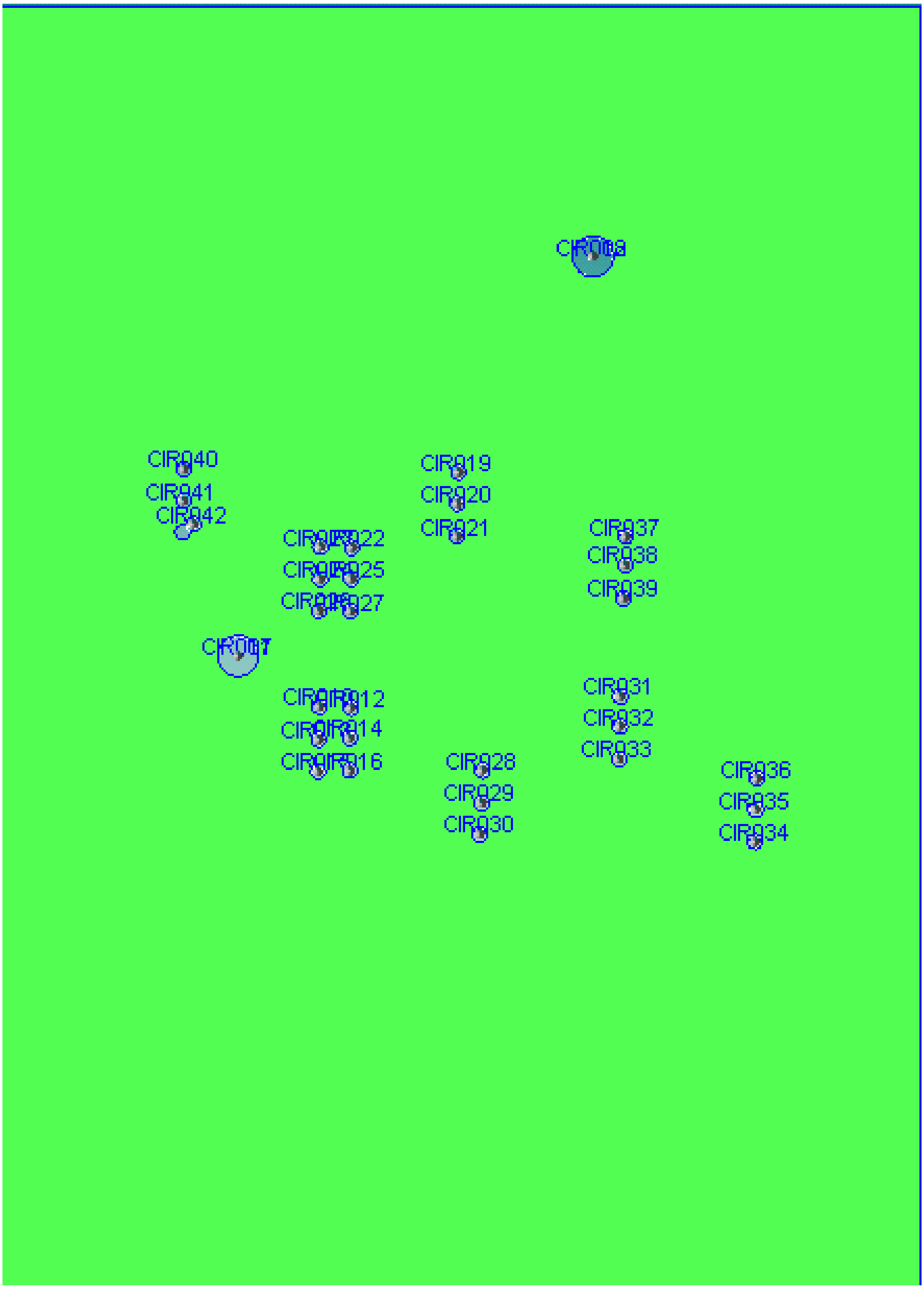

E.4 HdH CMM data – Numerical

Table E.57 - CMM data of plates supplied by HdH

Plate 1		ID	x		Y		dist from A		variation		
pattern			nominal	Actual	Nominal	actual	Nominal	actual	nominal	actual	dist
40	A	33	182.9692	182.827	20.5733	20.785					
40	B	31	168.9725	168.532	68.8652	69.315	50.27937	50.59158	0.279372	0.59158	0.59158
40	C	36	231.8715	232.049	9.4208	9.704	50.15788	50.45388	0.157883	0.453878	0.453878
40	D	35	148.8864	148.999	-15.362	-15.146	49.52782	49.34947	-0.47218	-0.65053	0.650528
50	A	34	186.0507	185.988	11.3549	11.577					
50	B	32	171.7766	171.46	59.2168	59.597	49.94508	50.16954	-0.05492	0.169544	0.169544
50	C	37	234.7956	235.022	-0.2841	0.001	50.11518	50.38191	0.115183	0.381911	0.381911
50	D	30	151.6786	151.79	-24.967	-24.814	50.00722	49.93804	0.007216	-0.06196	0.061958

Plate 2		ID	x		Y		dist from A		variation		
pattern			nominal	Actual	Nominal	actual	Nominal	actual	nominal	actual	dist
140	A	10	58.9685	-17.473	59.106	-17.292					
140	B	6	84.7063	-60.179	84.986	-60.247	49.86226	50.14884	-0.13774	0.148843	0.148843
140	C	16	9.1492	-18.484	9.47	-18.2	49.82957	49.6443	-0.17043	-0.3557	0.355696
140	D	24	83.1667	26.2298	82.966	26.601	49.95529	49.95893	-0.04471	-0.04107	0.041066
150	A	11	53.9124	-9.0958	53.991	-8.877					
150	B	5	79.5948	-51.602	79.857	-51.3	49.66292	49.68663	-0.33708	-0.31337	0.313373
150	C	59	4.0132	-9.8302	4.612	-9.127	49.9046	49.37963	-0.0954	-0.62037	0.620367
150	D	23	78.1036	34.7887	78.323	35.19	50.11051	50.33832	0.110513	0.338323	0.338323
240	A	60	75.299	17.0221	75.297	17.448					
240	B	26	101.3128	-25.920	101.48	-25.851	50.20725	50.59993	0.207246	0.59993	0.59993
240	C	13	25.3676	16.1047	25.626	16.335	49.93983	49.68347	-0.06017	-0.31653	0.316532
240	D	19	99.3884	60.9769	99.32	61.242	50.12308	49.95016	0.123085	-0.04984	0.049835
250	A	8	66.6334	11.6527	66.868	11.867					
250	B	27	92.2496	-30.873	92.466	-30.667	49.64507	49.64271	-0.35493	-0.35729	0.357289
250	C	14	16.4997	10.8841	16.735	11.007	50.13959	50.14038	0.139591	0.140376	0.140376
250	D	20	90.5049	55.7903	90.543	56.196	50.17944	50.25501	0.17944	0.255008	0.255008
260	A	9	57.9953	6.6477	58.24	6.954					
260	B	3	83.6349	-35.773	83.771	-35.646	49.56718	49.6648	-0.43282	-0.3352	0.335204
260	C	15	7.7496	6.0117	7.907	6.323	50.24973	50.33696	0.249725	0.336955	0.336955
260	D	21	81.7954	50.905	81.913	51.383	50.2509	50.3423	0.250904	0.342298	0.342298
270	A	12	49.4479	1.4226	49.542	1.685					
270	B	4	75.4691	-41.681	75.735	-41.48	50.34901	50.4905	0.349014	0.490499	0.490499
270	C	17	-0.2147	-0.257	-0.001	0	49.69099	49.57165	-0.30901	-0.42835	0.428354
270	D	22	73.75	45.0104	73.819	45.452	49.90479	50.04921	-0.09521	0.049206	0.049206
440	A	40	219.4569	-0.6718	218.946	-0.676					
440	B	18	193.1665	41.7441	192.602	41.799	49.90284	49.98132	-0.09716	-0.01868	0.018684
440	C		273.5692	-0.2376	273.134	-0.001	54.11404	54.1922	4.114042	4.192204	4.192204
440	D	46	200.02	-45.299	199.937	-45.414	48.67674	48.60896	-1.32326	-1.39104	1.391043
450	A	38	210.7056	-5.8277	210.019	-5.683					
450	B	29	184.3606	36.6638	184.097	36.784	49.99587	49.75335	-0.00413	-0.24665	0.246647
450	C		265.1234	-5.1436	264.743	-4.977	54.4221	54.72855	4.4221	4.728554	4.728554
450	D	45	191.6053	-50.936	191.519	-50.741	48.98588	48.70804	-1.01412	-1.29196	1.291958
460	A	36	202.1175	-10.975	201.677	-10.963					
460	B	32	175.8673	31.459	175.496	31.556	49.89732	49.93306	-0.10268	-0.06694	0.066944
460	C		256.7424	-10.608	256.219	-10.752	54.62613	54.54241	4.62613	4.542408	4.542408

460	D	48	183.1968	-56.226	182.841	-56.331	49.04729	49.12281	-0.95271	-0.87719	0.877191
540	A	41	212.2456	9.6841	211.884	9.732					
540	B	28	185.3299	52.065	185.14	52.175	50.20553	50.16622	0.205533	0.166222	0.166222
540	C		262.3687	11.556	261.951	11.516	50.15804	50.09877	0.158042	0.098774	0.098774
540	D	35	189.3964	-35.011	189.136	-35.073	50.19779	50.24898	0.197792	0.248975	0.248975
550	A	39	203.8132	4.3628	203.543	4.452					
550	B	30	176.9634	46.6784	176.328	46.68	50.11509	50.23804	0.115085	0.238035	0.238035
550	C		253.9829	6.0914	253.682	5.998	50.19947	50.16283	0.199471	0.162829	0.162829
550	D	43	181.1239	-40.413	181.041	-40.414	50.19709	50.19261	0.197094	0.192609	0.192609
560	A	37	195.2813	-1.1026	194.895	-1.015					
560	B	31	168.3466	41.3617	168.252	41.688	50.28613	50.33285	0.28613	0.332849	0.332849
560	C		245.5178	0.7971	245.111	0.81	50.27241	50.24915	0.272406	0.249152	0.249152
560	D	42	172.5971	-45.728	172.223	-45.774	50.05996	50.17358	0.059957	0.173575	0.173575

Plate 3 pattern Number		ID	x nominal	actual	Y Nominal	actual	dist from A nominal	actual	variation nominal	actual	dist
340	A	31	70.566	-98.584	70.566	-98.584					
340	B	37	109.273	-66.326	109.273	-66.326	50.38661	50.38661	0.386609	0.386609	0.386609
340	C	36	79.861	-147.843	79.861	-147.843	50.1283	50.1283	0.128296	0.128296	0.128296
340	D	28	24.257	-81.54	24.257	-81.54	49.34594	49.34594	-0.65406	-0.65406	0.654064
350	A	32	63.45	-104.722	63.45	-104.722					
350	B	38	102.449	-72.157	102.449	-72.157	50.80749	50.80749	0.807492	0.807492	0.807492
350	C	35	72.398	-154.074	72.398	-154.074	50.15662	50.15662	0.156621	0.156621	0.156621
350	D	29	16.51	-88.118	16.51	-88.118	49.79012	49.79012	-0.20988	-0.20988	0.209876
360	A	33	55.509	-111.26	55.509	-111.26					
360	B	39	94.352	-78.807	94.351	-78.807	50.61596	50.6152	0.615964	0.615197	0.615197
360	C	34	64.643	-160.501	64.643	-160.501	50.08099	50.08099	0.080995	0.080995	0.080995
360	D	30	8.788	-94.272	8.788	-94.272	49.71362	49.71362	-0.28638	-0.28638	0.28638
640	A	26	27.684	-9.607	27.684	-9.607					
640	B	15	-10.377	-43.056	-10.377	-43.056	50.67026	50.67026	0.670261	0.670261	0.670261
640	C										
640	D	21	73.978	-26.523	73.978	-26.523	49.28778	49.28778	-0.71222	-0.71222	0.712218
650	A	24	35.213	-3.343	35.213	-3.343					
650	B	13	-2.739	-36.498	-2.739	-36.498	50.39453	50.39453	0.394527	0.394527	0.394527
650	C	41	24.998	45.304	24.998	45.304	49.70792	49.70792	-0.29208	-0.29208	0.292085
650	D	20	81.77	-19.777	81.77	-19.777	49.37237	49.37237	-0.62763	-0.62763	0.627633
660	A	23	42.859	3.376	42.859	3.376					
660	B	10	5.183	-29.779	5.183	-29.779	50.187	50.187	0.187	0.187	0.187
660	C	40	32.603	51.813	32.603	51.813	49.51089	49.51089	-0.48911	-0.48911	0.489107
660	D	19	89.317	-13.436	89.317	-13.436	49.40637	49.40637	-0.59363	-0.59363	0.593633
740	A	27	34.078	-17.168	34.078	-17.168					
740	B	16	-3.503	-50.298	-3.503	-50.298	50.09919	50.09919	0.099186	0.099186	0.099186
740	C	42	21.618	38.099	21.618	38.099	56.65415	56.65415	6.654152	6.654152	6.654152
740	D										
750	A	25	41.81	-10.595	41.81	-10.595					
750	B	14	4.152	-43.544	4.152	-43.544	50.0376	50.0376	0.037602	0.037602	0.037602
750	C										
750	D										
760	A	22	49.321	-4.196	49.321	-4.196					

760	B	12	11.426	-37.488	11.426	-37.488	50.44193	50.44193	0.44193	0.44193	0.44193
760	C										
760	D										

E.5 Test results

Table E.58 - Positional error of robotic drill tests

Robot only testing		IPS positioning		Bump 1		Bump 2	
Trial	error	Trial	Error	Trial	Error	Trial	error
1	0.565329	1	0.322099	1	0.469909	1	0.171324
2	0.204471	2	0.250891	2	0.512868	2	0.197824
3	0.181868	3	0.338152	3	0.314712	3	0.251859
4	0.424021	4	0.389657	Mean	0.432496	4	0.460826
Mean	0.343922	5	0.39133			5	0.438082
		6	0.327524			6	0.423247
		20 sample	0.322686			mean	0.32386
		Mean	0.33462				

Table E.59 - Summary of positional error of robotic drill tests

Test	Error
Robot only	0.343922
IPS	0.33462
IPS 20 sample	0.322686
Bump 1	0.432496
Bump 2	0.32386

E.6 Data analysis

The calculation of data is performed using Microsoft excel, using a best fit analysis. Extensive data is far too large in include in printed form, and is therefore not deemed necessary for this dissertation. A methodology was therefore included here The stages are as follows:

1. Determine arrangement for receivers on end effector and workpieces.

2. Record locations of each workpiece and end effector receivers.

3. Use best fit analysis to determine position and orientation of each part in the system.

4. Identify displacement from the TCP to required drilling location.

At this point, the displacement is known in global coordinates.

5. The data is then converted to Robot end effector coordinates for movement.

6. This process is repeated until the location is within 0.1mm, then the location is drilled.

7. This process is repeated for each drilling location.

The mathematics and process behind this is shown in the following sections.

E.6.1 Calculations

The calculation for determining position and orientation is completed using the following translation of rotation and translation matrices. These are an adaptation from Labrooy [1991], Paul [1981] and Roskam [1995].

$$Roll(\phi) = \begin{bmatrix} \cos\phi & -\sin\phi & 0 & 0 \\ \sin\phi & \cos\phi & 0 & 0 \\ 0 & 0 & 1 & 0 \\ 0 & 0 & 0 & 1 \end{bmatrix}$$

$$Pitch(\theta) = \begin{bmatrix} \cos\theta & 0 & -\sin\theta & 0 \\ 0 & 1 & 0 & 0 \\ \sin\theta & 0 & \cos\theta & 0 \\ 0 & 0 & 0 & 1 \end{bmatrix}$$

$$Yaw(\psi) = \begin{bmatrix} 1 & 0 & 0 & 0 \\ 0 & \cos\psi & -\sin\psi & 0 \\ 0 & \sin\psi & \cos\psi & 0 \\ 0 & 0 & 0 & 1 \end{bmatrix}$$

$$Trans(x, y, z) = \begin{bmatrix} 1 & 0 & 0 & x \\ 0 & 1 & 0 & y \\ 0 & 0 & 1 & z \\ 0 & 0 & 0 & 1 \end{bmatrix}$$

It is also important to retain the order of translation and rotation, therefore the process for these calculations between a frame (noted A) and a second frame (noted B) is shown to be:

Frame A → Roll(ϕ) → Pitch(θ) → Yaw(ψ) → Trans(x,y,z) → Frame B

The reverse of each translation is required, to calculate the inverse of a matrix, we use the following relationship.

If :
$$[A_n] = \begin{bmatrix} n_x & o_x & a_x & p_x \\ n_y & o_y & a_y & p_y \\ n_z & o_z & a_z & p_z \\ 0 & 0 & 0 & 1 \end{bmatrix}$$

Then:
$$[A_n]^{-1} = \begin{bmatrix} n_x & n_y & n_z & -\vec{p} \bullet \vec{n} \\ o_x & o_y & o_z & -\vec{p} \bullet \vec{o} \\ a_x & a_y & a_z & -\vec{p} \bullet \vec{a} \\ 0 & 0 & 0 & 1 \end{bmatrix}$$

Therefore the inverse of the process is as follows:

Frame B → Trans(x,y,z)$^{-1}$ → Yaw(ψ)$^{-1}$ → Pitch(θ)$^{-1}$ → Roll(ϕ)$^{-1}$ → Frame A

To determine the required translation and rotation values, a spreadsheet is developed, a reduced example of this is presented in Figure E.82.

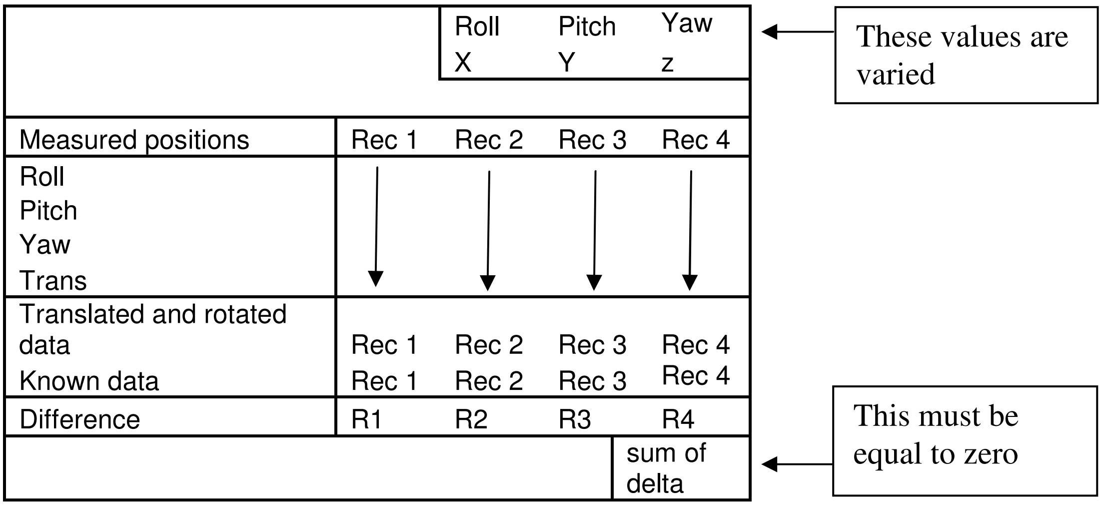

Figure E.82 - Presentation of rotation and translation matrix determination

The flowchart in Figure E.83 depicts the process by which this data is analyzed using Microsoft excel.

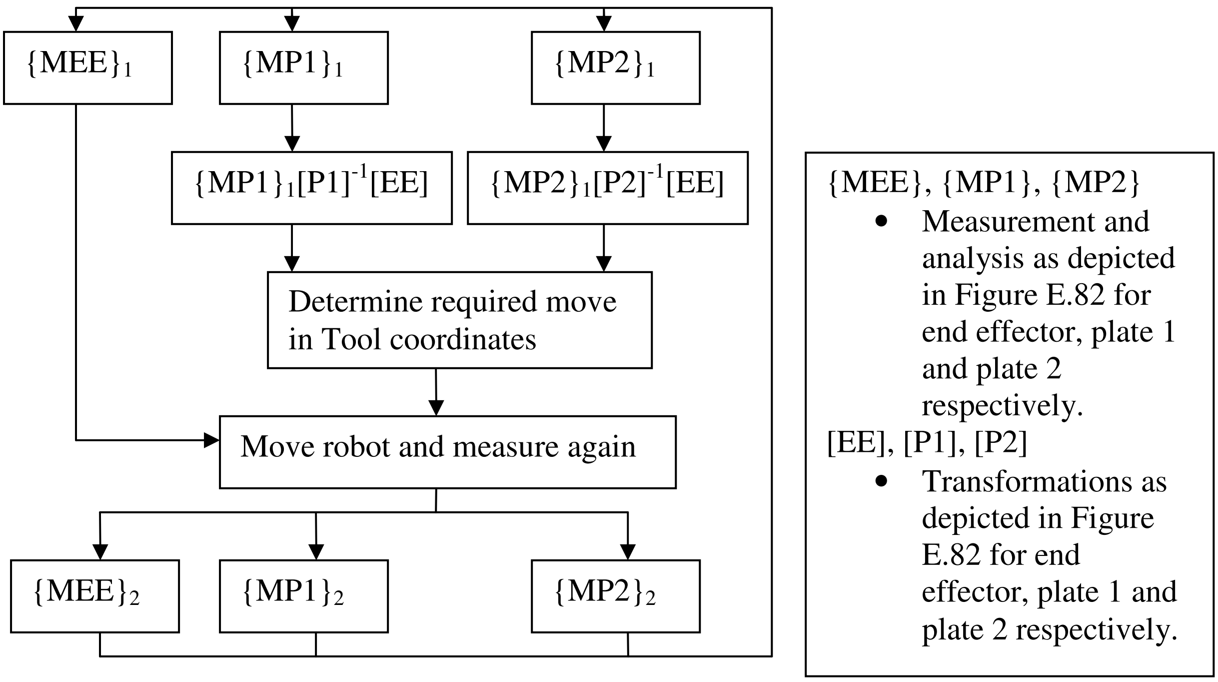

Figure E.83 - Data analysis for robot positioning